CHAPTER ONE

Oscillator Dynamics

1.1 INTRODUCTION

A well-designed free-running oscillator provides a periodic signal of constant amplitude and frequency f_o from the energy delivered by direct-current (dc) sources. This has an immediate application for the realization of local oscillators used in the frequency-conversion stages of communication systems [1]. In receivers, the modulated signal at radio-frequency (RF) f_{RF} is mixed with the output of a local oscillator at f_o, selecting the intermodulation product that corresponds to the frequency difference $f_{IF} = f_{RF} - f_o$, This allows down-conversion of the carrier frequency from f_{RF} to f_{IF}. An analogous procedure is followed in transmitters. The intermediate frequency f_{IF} is mixed with the output of the local oscillator, selecting the intermodulation product $f_{RF} = f_{IF} + f_o$. This allows up-conversion of the carrier frequency. The free-running oscillator is usually inserted into a phase-locked loop for this application [2].

A single oscillator having dc sources only is said to operate in free-running mode. However, other forms of behavior are possible. In injection-locked operation [3], the oscillation is synchronized with an independent periodic source, which means that the oscillation frequency, influenced by the input source, becomes equal to the input frequency $f_o = f_{in}$, with a constant phase shift between the oscillation and the input signal. The injection-locked mode is used for phase noise reduction, frequency division, or phase shifting. In coupled operation, several oscillators are interconnected by means of linear coupling networks [4] and oscillate in a synchronous manner. Coupled-oscillator systems can be used for power combination

Analysis and Design of Autonomous Microwave Circuits, By Almudena Suárez

or beam steering. In this chapter only the free-running mode of an oscillator circuit is considered. Familiarity with the behavior and properties of free-running oscillation is essential for an understanding of any other form of operation (e.g., injection-locked, coupled) treated in subsequent chapters.

Free-running oscillators have essential differences from other RF circuits, such as amplifiers, mixers, and frequency multipliers [5,6]. The operation frequency or frequencies (in the case of a mixer) of these circuits are determined by the input sources. In contrast, the fundamental frequency of an oscillator is self-generated or autonomous and depends on the values of the circuit elements. Thus, the circuit must be designed accurately to obtain the value desired for the oscillation frequency f_o. Due to the absence of time-varying sources, any free-running oscillator can be solved for a mathematical dc solution. The oscillation starts up from any small perturbation of this dc solution and must grow from noise level to a steady-state oscillatory solution with constant amplitude and period. As will be shown, the self-sustained oscillation is only possible in nonlinear, nonconservative systems. Stability concepts are also essential to the understanding of the oscillator behavior. The oscillation startup and the physical observation of the periodic solution are explained from the different stability properties of dc and the steady-state oscillation [7]. Because of the absence of an input periodic source establishing a time reference, arbitrary translations of the periodic waveform along the time axis give other solutions. There is an "irrelevance" with respect to time translations, or in the frequency domain, with respect to the phase origin. Thus, any phase-shifted solution constitutes a valid solution of the oscillator circuit. The absence of a restoring mechanism in the phase value gives rise to the phase noise problem in oscillator circuits [8,9].

In this chapter we deal with the main aspects of oscillator behavior. Oscillators are studied in the time domain and in the frequency domain, using impedance–admittance descriptions, which are very helpful for oscillator design, and the describing function approach, which allows nonlinear analysis at the fundamental frequency only. This one-harmonic approach will set the conceptual basis for harmonic balance analysis, covered in detail in Chapter 5. We relate various analysis techniques and unify concepts and properties, derived in the literature from very different viewpoints. Chapter 1 provides a general background for Chapter 2, which is devoted to phase noise analysis; Chapter 3, devoted to global stability analysis; and Chapter 4, devoted to an analysis of injection-locked oscillators and frequency dividers. The chapter is organized as follows. Section 1.2 provides intuitive explanations for oscillation startup and for the mechanism of self-sustained oscillation. In Section 1.3 we present the frequency-domain formulation based on the use of impedance or admittance functions, covering steady-state analysis and the stability of dc and periodic solutions. In Section 1.4 we extend the previous formulation to multiple harmonic components, for conceptual purposes, as this will be necessary for accurate stability analysis of oscillator circuit without limiting assumptions. In Section 1.5 we deal with oscillator circuits from the viewpoint of nonlinear dynamics, with the circuit described by a system of nonlinear differential equations. The main types of steady-state solutions and their properties are presented. In Section 1.6 we introduce formal mathematical procedures for the stability analysis of dc and periodic regimes and provide the necessary background for global stability analysis (i.e., versus variation in a circuit parameter), which is covered in Chapter 3. Finally, in Section 1.7 we emphasize the irrelevance of the oscillator solution versus time translations and show examples of phase shift response versus impulse perturbations. We establish the necessary background for Chapter 2, dealing with stochastic characterization of the spectrum of a noisy oscillator. Two different circuits are considered in this chapter: a parallel resonance oscillator with a two-terminal active element, and a FET-based oscillator at $f_o = 4.36$ GHz. The simplicity of the first circuit makes possible the derivation of meaningful analytical expressions. Comparison with a FET-based oscillator clarifies our understanding of deviations from ideal behavior in practical circuits.

1.2 OPERATIONAL PRINCIPLE OF FREE-RUNNING OSCILLATORS

An ideal circuit given by the parallel connection of an inductor L and a capacitor C, without resistance, will under any initial condition exhibit oscillation at the frequency $\omega_o = 1/\sqrt{LC}$, at which the average energies stored in the magnetic and electric fields are equal, so the sum of the inductor and capacitor susceptances is equal to zero [5]. The total energy in the circuit remains constant during the entire oscillation period, so it is a conservative system [10]. When the electrical energy stored in the capacitor is maximal, the magnetic energy stored in the inductor is zero, and vice versa. The energy displacement from one element to another gives rise to the oscillation observed in the node voltage and branch currents. By Kirchhoff's laws, the sum of the inductor plus capacitor current must be equal to zero, $i_C + i_L = 0$, which after some simple manipulations provides the linear differential equation

$$\frac{d^2v(t)}{dt^2} + \frac{1}{LC}v(t) = 0 \tag{1.1}$$

with $v(t)$ the node voltage. Equation (1.1) is a second-order differential equation with constant coefficients which can be transformed into two first-order equations by performing the variable change $x_1(t) = v(t)$, $x_2(t) = dv(t)/dt$. Then, equation (1.1) becomes

$$\begin{bmatrix} \dot{x}_1(t) \\ \dot{x}_2(t) \end{bmatrix} = \begin{bmatrix} 0 & 1 \\ \frac{-1}{LC} & 0 \end{bmatrix} \begin{bmatrix} x_1(t) \\ x_2(t) \end{bmatrix} \tag{1.2}$$

System (1.2) belongs to the general class of linear differential equations with constant coefficients, which can be written in the general manner $\dot{\overline{x}}(t) = A\overline{x}(t)$, where $\overline{x}(t)$ is a vector of system unknowns and A is a constant matrix. For M variables in $\overline{x}(t)$, the general solution of $\dot{\overline{x}}(t) = A\overline{x}(t)$ has the form $\overline{x}(t) = c_1\overline{v}_1 e^{\lambda_1 t} + c_2\overline{v}_2 e^{\lambda_2 t} + \cdots + c_M \overline{v}_M e^{\lambda_M t}$, where the exponents λ_k are the eigenvalues of the matrix A, assumed different, and the vectors $\overline{v}_k$ are the eigenvectors of A. Because any physical variable $x(t)$ is real valued in the time domain, the constants c_k, v_k, and λ_k will be either real or complex conjugate. The constants c_k depend on the initial value $t_o, \overline{x}(t_o)$.

In the particular case of system (1.2), the eigenvalues of the 2×2 matrix A are $\lambda_{1,2} = \pm j\omega_o = \pm j1/\sqrt{LC}$ and the eigenvectors are given by $[1, j\omega_o]$ and $[1, -j\omega_o]$. Then the solution of (1.1) has, for $x_1(t) = v(t)$, the general form

$$v(t) = ce^{j\omega_o t} + c^* e^{-j\omega_o t} = 2(c_r \cos\omega_o t - c_i \sin\omega_o t) \tag{1.3}$$

with $c = c_r + jc_i$ being a complex constant, depending on the initial conditions $v(t_o)$ and $dv(t_o)/dt$. For a given initial value $v(t_o)$ and $dv(t_o)/dt$, this complex constant is calculated by means of the following system of boundary conditions:

$$\begin{aligned} v(t_o) &= 2(c_r \cos\omega_o t_o - c_i \sin\omega_o t_o) \\ \frac{dv(t_o)}{dt} &= -2(c_r\omega_o \sin\omega_o t_o + c_i\omega_o \cos\omega_o t_o) \end{aligned} \tag{1.4}$$

Thus, for each pair of possible initial conditions $v(t_o)$ and $dv(t_o)/dt$, an oscillatory solution with different amplitude would be obtained. This dependence of the oscillation amplitude on the initial conditions is unphysical and, of course, is never observed in the free-running oscillators measurements. An analogous situation would be found in an ideal pendulum with no friction in which the ball keeps oscillating at the amplitude of the initial elongation. In the case of the circuit described by (1.1), the unphysical situation is due to the absence of resistive elements in the ideal LC circuit. In practice it is not possible to have inductors or capacitors without resistive losses. Note that one of the solutions of (1.3) obtained from $v(t_o) = 0$ and $dv(t_o)/dt = 0$ is given by $v(t) = 0$ and $y(t) = 0$ $\forall t$. This solution, just one of the family $v(t) = ce^{j\omega t} + c^* e^{-j\omega t}$, provides no oscillation at all.

The eigenvalues λ_k of the matrix A in the general system $\dot{\overline{x}}(t) = A\overline{x}(t)$ can also be obtained from an application of the Laplace transform to this system, which provides $[sI_d - A]\overline{X}(s) = 0$, where I_d is the identity matrix and $\overline{X}(s)$ is the vector of the Laplace transforms of the different variables. (Note that the obtained system assumes a zero initial value $\overline{x}(0) = 0$, which otherwise should be taken into account in the transformation of the time-derivative to the Laplace domain.) The system $[sI_d - A]\overline{X}(s) = 0$ is a homogeneous linear system in $\overline{X}(s)$. Therefore, to obtain a solution $\overline{X}(s)$ different from zero, the matrix affecting $\overline{X}(s)$ must be singular. Thus, the condition $\det[sI_d - A] = 0$ must be fulfilled. The determinant introduced, known as the *characteristic determinant* of the linear system, provides a characteristic polynomial $P(s) = \det[sI_d - A] = 0$ of the same degree as the number of unknowns in $\overline{X}(s)$. In particular, application of the Laplace transform to (1.1) provides the characteristic polynomial $P(s) = s^2 + 1/LC = 0$. As can easily be seen, the roots of the characteristic polynomial agree with the eigenvalues $\lambda_{1,2} = \pm j\omega_o = \pm j1/\sqrt{LC}$ of matrix A of (1.2).

Now assume that a small-signal input $u(t)$ is introduced in the general linear system $\dot{\overline{x}}(t) = A\overline{x}(t)$. In the Laplace domain this will give rise to the equation $[sI_d - A]\overline{X}(s) = [G(s)]U(s)$, where $[G(s)]$ is a column matrix [11,12]. This matrix is necessary because we have not specified the nature of the input, so it may undergo time derivations when introduced in the system. Any possible output $Y(s)$ will be linearly related to the variable vector $\overline{X}(s)$, which in a general manner can be expressed as $Y(s) = [B][sI_d - A]^+$, where $[B][sI_d - A]^+$ is a row matrix. Thus, any possible single-input single-output transfer function will be written

$$H(s) = \frac{Y(s)}{U(s)} = \frac{[B][sI_d - A]^+[G(s)]}{P(s)} \tag{1.5}$$

with "+" being the transpose of the cofactor matrix. The roots of $P(s)$ will agree with the poles of the single-input single-output transfer function $H(s)$. Intuitively, the poles are associated with the zero-input solutions of the analyzed system, so they cannot depend on the particular input or output. However, pole–zero cancellations are possible due to the matrix product in the numerator, which will be different for different choices of the closed-loop transfer function. Pole–zero cancellations can be avoided through a suitable choice of $H(s)$. Provided that no pole–zero cancellations occur, it will be possible to calculate the roots λ_k of $P(s)$ indirectly from the pole analysis of a transfer function $H(s)$.

As an example, consider the connection of a small-signal current source $I_{\text{in}}(s)$ to the middle node of the LC resonator in Fig. 1.1. The input signal $U(s) = I_{\text{in}}(s)$ is the current introduced, and the output selected is the node voltage $Y(s) = V(s)$. Applying (1.5), the closed-loop transfer function is

$$Z(s) = \frac{V(s)}{I_{\text{in}}} = \frac{[1\ 0]\begin{bmatrix} s & -1/(LC) \\ 0 & s \end{bmatrix}\begin{bmatrix} 0 \\ s/C \end{bmatrix}}{P(s)} = \frac{Ls}{CLs^2 + 1} \tag{1.6}$$

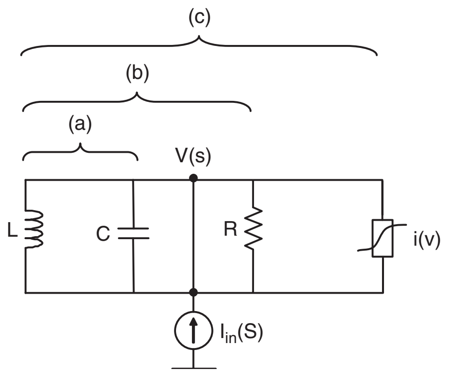

FIGURE 1.1 Parallel resonance oscillator. The element values are $L = 1$ nH, $C = 10$ pF, $R = 100\Omega$, and $i(v) = -0.03v + 0.01v^3$. Three different situations are considered in the text: (a) the connection of the two reactive elements LC only, without a resistor; (b) the inclusion of a positive resistor R; (c) the addition of the nonlinear element $i(v) = av + bv^3$. The current source $I_{\text{in}}(s)$ is introduced for the calculation of a closed-loop transfer function, defined as $Z(s) = V(s)/I_{\text{in}}(s)$.

with s the Laplace frequency. Clearly, the denominator agrees with the characteristic polynomial associated with (1.1), and the transfer function poles $p_{1,2} = \pm j\omega = \pm j\sqrt{1/LC}$ agree with the polynomial roots λ_1 and λ_2. The term *poles* is used often in the book to refer to the roots of the characteristic polynomial of a linear system, due to their equivalence. In the case of the second-order system (1.1), complex-conjugate poles are located on the imaginary axis. Therefore, the solution originating from given initial values $v(t_o)$ and $dv(t_o)/dt$ neither grows (which would correspond to poles on the right-hand side of the complex plane) nor vanishes (which would correspond to poles on the left-hand side of the plane), but remains with its initial amplitude. This is never observed in physical systems.

If a resistor is now introduced in the circuit of Fig. 1.1, the situation becomes totally different. The energy contained in the system no longer remains constant in time. The resistor dissipates energy as heat, at the rate $R\int_0^{t_{\max}} i_R^2(t)\,dt$, where $t_{\max}$ is the duration of the time interval considered and i_R is the current through the resistor. So the longer the time, the less energy is available for storage at the inductor and capacitor and the smaller is the oscillation amplitude. Thus, in an *RLC* circuit with $R > 0$, the oscillation amplitude decays to zero. When the resistor R is introduced in parallel, the circuit equations become

$$\frac{d^2v(t)}{dt^2} + \frac{1}{RC}\frac{dv(t)}{dt} + \frac{1}{LC}v(t) = 0 \tag{1.7}$$

Because of introduction of the resistor R, a new term has appeared in dv/dt, called the *damping term* [10]. The name *damping* indicates that the rate of extinction of the oscillation depends on the coefficient associated with dv/dt. The smaller the resistance value R, the higher its influence over the parallel resonator and the faster the oscillation extinction. As in the former case, equation (1.7) is a second-order linear system with constant coefficients. The associated characteristic polynomial $P(s)$ is obtained through application of the Laplace transform to (1.7). The two roots of this polynomial are given by

$$\lambda_{1,2} = -\frac{1}{2RC} \pm \sqrt{\frac{1}{(2RC)^2} - \frac{1}{LC}} \tag{1.8}$$

Provided that $1/LC > 1/(2RC)^2$, an exponentially decaying oscillation of the form $v(t) = e^{-(1/2CR)t}2(c_r\cos\omega t - c_i\sin\omega t)$ is obtained, with $\omega = \sqrt{1/LC - 1/(2RC)^2}$ and c_r and c_i constants that depend on the initial conditions. Note that the transient decay is ruled by the amplitude envelope $e^{(-1/2CR)t}$. The quality factor of the parallel resonance is given by $Q = RC\omega_o$, with $\omega_o = 1/\sqrt{LC}$. Therefore, the exponential transient can be described as $v(t) = e^{(-\omega_o/2Q)t}2(c_r\cos\omega t - c_i\sin\omega t)$, so the smaller the quality factor of the parallel circuit, the faster the oscillation extinction. Because the oscillation amplitude decays to zero for any initial value, the only steady-state solution of equation (1.7) is a dc regime with $v = 0$ and $dv/dt = 0$. This will be the only solution observed physically. The small noise perturbations will give rise to oscillatory transients, seen simply as noise about this dc regime.

As in the previous case, it is possible to define a closed-loop transfer function associated with the RLC circuit. This transfer function can be obtained by connecting a small-signal current source I_{in} in parallel and obtaining the ratio between the node voltage V and the current introduced, I_{in}. The poles of this transfer function, which agree with the roots of the characteristic polynomial $P(s)$, are located on the left-hand side of the complex plane. This indicates that whatever the initial condition, the linear system evolves to the steady state $v = 0$ and $dv/dt = 0$. The solution $v = 0$ and $dv/dt = 0$ also existed in the conservative system, but was just one of the infinite solutions in the family $v(t) = ce^{j\omega t} + c^*e^{-j\omega t}$. In contrast, the solution $v = 0$ and $dv/dt = 0$ is the only steady state of (1.7). Once this solution is reached, any instantaneous perturbation applied at a particular time value t_{o} only, and setting the initial values $v(t_{\text{o}})$ and $dv(t_{\text{o}})/dt$, will start a transient leading back to the dc solution $v = 0$ and $dv/dt = 0$. This dc solution is robust versus perturbations, or stable.

Clearly, to observe a steady-state oscillation, the effect of the resistor $R > 0$ must be compensated. Introduction of a negative-resistance element will provide an energy source to compensate for the energy loss in the resistor. This element can be a negative-resistance diode or a transistor under suitable configuration and bias conditions. The energy delivered will be taken from dc sources. Assuming a constant negative resistance R_N connected in parallel, the total resistance will be $R_T = 1/(G_N + G)$, with $G_N = 1/R_N$ and $G = 1/R$. The general circuit solution will be $v(t) = e^{[-(G+G_N)/2C]t} \cdot 2(c_r \cos \omega t - c_i \sin \omega t)$. For $G + G_N > 0$, which implies dominant positive resistance, the negative resistance introduced is not sufficient. The damping term will be positive and the oscillation amplitude will decay exponentially to zero from any initial condition. Thus, the dc solution will be the only one observable. For $G + G_N = 0$, a conservative LC circuit, with no effective resistance, is obtained again, which as discussed earlier, corresponds to a nonphysical situation. For $G + G_N < 0$, which implies dominant negative resistance, the damping term will be negative and the oscillation amplitude will increase exponentially ad infinitum. This is also nonphysical. The negative resistance cannot be insensitive to the growth of the node voltage. It has to depend on this voltage, or equivalently, it has to be nonlinear to enable saturation of the oscillation amplitude.

To illustrate the mechanism of self-sustained oscillation, a nonlinear element with the instantaneous characteristic $i(v)$ is introduced in the resonant circuit (see Figure 1.1). This provides the nonlinear differential equation

$$\frac{d^2v(t)}{dt^2} + \left[\frac{1}{RC} + \frac{1}{C}\frac{di}{dv}(v)\right]\frac{dv(t)}{dt} + \frac{1}{LC}v(t) = 0 \tag{1.9}$$

To obtain sustained oscillation, the damping term affecting dv/dt must be nonlinear and thus sensitive to $v(t)$. A common example of nonlinearity in oscillator theory is $i(v) = av + bv^3$, with $a < 0$ and $b > 0$. This is an ideal element providing negative conductance at small signal $G_N = di(v = 0)/dv = a + 3bv^2|_{v=0} = a$ about $v = 0$.

In physical systems, bias sources delivering energy to the circuit will, of course, be required. Placing the derivative di/dv into (1.9) yields the following equation:

$$\frac{d^2v(t)}{dt^2} + \frac{1}{C}(a + G + 3bv^2)\frac{dv(t)}{dt} + \frac{1}{LC}v(t) = 0 \tag{1.10}$$

where $G = 1/R$. Thus, the nonlinear damping term is given by $\mu(v) = (a + G + 3bv^2)/C$. Equation (1.10) constitutes a good behavioral model of the oscillator circuit, with reduced analytical complexity. Clearly, equation (1.10) admits the steady-state solution $v(t) = 0$, $dv/dt = 0$, which corresponds to the constant or dc solution of the ideal circuit of Fig. 1.1. Note that any oscillator circuit can always be solved for a constant solution, even when it exhibits self-sustained oscillation. This can easily be verified by the reader and is due to the absence of time-varying generators. When the dc generators are first powered on, oscillation has not yet builtup and the circuit is at this dc solution, due to the existence of dc sources only. The reaction of the dc solution to small perturbations can be predicted by linearizing the nonlinear element $i(v) = av + bv^3$ about the dc solution $v = 0$. Thus, the nonlinear element is replaced by the constant conductance $G_N = di(v = 0)/dv = a$. This allows us to apply linear analysis techniques to the circuit constituted by the parallel connection of G, G_N, L, and C. The resulting poles [or roots of the characteristic determinant $P(s)$] are given by

$$p_{1,2} = -\frac{G_T}{2C} \pm \frac{\sqrt{G_T^2L^2 - 4LC}}{2LC} \tag{1.11}$$

with $G_T = G_N + G$. The two poles in (1.11) are associated with nonlinear circuit linearization about the dc solution, thus are often called poles of the dc solution. They determine the response of the dc solution of an oscillator circuit to a small instantaneous perturbation.

From an inspection of (1.11), to obtain an oscillatory transient with exponentially growing amplitude, the poles must be complex conjugate $p_{1,2} = \sigma \pm j\omega$, with $\sigma > 0$. The oscillatory transient requires a negative value of the term under the square root. Assuming that $4LC \gg G_T^2L^2$, the pole frequency will correspond approximately to the resonance frequency $\omega_o = 1/\sqrt{LC}$. For the oscillation amplitude to grow exponentially in time, the condition $\sigma = -G_T/2C > 0$ must be fulfilled, which in the circuit of Fig. 1.1 implies that $G_T = a + G < 0$. At small signal, we can consider the circuit of Fig. 1.1 (including the nonlinear element) as a feedback system with a direct-trajectory transfer function $Y_N = a$ and a feedback transfer function $Z(s) = (Cs + 1/(Ls) + G)^{-1}$. The combination of gain and feedback with a resonant network leads to a characteristic system with two complex-conjugate poles responsible for the oscillation startup. As in the case of a linear *RLC* circuit, the positive real part $\sigma = -G_T/2C$ can be expressed in terms of the quality factor $Q = C\omega_o/G$ of the linear part of the circuit as $\sigma = -\omega_o G_T/2GQ$. Thus, the duration of the startup transient depends on the quality factor and on the ratio between the total conductance G_T (with negative sign) and the load conductance G. The startup transient will be shorter for larger ratio G_T/G and smaller quality factor Q of the resonant circuit, which implies larger $\sigma > 0$. As the oscillation amplitude increases, the actual nonlinearity of the total conductance will give rise to continuous variation of σ, which must take a zero value at steady state.

The initial exponential growth of the oscillation amplitude is in agreement with the fact that for $v \cong 0$, the damping term $\mu(v) = (a + G + 3bv^2)/C$ is nearly constant and given by $\mu = (a + G)/C < 0$ and delivers energy continuously to the incipient oscillatory solution. Note, however, that this linearized analysis is valid as long as $|v(t)|$ is small enough for the linearization of $i(v)$ about the dc solution to be accurate. For not so small $|v(t)|$, the damping term $\mu(v)$ will no longer be constant and the oscillation amplitude will start to grow more slowly than the exponential prediction, until it reaches a constant value at the steady-state regime. None of this can be predicted with the linearization about the dc solution and the pole analysis. Evolution of the oscillatory solution to its steady-state regime has to be determined through numerical integration.

The results of the numerical integration of (1.10) are shown in Fig. 1.2, where the node voltage amplitude $|v(t)|$ and the associated evolution of the damping term $\mu(v) = [a + G + 3bv^2(t)]/C$ are represented. For small-signal $|v(t)|$, the damping term is nearly constant and negative, with the value $\mu(0) = (a + G)/C$. This negative damping term is responsible for the initial exponential growth of the oscillation amplitude as $e^{-[\mu(0)]/2t}$. As this amplitude increases, the nonlinearity of $\mu(v)$ starts to be noticeable. The nonlinear component of $\mu(v)$, given by $3bv^2(t)/C$, is always positive since $b > 0$, and constitutes a positive contribution to the damping term. For smaller amplitude $|v(t)|$, the damping term will be more negative than for larger amplitude $|v(t)|$, so more energy will be delivered to the oscillatory solution by the active element. Note that the damping term has oscillatory variation, as it is a function of the periodic $v(t)$. This can be seen in Fig. 1.2. The local

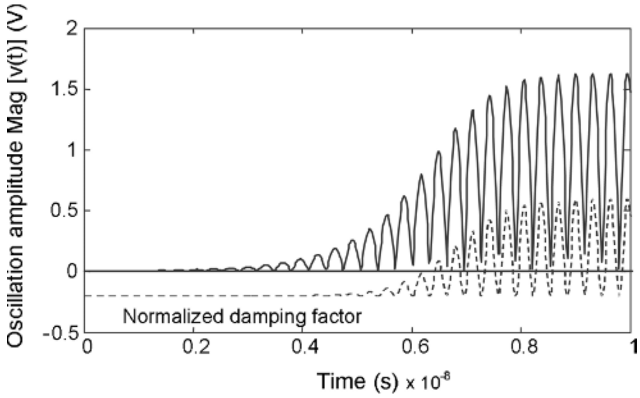

FIGURE 1.2 Analysis of the second-order oscillator of Fig. 1.1. Nonlinear equation (1.10) has been integrated for initial conditions different from $v = 0$ and $dv/dt = 0$. Both $|v(t)|$ and the normalized nonlinear term $(a + G + 3bv^2)/C$ have been represented.

maxima of $\mu(v)$ correspond to the local maxima of $|v(t)|$, and the local minima (most negative values) to the local minima of $|v(t)|$. The local maxima of $\mu(v)$ increase with $|v(t)|$ until steady state is reached. In steady state, both $v(t)$ and the damping term $\mu(v) = [a + G + 3bv^2(t)]/C$ exhibit periodic oscillation. As can be seen, the cubic nonlinearity provides a good model of the physical reduction of the device negative conductance when increasing the voltage amplitude across its terminals. This is why it is often chosen for a simple mathematical description of the oscillator behavior.

The circuit capability to self-sustain a steady-state oscillation is explained as follows. For small $|v(t)|$ during the oscillation period, the damping term $\mu(v)$ is negative (Fig. 1.2), so the energy delivered by the active element exceeds the resistor dissipation and makes $|v(t)|$ grow again. For large $|v(t)|$, a positive damping term is obtained and the dissipation exceeds the energy delivery, which makes $|v(t)|$ decrease. This mechanism allows sustaining the periodic oscillation with perfect balance between energy pumped in and energy dissipated over one cycle. Unlike the situation for a conservative system, with no energy dissipation at any time during the oscillation period, there is energy dissipation in the fraction of the oscillation period with $\mu(v) > 0$. Except in the case of coexistence of stable solutions (which has not yet been considered), the oscillation amplitude and frequency are independent of initial conditions. They are determined solely by the nonlinear characteristic of the damping term and the circuit topology and component values. Thus, for a system to exhibit sustained oscillation, it must be nonlinear and nonconservative.

Due to the nonexplicit time dependence of the differential equations describing an autonomous circuit, the time integration from different values at the same initial time t_o gives rise to time-shifted steady-state waveforms. This is illustrated in Fig. 1.3a, where different initial conditions have been considered in the time-domain integration of equation (1.10). The initial conditions are not known by the designers, as they come from noise or fluctuations at the experimental stage. Assuming that the voltage waveform $v(t)$ is a solution of (1.10), any time-delayed version of this voltage waveform $v(t - \tau)$ will be also a solution of (1.10). This is easily verified by defining the new time variable $t' = t - \tau$ and introducing $v(t')$ in (1.10). Note that the shape and period of the waveform are independent of these initial conditions. They satisfy the mathematical conditions for the self-sustained oscillation with zero net energy consumption. Nonautonomous circuits such as amplifiers and frequency multipliers are ruled by differential equations having coefficients with explicit time dependence. As an example, consider the parallel connection of an independent current generator $i_g(t)$ to a parallel RLC resonator. This circuit is governed by the linear equation $\ddot{v}(t) + G\dot{v}(t)/C + 1/(LC)v(t) - (di_g(t)/dt)/C = 0$, with the independent term $di_g(t)/dt$. This independent term establishes a time reference, so all the solutions obtained integrating the equations from different values v_o at the same initial time t_o converge to the same steady-state waveform. An example is shown in Fig. 1.3b, where the equations of a nonautonomous circuit have been integrated from totally different initial conditions $t = 0$, $v_o = -1V$, and $t = 0$, $v_o =$

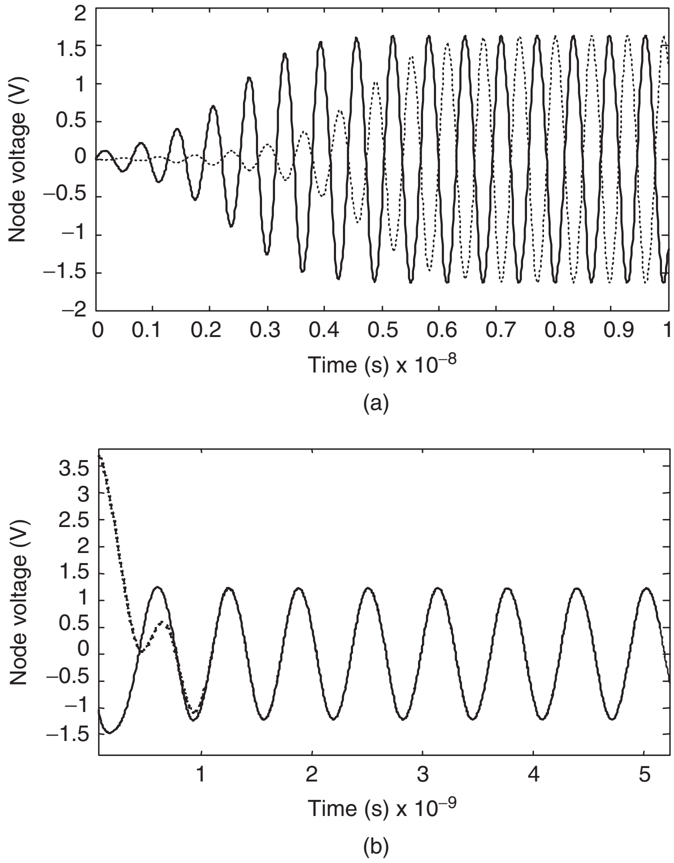

FIGURE 1.3 Time-domain integration of differential equations describing an autonomous and a forced circuit. (a) Integration of the nonlinear differential equation (1.10) describing the oscillator of Fig. 1.1, from different initial values at $t_o = 0$. This gives rise to time-shifted steady-state waveforms. (b) Integration of a forced circuit from different voltage values v_o at $t_o = 0$. The same waveform, without a time shift, is obtained for all the initial values.

4 V, obtaining the same steady-state waveform without a time shift. Compare with the situation shown in Fig. 1.3a.

Although the explanation above was based on a simple second-order nonlinear circuit, all the major conclusions are applicable to practical oscillators of much higher complexity. In a free-running oscillator, the oscillatory solution always coexists with a dc solution. When the dc generators are first powered on, the oscillation has not built yet up and the circuit is at the dc solution. In a well-designed oscillator, the dc solution is unstable and contains a pair of complex-conjugate poles on the right-hand side of the complex plane. This is due to the imbalance between the energy delivered by the active element and the energy dissipated by the resistors at the frequency of the poles. The unstable poles will give rise to oscillation startup under any small perturbation. For the circuit to be able to exhibit a self-sustained oscillation, the negative-resistance device must be nonlinear and thus sensitive to the oscillation amplitude. In the steady-stage regime, energy is alternately consumed and delivered during the oscillation period, so the system must be nonconservative (i.e., it must contain resistive elements).

1.3 IMPEDANCE–ADMITTANCE ANALYSIS OF AN OSCILLATOR

As noted in Section 1.2, an oscillator is ruled by a set of nonlinear differential equations that can only be accurately solved using numerical techniques. Time-domain analysis makes it possible to obtain the entire time evolution of the circuit variables, including transient and steady state. In frequency-domain analysis, each variable is represented by a Fourier series $v(t) = \sum_k V_k e^{jk\omega t}$, with constant complex coefficients V_k and constant ω, so only the steady-state regime can be determined. Note that due to the circuit nonlinearity, the saturation of the waveform amplitude gives rise inherently to some harmonic content. Due to the orthogonally of the Fourier basis, the circuit will be described by a set of equations, one at each harmonic frequency, relating the harmonic coefficients of the circuit variables. When limiting the analysis to one harmonic term (i.e., when assuming a sinusoidal oscillation), it will be possible to obtain meaningful analytical expressions for the oscillation frequency and amplitude. In what follows, an admittance–impedance analysis of the oscillator circuit is presented, assuming a sinusoidal waveform. This frequency-domain analysis offers a different viewpoint of the oscillator circuit and allows the derivation of useful design criteria. Note that the accuracy of the sinusoidal approach will be higher for a larger quality factor Q of the resonant circuit, due to the high attenuation of the harmonic frequencies.

As shown in Section 1.2, in a free-running oscillator, a negative-resistance element delivering energy to a resonator and a load or utilization resistance are necessary for oscillation buildup from the noise level. This negative resistance can be obtained from negative-resistance diodes, such as tunnel, Gunn, or Impatt [5], or by using transistors, which generally requires the introduction of suitable feedback between the two transistor ports [13,14]. Figure 1.4 shows a simple representation of an oscillator circuit. There are no periodic generators and the circuit is divided into a nonlinear block, providing the negative resistance, and a linear block, containing the output load. This block division is straightforward for a diode-based oscillator such as the one depicted in Fig. 1.1. For a transistor-based oscillator, the block division is more involved. In single-ended oscillators, the sketch shown in Fig. 1.5 is often used. Since there are no external RF sources, one of the transistor ports is ended by a given impedance (the termination), used only to obtain negative resistance at the other port. To avoid power loss, a reactive termination is often preferred. In addition to a proper choice of this termination and suitable biasing,

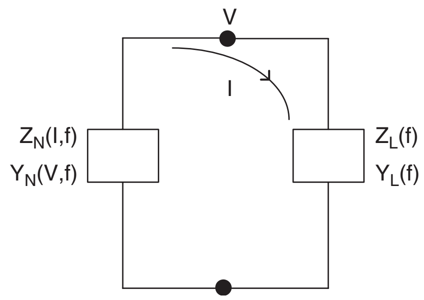

FIGURE 1.4 One-port representation of a free-running oscillator.

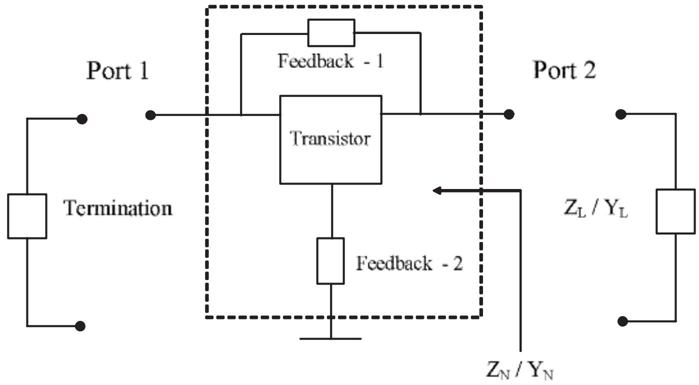

FIGURE 1.5 Schematic representation of a transistor-based oscillator. A one-port description is used for the block, consisting of the transistor, its termination at port 1, and the feedback elements.

the transistor often requires an additional parallel or series feedback network to exhibit negative resistance about the oscillation frequency that is desired [15]. The transistor is loaded with an impedance Z_L containing the resistive load from which the oscillation output power is extracted.

A one-port definition of the subcircuit, consisting of the transistor, together with its termination at the other port and the series or parallel feedback network (the nonlinear block), is often assumed at the design stage. This allows modeling the transistor-based oscillator as in Fig. 1.4. Note that although this block contains nonlinear and linear elements, it is globally nonlinear. By taking into account the boundary condition imposed by the transistor termination, the admittance of the nonlinear block can be expressed as a function of the voltage V at the output port. This admittance will also depend on the frequency ω, due to the existence of reactive elements inside the nonlinear block. Thus, it is possible to define the function $Y_N(V, \omega)$. In turn, the load circuit exhibits the linear admittance $Y_L(\omega)$. This type of representation is not sufficient for an accurate analysis of transistor-based oscillators, which actually depend on the two state variables of the nonlinear model of the transistor (e.g., the gate-to-source voltage and the drain-to-source voltage of FET transistors). However, it will be very helpful for a general understanding of the oscillator behavior and for oscillator design.

Next, we analyze an oscillator in terms of general admittance–impedance functions from a single observation port, following Fig. 1.4.

1.3.1 Steady-State Analysis

When applying Kirchhoff's laws to the circuit of Fig. 1.4, either a series or a parallel connection may be considered between the linear and nonlinear blocks. For a series connection, an impedance analysis is carried out, in terms of the branch current, as this provides simpler equations. For a parallel connection, an admittance analysis is carried out in terms of the node voltage. Depending on the actual circuit topology, one or another analysis may be more convenient. Here, only the admittance analysis is considered. One based on an impedance description, in terms of the loop current, is totally analogous.

A steady-state oscillation with a sinusoidal node voltage $v(t) = V_o \cos(\omega_o t + \phi)$ will be assumed initially. In contrast to forced circuits, the fundamental frequency ω_o of the solution depends on the values of the circuit elements, bias sources, and other parameters, since it is not delivered to the circuit by an external source. Due to this fact, the oscillation frequency will be an unknown to be determined. Application of Kirchhoff's laws at the frequency ω_o provides the following complex equation, which relates the total branch current at ω_o to the node voltage at the same frequency:

$$Y_T(V, \omega_o)Ve^{j\phi} = [Y_N(V, \omega_o) + Y_L(\omega_o)]Ve^{j\phi} = 0 \qquad (1.12)$$

where Y_L is the linear block admittance and Y_N the nonlinear block admittance, which, in general, will be frequency dependent, as it may contain reactive elements. Note that the nonlinear admittance function $Y_N(V, \omega_o)$ does not depend on the phase value of the periodic exciting signal $Ve^{j\phi}$. This is understood by comparison with the behavior of any circuit forced with a sinusoidal generator. A change $\Delta\phi$ in the phase of the periodic exciting source simply gives rise to the same phase increment in all the circuit variables. Thus, the solution phase shift with respect to this exciting source remains the same as before the application of $\Delta\phi$.

By inspecting (1.12), it is clear that at least two solutions coexist in the oscillator circuit. One is given by $V = 0$. This solution, with zero oscillation amplitude, is in fact the dc solution discussed in Section 1.2, for which any circuit with no time-varying external sources can be solved. The other solution is obtained from the nonlinear equation $Y_T(V_o, \omega_o) = 0$ and corresponds to a sinusoidal voltage $v(t) = \mathrm{Re}\{V_o e^{j(\omega_o t + \phi)}\}$, as assumed when writing the admittance equation (1.12). Thus, the steady-state oscillation equation is written

$$Y_T(V_o, \omega_o) = [Y_N(V_o, \omega_o) + Y_L(\omega_o)] = 0 \qquad (1.13)$$

The complex equation (1.13) can be split into two real equations in two real unknowns V_o and ω_o by considering the real and imaginary parts of Y_T: $\text{Re}[Y_T] = 0$ and $\text{Im}[Y_T] = 0$. It is actually the voltage dependence of $Y_N(V, \omega)$ (i.e., the circuit nonlinearity) which makes it possible to solve $Y_T = 0$ for the constant oscillation amplitude V_o. Note that any phase value ϕ provides a valid solution, as Y_T does not depend on ϕ. This is due to the absence of an independent periodic generator at the same frequency ω_o, establishing a phase reference. When this is the case, the coefficients of the differential equations ruling circuit behavior have no explicit time dependence, so any arbitrary time shift of the periodic waveform provides another solution. In the frequency domain, the different time shifts correspond to different phase origins, as $\Delta\phi = \omega_o(\tau' - \tau)$.

The complex equation $Y_T(V_o, \omega_o) = 0$ is in total agreement with the conclusions of Section 1.2. The first real equation, $\text{Re}[Y_T] = 0$, implies balance between average power delivered and consumed, as resulting from $\frac{1}{T}\int_0^T v(\lambda)i(\lambda)d\lambda = \frac{1}{2}\text{Re}[Y_T]V_o^2$, with T being the oscillation period $T = 2\pi/\omega_o$. The second equation, $\text{Im}[Y_T] = 0$, implies the existence of a resonance at the oscillation frequency.

The next objective is to obtain the nonlinear admittance function $Y_N(V, \omega)$, which constitutes the model of the active element in the approximate oscillator analysis. The model is based on use of the describing function. For a sinusoidal describing function [16], the input signal is represented by a sinusoid. Considering the nonlinearity $i(t) = i(v(t))$, the describing function will provide an admittance model $Y_N(V)$, depending on the voltage amplitude V. To obtain a sinusoidal describing function, the voltage $v(t) = V\cos(2\pi f_o t + \phi)$ is introduced into the nonlinearity $i(v)$, obtaining the ratio between the first harmonic of the resulting current and the voltage phasor $\frac{V}{2}e^{j\phi}$:

$$Y_N(V) = \frac{i(v)|_f}{Ve^{j\phi}} = \frac{2}{T}\frac{\int_0^T i(v(t))e^{-j\omega_o t}\,dt}{Ve^{j\phi}} \tag{1.14}$$

where $T = 2\pi/\omega_o$. Clearly, Y_N depends on the amplitude V of the voltage introduced but not on its phase ϕ, in agreement with previous discussions. To see this more clearly, a phase shift $\Delta\phi$ will be considered. This phase shift can be represented as $\Delta\phi = -\omega_o\tau$. Next, the variable change $t' = t - \tau$ is performed in (1.14), which provides

$$Y_N(V) = \frac{2}{T}\frac{\int_0^T i(v(t'))e^{-j\omega_o t'}e^{-j\omega_o\tau}\,dt'}{Ve^{j\phi}e^{-j\omega_o\tau}} \tag{1.15}$$

So the same nonlinear admittance $Y_N(V)$ is obtained. In polynomial nonlinearities, another way to obtain the same result would be to place $v(t) = V/2e^{j(\omega_o t+\phi)} + V/2e^{-j(\omega_o t+\phi)}$ into the nonlinear function $i(v)$, expand the function, and divide the resulting harmonic term at $j\omega_o$ by $V/2e^{j(\omega_o t+\phi)}$.

To illustrate the admittance analysis will be applied to the parallel resonance oscillator of Fig. 1.1. Using (1.14), the sinusoidal describing function associated with the constitutive relationship $i(v) = av + bv^3$ (with $a < 0$ and $b > 0$) is given by $Y_N(V) = a + 3/4bV^2$. From an inspection of this expression, the small-signal conductance is $Y_N(0) = a$, with a negative value. Because $b > 0$, the nonlinear conductance decreases with the voltage amplitude across the nonlinear element. Note that this physical behavior of the active element leads to an increase in the damping ratio $\mu(v)$ with the amplitude $|v(t)|$, discussed in Section 2.2, which allows us to reach a constant steady-state oscillation amplitude. Replacing the describing function obtained in (1.13) yields the following equations:

$$\begin{aligned} a + \frac{3bV^2}{4} + G_L = 0 \\ C\omega_o - \frac{1}{L\omega_o} = 0 \end{aligned} \tag{1.16}$$

Resolving equation (1.16), the oscillation amplitude is $V_o = \sqrt{(-a - G_L)/(3b/4)}$ $= 1.64$ V and the oscillation frequency is $f_o = 1/(2\pi\sqrt{LC}) = 1.59$ GHz. From the expression of the oscillation amplitude, it is clear that the small-signal conductance $Y_N(V \cong 0) = a$ must have a larger absolute value than the positive linear conductance G_L to obtain a steady-state oscillation. Otherwise, the root of a negative value is obtained in $V_o = \sqrt{(-a - G_L)/(3/4b)}$. This agrees with the results of Section 1.2. The total circuit conductance G_T is negative in small-signal mode but equal to zero in the steady state, as $\text{Re}[Y_T(V_o)] = 0$. To understand this, note that the negative conductance exhibited by the active element decreases with the voltage amplitude, as gathered from $Y_N(V) = a + 3/4bV^2$. The oscillation reaches steady state at the voltage amplitude for which $|Y_N(V_o)| = \text{G}_L$.

It must be emphasized that the steady-state analysis (1.16) is very simplified, as it is limited to a single harmonic component. From (1.16), the oscillation frequency is given by the resonance frequency of the LC resonator. A time-domain simulation would show that depending on the quality factor, the oscillation frequency can differ noticeably from the resonance frequency. The one-harmonic limitation of (1.16) prevents prediction of this effect. To discuss the influence of the harmonic content, a voltage expression $v(t) = V_1 \cos \omega t + V_3 \cos(3\omega t + \phi)$ will be considered. In this expression it has been taken into account that in the circuit being analyzed with no dc sources, no dc or even harmonic components are generated by the cubic nonlinearity $i(v)$. To obtain the first- and third-harmonic admittance functions $Y_{N1}(V_1, V_3, \phi)$ and $Y_{N3}(V_1, V_3, \phi)$, the waveform $v(t)$ is introduced into the transfer characteristic $i(v)$. The admittance functions are calculated as

$$\begin{aligned} Y_{N1} &= \frac{I_1(V_1, V_3, \phi)}{V_1} \\ Y_{N3} &= \frac{I_3(V_1, V_3, \phi)}{V_3 e^{j\phi}} \end{aligned} \tag{1.17}$$

Kirchhoff's laws are written at the first- and third-harmonic components, which provides a two-complex-equation system $Y_{T1} = 0$ and $Y_{T3} = 0$ in the four unknowns V_1, V_3, ϕ and, ω. Solving this system, the oscillation frequency does not exactly agree with the resonance frequency $1/\sqrt{LC}$. This is because unlike the case of the nonlinear admittance function $Y_N(V, \omega)$, in one-harmonic analysis, the imaginary part of Y_{N1} is different from zero. As an example, for $L = 4$ nH and $C = 2.5$ pF, $Y_{N1} = -0.01 + j0.002\Omega^{-1}$ and $Y_{N3} = -0.02 - j0.063\Omega^{-1}$, the oscillation frequency is $f_o = 1.52$ GHz instead of $1/(2\pi\sqrt{LC}) = 1.59$ GHz. The high discrepancy is due to the extremely low quality factor Q of the RLC resonator for these element values. This discrepancy is higher for a smaller quality factor Q, due to the lower filtering of the harmonic components $n\omega_o$ with $n > 1$.

1.3.2 Stability of Steady-State Oscillation

As already pointed out, for a given mathematical solution to be observable physically, it must be stable or robust versus small perturbations. Earlier we considered only the stability of the dc solution that coexists with steady-state oscillation. For the steady-state oscillation of (1.13), given by $v_o(t) = \mathrm{Re}[V_o e^{j\omega_o t}]$, to be stable, the circuit must return to it exponentially under any small perturbation. To verify mathematically if this is the case, a small perturbation is applied at a given time instant t_o. This takes the circuit out of the steady state. However, because the perturbation is small at the beginning of the transient being generated, the circuit variables cannot differ much from their values in a steady-state regime. In the stability analysis proposed by Kurokawa [17], small variations are assumed in both the oscillation amplitude and frequency. The perturbation applied gives rise to time-varying amplitude, which can be expressed as $V_o + \Delta V(t)$. In turn, the frequency takes the time-varying value $\omega_o + \Delta\omega(t)$. Before continuing, the reader should be warned that the assumption of a small frequency variation $\Delta\omega(t)$ limits the validity of this analysis technique. This is because the small perturbation can actually have any frequency, not necessarily one fulfilling $\Delta\omega \ll \omega_o$. As an example, a common instability phenomenon is the onset of a subharmonic component at $\omega_o/2$, generated from a low-amplitude perturbation that clearly does not fulfill the assumption $\Delta\omega \ll \omega_o$. The stability analysis under the assumption $\Delta\omega \ll \omega_o$ is also called *quasistatic*. Despite of this limitation, the stability conditions obtained are extremely helpful use at the oscillator design stage.

Due to the use of instantaneous perturbation, the oscillator is no longer in steady state. The perturbed frequency is written as $j\omega_o + s$, where s is a complex frequency increment. Because the perturbation is small, the perturbed oscillation can be analyzed by performing a first-order Taylor series expansion of the total admittance function about the free-running solution (V_o, ω_o), fulfilling $Y_{To} = 0$. This provides the equation

$$\begin{aligned} Y_T[V_o + \Delta V(t)]e^{j\phi(t)} = {} & \frac{\partial Y_{To}}{\partial V}\Delta V(t)[V_o + \Delta V(t)]e^{j\phi(t)} \\ & + \frac{\partial Y_{To}}{\partial j\omega}\frac{d[(V_o + \Delta V(t))e^{j\phi(t)}]}{dt} = 0 \end{aligned} \tag{1.18}$$

with the increment s giving rise to a time derivation in the slow time scale of the perturbed voltage. After performing this derivation, equation (1.18) is written

$$\frac{\partial Y_{To}}{\partial V}\Delta V(t)V_o \mathrm{e}^{j\phi(t)} + \frac{\partial Y_{To}}{\partial \omega}[\dot{\phi}(t)V_o \mathrm{e}^{j\phi(t)} - j\Delta\dot{V}(t)\mathrm{e}^{j\phi(t)}] = 0 \tag{1.19}$$

where higher-order terms have been neglected. Dividing by $V_o e^{j\phi(t)}$, equation (1.19) can be simplified to

$$\frac{\partial Y_{To}}{\partial V}\Delta V(t) + \frac{\partial Y_{To}}{\partial \omega}\left[-j\frac{\Delta \dot{V}(t)}{V_o} + \Delta\omega_o(t)\right] = 0 \tag{1.20}$$

where $\dot{\phi}(t)$ has been renamed $\dot{\phi}(t) = \Delta\omega_o(t)$. The complex nature of the frequency increment in (1.20) is due to the fact that the oscillator solution has been kicked out of the steady-state solution $V_o e^{j\omega_o t}$, so the amplitude must have an exponential variation associated with the imaginary term $-j[\Delta\dot{V}(t)/V_o]$. Splitting (1.20) into real and imaginary parts, the following linear system is obtained:

$$\begin{aligned} \frac{\partial Y^i_{To}}{\partial \omega}\frac{1}{V_o}\Delta\dot{V}(t) + \frac{\partial Y^r_{To}}{\partial \omega}\Delta\omega_o(t) &= -\frac{\partial Y^r_{To}}{\partial V}\Delta V(t) \\ -\frac{\partial Y^r_{To}}{\partial \omega}\frac{1}{V_o}\Delta\dot{V}(t) + \frac{\partial Y^i_{To}}{\partial \omega}\Delta\omega_o(t) &= -\frac{\partial Y^i_{To}}{\partial V}\Delta V(t) \end{aligned} \tag{1.21}$$

where the superscripts r and i indicate real and imaginary parts, respectively. Note that all the coefficients of (1.21) are constant and constitute the derivatives of the nonlinear function $Y_T(V, \omega)$, calculated at the free-running oscillation point, given by V_o and ω_o. By solving for $\Delta\dot{V}(t)$ in terms of $\Delta V(t)$, the following relationship is obtained:

$$\begin{aligned} \frac{d\Delta V(t)}{dt} &= \frac{-\left[(\partial Y^r_{To}/\partial V)(\partial Y^i_{To}/\partial\omega) - (\partial Y^i_{To}/\partial V)(\partial Y^r_{To}/\partial\omega)\right] V_o}{|\partial Y_{To}/\partial\omega|^2}\Delta V(t) \\ &= \sigma_o \Delta V(t) \end{aligned} \tag{1.22}$$

where the constant coefficient has been called σ_o. The amplitude increment $\Delta V(t)$ evolves according to $\Delta V(t) = \Delta V_o e^{\sigma_o t}$, where ΔV_o depends on the value of the initial instantaneous perturbation. The exponential reaction to small perturbations was also shown in Section 1.2 in the case of perturbed dc solutions. For the oscillation to be stable, the perturbation must vanish exponentially in time. Thus, the coefficient in (1.22) must fulfill $\sigma_o < 0$. Because the denominator of σ_o, given by $|\partial Y_{To}/\partial\omega|^2$, is necessarily positive, the stability condition is given by [17]

$$S = \frac{\partial Y^r_{To}}{\partial V}\frac{\partial Y^i_{To}}{\partial \omega} - \frac{\partial Y^i_{To}}{\partial V}\frac{\partial Y^r_{To}}{\partial \omega} > 0 \tag{1.23}$$

Expression (1.23) is very useful for oscillator design. Due to the physical reduction in negative resistance with signal amplitude, the factor $\partial Y^r_{To}/\partial V$ will generally have a positive sign. Then a sufficiently high value of $\partial Y^i_{To}/\partial\omega$ facilitates the oscillation stability. Actually, the second term, $(\partial Y^i_{To}/\partial V)(\partial Y^r_{To}/\partial\omega)$, is often small compared to the first term, which is explained as follows. The real part of Y_T usually has a small frequency dependence, because the dependence comes from the reactive elements. On the other hand, the imaginary part of Y_T usually has a small amplitude dependence, because the nonlinearities responsible for the free-running oscillation are usually voltage-controlled current sources.

The duration of the transient response to perturbation is considered next. Assuming that $\partial Y_{To}^i/\partial\omega \gg \partial Y_{To}^r/\partial\omega$, the denominator in (1.22) can be approached $|\partial Y_{To}/\partial\omega|^2 \cong (\partial Y_{To}^i/\partial\omega)^2$. A commonly used definition for the oscillator quality factor is $Q = (\omega_o/2G_L)(\partial Y_{To}^i/\partial\omega)$, with the derivative being evaluated at the oscillation frequency and G_L being the passive conductance. Thus, the coefficient σ_o is inversely proportional to the quality factor, meaning that the transient reaction to the perturbation will be slower for larger Q. A similar conclusion had been obtained in Section 1.2 for the oscillation startup transient. In the case of a stable steady-state oscillation, the system will return more slowly to this steady-state regime.

The nonlinear circuit of Fig. 1.1 fulfills the stability criterion. The real part of the total admittance is $\text{Re}[Y_T(V)] = a + 3/4bV^2 + G_L$, so the amplitude derivative in the first term is given by $\text{Re}[\partial Y_{To}/\partial V] = 3/2bV_o$. Note that V_o is the oscillation amplitude, defined as positive, so the term $3/2bV_o$ necessarily takes a positive value. On the other hand, the derivative of the imaginary part of the total admittance function, evaluated at the free-running oscillation, is given by $\text{Im}[\partial Y_{To}/\partial\omega] = 2C$. In turn, the derivatives in the second term of (1.23) are equal to zero. Thus, the condition $S > 0$ is satisfied and the oscillation is stable. Under any small perturbation, the amplitude increment of the perturbed oscillation evolves according to $\Delta V(t) = \Delta V_o e^{\sigma_o t}$, with $\sigma_o = -(3bV_o^2/4)(\omega_o/G_L Q)$ and $Q = C\omega_o/G_L$.

Note that condition (1.23) was derived under a quasistatic approximation, assuming a very small value of the perturbation frequency $\Delta\omega \ll \omega_o$ and using a single observation port. As already stated, this analysis is helpful for oscillation design, as it provides criteria for *likely* stable behavior from admittance functions accessible to the designer. However, the design procedure should be complemented by a rigorous verification of oscillator stability without the limiting assumption $\Delta\omega \ll \omega_o$ and taking into account the actual multidimensional nature of the circuit equations. Note that some unstable resonances may be hidden when inspecting the total impedance or admittance from a single observation port. At the end of the section, some hints about the basis for a more general stability analysis in the frequency domain are provided.

1.3.3 Oscillation Startup

As already known, stable oscillation, with steady-state amplitude V_o and frequency ω_o, must grow from the noise level. This growth is due to the instability of the dc solution, which under any small perturbation gives rise to an oscillatory transient. As shown in Section 1.2, the envelope of the initial transient follows an exponential law. From a certain oscillation amplitude, linearization is no longer valid and the device nonlinearity gives rise to saturation of the oscillation amplitude. When using admittance analysis, the instability of the dc solution is generally associated with fulfillment of the following conditions:

$$\begin{aligned} Y_T^r(V \cong 0, \omega'_o) &< 0 \\ Y_T^i(V \cong 0, \omega'_o) &= 0 \\ \frac{\partial(Y_T^i(V \cong 0, \omega'_o))}{\partial\omega} &> 0 \end{aligned} \tag{1.24}$$

where $V \cong 0$ refers to the admittance function evaluated in small-signal mode. Note that an analysis of conditions (1.24) constitutes a stability analysis of this dc solution. Actually, the small-signal admittance $Y_T(V \cong 0, \omega)$ depends on the dc solution about which the active element is linearized. That is, for different bias points, different $Y_T(V \cong 0, \omega)$ functions are obtained, fulfilling conditions (1.24) or not fulfilling them. The main point of conditions (1.24) is that they help in synthesizing a pair of complex-conjugate poles with positive σ at the desired oscillation frequency ω'_o. As shown in Section 1.2, this pair of complex-conjugate poles should give rise to an oscillatory transient of growing amplitude. To understand the relationship between (1.24) and the poles of the dc solution, consider the introduction of a small-signal current source $I_{in}(s)$ in parallel at the observation port. The ratio between the node voltage $V(s)$ and the current delivered, $I_{in}(s)$, provides the closed-loop transfer function $Z(s)$. Assuming that no pole–zero cancellations occur, the poles of $Z(s)$ will agree with the roots of the characteristic function $P(s)$ associated with circuit linearization about the dc solution. A pair of complex-conjugate poles $\sigma \pm j\omega_o$ provides a contribution of the form $Z_p(s) = A\omega_o^2/(s^2 + \sigma^2 - 2s\sigma + \omega_o^2)$, with A a constant value. We will assume that this is the dominant contribution of the pole-residue expansion of $Z_p(s)$ [16] from the observation port. Replacing s with $j\omega$, the impedance function becomes $Z_p(\omega) = A\omega_o^2/(\sigma^2 + \omega_o^2 - \omega^2 - 2\sigma j\omega)$. The property sign $(d\phi/dx) = sign(d\tan(\phi)/dx)$ is fulfilled for any angle ϕ and independent variable x. In the case of the impedance function $\tan(ang(Z_p(\omega)) = 2\sigma\omega/(\sigma^2 + \omega_o^2 - \omega^2)$ for positive σ, the phase associated with $Z_p(\omega)$ has positive slope at the resonance frequency ω_o. The function $Z(\omega)$ agrees with the inverse of the total admittance analyzed, $Y_T(\omega) = Y_T^r(\omega) + jY_T^i(\omega)$. In terms of $Y_T(\omega)$, it is possible to write $\tan(ang(Z_p(\omega))) = -Y_T^i(\omega)/Y_T^r(\omega)$. Assuming a small frequency variation of $Y_T^r(\omega)$, a resonance of the form $Y_T^r(\omega_o) < 0$, $Y_T^i(\omega_o) = 0$, $\partial(Y_T^i(\omega_o))/\partial\omega > 0$ will give rise to a positive slope of the phase associated with $Z(\omega)$, corresponding to a pair of unstable complex-conjugate poles. For a rigorous determination of the dc solution poles, pole–zero identification techniques [11] should be applied to the closed-loop transfer function $Z(\omega)$.

The result on the positive slope $\partial(Y_T^i(\omega_o))/\partial\omega > 0$ is in agreement with the preceding discussion on the stability conditions of steady-state oscillation. As already stated, the second term of (1.23) usually has little influence on the S value. The imaginary part, $Y_T^i(\omega)$, contributed primarily by the linear elements, is not typically very dependent on the oscillation amplitude. Thus, achieving the resonance condition at the oscillation frequency desired $Y_T^i(V \cong 0, \omega'_o) = 0$, with positive slope $\partial(Y_T^i(V \cong 0, \omega_o')/\partial\omega > 0$, will facilitate stable oscillation at about ω_o'. Although small, there is usually a dependence of the susceptance Y_T^i on the signal amplitude. Therefore, the resonance frequency ω_o' under small-signal conditions will be similar to the oscillation frequency ω_o but generally not equal. In addition, the inherent nonlinearity of the oscillator circuit will generate a certain harmonic content that, as explained earlier, may give rise to a shift in the oscillation frequency.

The initial stage of oscillation startup will be ruled by the pair of unstable complex-conjugate poles $\sigma \pm j\omega$ of the dc solution, so the amplitude will grow according to $e^{\sigma t}$ from any small perturbation of this solution. The σ value is related linearly to $Y_T^r(\omega_o)$, fulfilling $Y_T^r(\omega_o) < 0$, and in general, σ will be more positive for larger absolute value $|Y_T^r(\omega_o)|$ [18]. This will imply a shorter initial transient. Actually, two different stages can be distinguished in the oscillation startup. In the initial stage, the oscillation amplitude is small and its variation can be predicted with circuit linearization about the dc solution. However, from a certain transient amplitude, the circuit will no longer be under small-signal conditions, and the real exponent σ will be different from the real part of the poles. In a simplified model it will exhibit an amplitude dependence $\sigma(V)$ coming from the amplitude dependence of the nonlinear conductance $G_N(V)$. The transient evolution depends on the function $\sigma(V)$. Usually, the positive exponent $\sigma(V)$ decreases monotonically to the value $\sigma = 0$, corresponding to steady state. However, in some cases, before reaching steady state, the positive σ increases, which is due to $G_N(V)$ becoming more negative versus V. After passing through a minimum, the conductance will increase (i.e., it will become less negative) until the steady-state condition $G_N(V) + G_L = 0$ is fulfilled. This type of behavior gives rise to an apparent delay in the startup transient as the amplitude growth becomes more noticeable for larger σ. It can be obtained in transistor-based oscillators that have power expansions of the nonlinear conductance of the form $G_N(V) = a_1 + a_2V^2 + a_3V^3 + \cdots$, with $a_1 < 0, a_2 < 0, a_3 > 0$ [18].

1.3.4 Formulation of Perturbed Oscillator Equations as an Eigenvalue Problem

For a better understanding of oscillator behavior, it will be convenient to formulate the perturbed oscillator equations as an eigenvalue problem. This will be done in terms of the amplitude and phase V and ϕ of the oscillator solution. The objective is to obtain a perturbed oscillator system of the form

$$\begin{bmatrix} \Delta\dot{V} \\ \Delta\dot{\phi} \end{bmatrix} = [M] \begin{bmatrix} \Delta V \\ \Delta\phi \end{bmatrix} \tag{1.25}$$

The matrix $[M]$ is derived directly from (1.21), taking into account that $\Delta\dot{\phi}(t) = \Delta\omega(t)$ and that $\partial Y_T/\partial\phi = 0$ due to the irrelevance with respect to the phase origin.

Thus, system (1.21) becomes

$$\begin{bmatrix} \Delta\dot{V}(t) \\ \Delta\dot{\phi}(t) \end{bmatrix} = \begin{bmatrix} \dfrac{1}{V_o}\dfrac{\partial Y_{To}^i}{\partial\omega} & \dfrac{\partial Y_{To}^r}{\partial\omega} \\ -\dfrac{1}{V_o}\dfrac{\partial Y_{To}^r}{\partial\omega} & \dfrac{\partial Y_{To}^i}{\partial\omega} \end{bmatrix}^{-1} \begin{bmatrix} -\dfrac{\partial Y_{To}^r}{\partial V} & \dfrac{\partial Y_{To}^r}{\partial\phi} \\ -\dfrac{\partial Y_{To}^i}{\partial V} & \dfrac{\partial Y_{To}^i}{\partial\phi} \end{bmatrix} \begin{bmatrix} \Delta V(t) \\ \Delta\phi(t) \end{bmatrix}$$

$$= \frac{\begin{bmatrix} -S & 0 \\ B & 0 \end{bmatrix}}{|\partial Y_{To}/\partial\omega|^2} \begin{bmatrix} \Delta V(t) \\ \Delta\phi(t) \end{bmatrix} \tag{1.26}$$

where the coefficient B is deduced directly from the matrix product. One of the eigenvalues of the matrix on the right-hand side is $\lambda_1 = \sigma_o$. The second eigenvalue, $\lambda_2 = 0$, is due to the irrelevance of the oscillator solution versus any phase shift. From basic linear algebra [19,20], the general solution of linear differential equation system (1.26) with constant coefficients is

$$\begin{bmatrix} \Delta V(t) \\ \Delta\phi(t) \end{bmatrix} = c_1 e^{\sigma_o t} \begin{bmatrix} 1 \\ -\dfrac{B}{SV_o} \end{bmatrix} + c_2 \begin{bmatrix} 0 \\ 1 \end{bmatrix} \tag{1.27}$$

Expression (1.27) evidences the irrelevance of the oscillator solution versus translations in the phase shift. Even if the oscillation is stable, which implies that $\sigma_o < 0$, the phase perturbation $\Delta\phi(t) = c_2$, with c_2 determined by the initial value, will remain in the steady-state solution. Equation (1.27) has a great conceptual interest. It enables the stability analysis of the steady-state oscillation, limited to two poles. Because one of the poles is necessarily zero, due to the autonomy of the free-running oscillator solution, the other pole must be real. In the case of an oscillator circuit with a single-resonant circuit, such as in Fig. 1.1, the system dimension (agreeing with the number of reactive elements) is $N = 2$. Thus, we only have two poles. The poles of the dc solution are complex-conjugate. The two poles of the steady-state oscillation are zero and real, respectively. The stability analysis derived by Kurokawa is limited to this real pole. In a "perfect" single-resonator oscillator, this should be sufficient. (A different problem is the limited accuracy of the analysis, considering only the fundamental frequency.) However, real-life oscillators, composed of several lumped reactive elements and distributed elements, will contain more poles. Therefore, the analysis from (1.27) will be unable to predict instabilities of the periodic solution coming from complex-conjugate poles or instabilities coming from two real poles on the right-hand side of the complex plane.

Clearly, for a free-running oscillator analyzed with one harmonic component and from a single observation port, the formulation above provides no advantage with respect to (1.23). However, when there is more than one state variable—two voltages, for instance, and/or several harmonic terms—phase variables will necessarily appear in the oscillator equations, as there is irrelevance with respect to the phase origin only. Then, use of a formulation of the type (1.26) will avoid a mixed system that includes the common frequency $\Delta\omega(t)$ in the set of circuit variables, together with the amplitudes and phases $\Delta V_n(t), n = 1$ to N, and $\Delta\phi_n(t), n = 2$ to N. An example of this type of formulation is the multiport stability analysis of a transistor-based oscillator, presented in the following. Other examples are shown throughout the book.

1.3.5 Generalization of Oscillation Conditions to Multiport Networks

As has been shown, in transistor-based oscillator design two of the transistor terminals are ended by particular immitance values, so it is possible to define the function $Y_N(V, \omega)$ depending only on the voltage amplitude at the reference plane. In turn, the load circuit exhibits the linear admittance $Y_L(\omega)$. Thus, fulfilment of the derived conditions (1.24) and (1.23) at the single-observation port considered will facilitate the stable oscillation. The same would be true for an impedance analysis in terms of the loop current. This is very helpful for circuit design, but does not fully guarantee stable operation of the oscillator circuit.

Alternatively, it is possible to use a generalization of the oscillation condition (1.13) in circuits containing multiport devices, which provides more accuracy and design flexibility. A brief explanation follows. The circuit is divided into two connected N-port networks, defined by their admittance matrixes $[Y_N(\overline{V}, \omega)]$ and $[Y_L(\omega)]$, with $\overline{V}$ the vector comprising voltage phasors at all N ports $\overline{V}^T$ with variables $[V_1, \ldots, V_N, \phi_1, \ldots, \phi_N]$. Note that the irrelevance with respect to the phase origin allows us to set any of the phase values to zero arbitrarily. Because there are no RF generators, the port voltages will be the same for the two connected multiport networks. The currents will have the same magnitude and opposite direction (or sign). Applying Kirchhoff's laws, it will be possible to write $([Y_N(\overline{V}, \omega)] + [Y_L(\omega)])\overline{V} = 0$. For $\overline{V}$ to differ from zero, the following oscillation condition must be fulfilled: $\det([Y_N(\overline{V}, \omega)] + [Y_L(\omega)]) = 0$. This condition generalizes (1.13) to multiport networks. Similar equations can be derived in terms of impedance or scattering matrixes.

The total admittance matrix of the circuit being considered can be defined as $[Y_T] = [Y_N(\overline{V}, \omega)] + [Y_L(\omega)]$. The circuit equations are written in matrix form as $\overline{H} = [Y_T]\overline{V} = 0$, the vector $\overline{V}$ comprising $[V_1, \ldots, V_N, \phi_1, \ldots, \phi_N]$. To balance the equation system, which must also be solved for ω, one of the phase variables is set arbitrarily to zero $\phi_k = 0$, which can be done due to the solution autonomy. For the quasistatic stability analysis of a given solution $\overline{V}_o^T = [V_1, \ldots, V_N, \phi_1, \ldots, \phi_N]$, the amplitudes and phases (except ϕ_k), as well as the frequency ω, must be perturbed about the steady-state values $\overline{V}_o^T$ and ω_o. Use of the frequency perturbation $\Delta\omega(t)$ leads to a mixed system, difficult to formulate in a compact manner. This can be avoided by considering the entire set of phase variables (including ϕ_k). Thus, the perturbations will be $\Delta V_1(t), \ldots, \Delta V_N(t), \Delta\phi_1(t), \ldots, \Delta\phi_N(t)$. The perturbed system will be derived by expanding the vector function $\overline{H}$ in a first-order Taylor series about the steady-state oscillation $(\overline{V}_o, \omega_o)$. Each H_k can be expressed as the product

$$H_k = [Y_T(\overline{V}, \omega)]_k^T \overline{V} \tag{1.28}$$

where $[Y_T]_k^T$ is a row matrix agreeing with the kth row of $[Y_T]$. The perturbed frequency will be given by $j\omega_o + s$. When performing the Taylor series expansion, it is taken into account that the multiplication by s acts like a time derivation of the perturbed variables, as shown in (1.18)–(1.20). Thus, the derivation of $[Y_T]_k^T$ with respect to frequency will give rise to terms of the form

$$\frac{\partial Y_{km}}{\partial \omega}\left(-j\frac{\Delta \dot{V}_m(t)}{V_m} + \Delta\dot{\phi}_m(t)\right)V_m e^{j\phi_m},$$

where k and m refer to the particular component of the kth row of the $[Y_T]$ matrix.

Using a development similar to the one in (1.18)–(1.20), each perturbed component H_k, with $k = 1, \ldots, N$, of the vector function $\overline{H}$ is given by

$$\begin{aligned}&\frac{\partial H_k}{\partial V_1}\Delta V_1(t) + \cdots + \frac{\partial H_k}{\partial V_N}\Delta V_N(t) + \frac{\partial H_k}{\partial \phi_1}\Delta\phi_1(t)\\ &+\cdots+\frac{\partial H_k}{\partial \phi_N}\Delta\phi_N(t) + \frac{\partial Y_{k1}}{\partial \omega_o}\left(-j\frac{\Delta\dot{V}_1(t)}{V_1} + \Delta\dot{\phi}_1(t)\right)V_1 e^{j\phi_1}\\ &+\cdots\frac{\partial Y_{kN}}{\partial \omega_o}\left(-j\frac{\Delta\dot{V}_N(t)}{V_N} + \Delta\dot{\phi}_N(t)\right)V_N e^{j\phi_N} = 0\end{aligned} \tag{1.29}$$

with all the derivatives calculated at the steady-state oscillation. In expression (1.29) In matrix form it is possible to write

$$\left[\frac{\partial \overline{H}}{\partial \overline{V}_o}\right]\Delta\overline{V} + \left[\frac{\partial \overline{H}}{\partial \overline{\phi}_o}\right]\Delta\overline{\phi} + \left[\frac{\partial \overline{H}}{\partial \omega_o}\right]\left(-j\frac{\Delta\dot{\overline{V}}(t)}{V} + \Delta\dot{\overline{\phi}}(t)\right) = 0 \tag{1.30}$$

where $\Delta\overline{V}$ is the vector of amplitude increments, $\Delta\overline{\phi}$ the vector of phase increments, and $\Delta\overline{V}/V$ the vector of normalized amplitude increments. This notation indicates that each voltage increment is normalized by the corresponding steady-state value. On the other hand, $\left[\partial\overline{H}/\partial\omega_o\right]$ is a square matrix with k and m elements of the form $(\partial Y_{km}/\partial\omega)V_m e^{j\phi_m}$. Rearranging equation (1.30) it is possible to obtain a system of the form

$$\begin{bmatrix}\Delta\dot{\overline{V}}\\ \Delta\dot{\overline{\phi}}\end{bmatrix} = [JH]\begin{bmatrix}\Delta\overline{V}\\ \Delta\overline{\phi}\end{bmatrix} \tag{1.31}$$

Due to the irrelevance with respect to variations in the phase origin, the Jacobian matrix [JH] above must be singular. This is due to the fact that the solution remains the same if the phases of all the state variables are incremented by the same amount, $\Delta\alpha$. This means that for any H component,

$$\frac{\partial H_k^x}{\partial \phi_1}\Delta\alpha + \frac{\partial H_k^x}{\partial \phi_2}\Delta\alpha + \cdots + \frac{\partial H_k^x}{\partial \phi_N}\Delta\alpha = \left(\frac{\partial H_k^x}{\partial \phi_1} + \frac{\partial H_k^x}{\partial \phi_2} + \cdots + \frac{\partial H_k^x}{\partial \phi_N}\right)\Delta\alpha = 0 \tag{1.32}$$

where the superscript x refers to either a real or an imaginary part. From (1.32) it is clear that all the columns in (1.31) are related linearly, so the matrix $[JH]$ must be singular, with one eigenvalue, $\lambda_1 = 0$. This is in agreement with the fact that we are using one unnecessary phase variable that could have been set arbitrarily to any value. For the perturbation to vanish in time, all the rest of the eigenvalues of the matrix $[JH]$ must have a negative real part. As can be seen, this analysis generalizes the one-port analysis of (1.26) to multiple ports.

Analysis using (1.31) allows more insight into circuit behavior than does one-port analysis (1.26), as more observation ports are being considered. Actually, the analysis reflected in (1.26) is limited to one real eigenvalue, whereas (1.31) can provide a total of N eigenvalues, which can be real or complex conjugate. However, the analysis remains quasistatic, as a small frequency perturbation $\Delta\omega \ll \omega_o$ is still considered. Despite this, the formulation presented is helpful for understanding purposes and will be applied to some oscillator systems later in the book. It is particularly useful in the case of oscillator circuits composed of two or more suboscillator elements, as N-push oscillators [13] used for multiplication of the oscillation frequency, or in coupled-oscillator systems [4] used for beamsteering in phased arrays. However, for ordinary oscillator design, use of the total admittance function derived from a single sensitive port is more practical and intuitive.

1.3.6 Design of Transistor-Based Oscillators from a Single Observation Port

One-port analysis of transistor-based oscillators from a single observation port yields a simple oscillator design. It requires only the choice of a sensitive observation port and identification of a nonlinear active block and linear load network. As stated earlier, the steady-state oscillation condition $Y_T = 0$ is fulfilled at any possible observation node. However, the results of startup evaluation using $Y_T(V \cong 0, \omega)$ will depend on this observation node and may also be different for admittance analysis in terms of the node voltage, or impedance analysis in terms of the loop current. To show this more clearly, assume a parallel connection of the two blocks in Fig. 1.4. The total admittance is $Y_T = (G_N(\omega) + G_L(\omega)) + j(B_N(\omega) + B_L(\omega))$. Now, assume a series connection. The total impedance is $Z_T = (G_N(\omega) + jB_N(\omega))^{-1} + (G_L(\omega) + jB_L(\omega))^{-1}$. Developing this impedance function, it is easily seen that if the startup conditions (1.24) are fulfilled in terms of parallel admittance at ω_o', the equivalent conditions in terms of series impedance might be fulfilled at a different frequency, ω_o', or might never be fulfilled. Similar problems occur when changing the analysis port. A pure LC parallel (series) resonance will give a positive slope for admittance (impedance) analysis. Therefore, attention should be paid to the actual form of resonance of the circuit being analyzed. However, the nonlinear block of a practical circuit will generally contain several reactive and resistive elements, so the function Y_N cannot be modeled in a simple manner. In agreement with the discussion in Section 1.3.3, negative conductance $Y_T^r < 0$ at the resonance frequency ω_o' with negative slope of the susceptance $\partial(Y_T^i(V \cong 0, \omega_o')/\partial\omega < 0$ does not generally represent instability in the dc solution. It is advisable to perform an impedance analysis or to change the observation port until a positive slope is obtained. As a rule, the one-port conditions are helpful at the design stage. Then, a rigorous stability analysis of the steady-state solution obtained should be carried out. The use of numerical pole–zero identification [11] or other techniques, such as Nyquist criterion [16,21,22], will be necessary.

The topology of the FET-based oscillator of Fig. 1.6 matches the schematic representation of Fig. 1.5. The capacitor C_T, connected between the gate terminal and ground, constitutes a reactive "termination" at port 1. The capacitor C_{fb}, connected between the source terminal and ground, provides series feedback to the transistor in use. C_T and C_{fb} are both calculated to obtain negative resistance at the analysis port (port 2), defined between the drain terminal and ground, at the oscillation frequency desired, $f_o = 5.0$ GHz. The load circuit, with equivalent admittance Y_L (or impedance Z_L), is calculated to ensure the fulfilment of oscillation startup conditions at this specified oscillation frequency. The introduction of a parallel inductance provides a negative slope versus frequency of the small-signal susceptance $\partial Y_T^i(V \cong 0, \omega_o)/\partial\omega < 0$. A series inductance $L = 0.2$ nH, fulfilling $Z_N^i(\omega_o) + L\omega_o = 0$, is introduced instead, which also reduces the harmonic content due to lowpass filtering. An equivalent load resistance seen from the drain terminal is chosen: $R_L = 20\ \Omega$. This value provides an excess negative resistance $Z_N^r(\omega_o) + 20 = -45\Omega$, which should allow oscillation startup. Note that in the design discussed, the resonator is formed by the capacitive output of the nonlinear block containing the transistor and the series inductance introduced. It is possible to reduce the influence of the nonlinear block on the resonance frequency by adding a series capacitance C_s (not represented in the circuit schematic), such that the resonance frequency is determined primarily by the linear load circuit. Provided that C_s is small enough, the total capacitance (including the one at the output of the nonlinear block C_{out}) will be $C_T = C_s C_{\text{out}}/(C_s + C_{\text{out}}) \cong C_s$, much smaller than the original value C_{out}. Because $L_s = 1/(C_s\omega_o^2)$ to maintain the same resonance frequency, the quality factor Q of the series load resonator must increase significantly, giving a high value for the derivative $\partial Y_T^i(\omega_o)/\partial\omega$. For example, in the design discussed, the introduction of a series capacitance $C_s = 0.1$ pF requires an inductance of $L = 10.1$ nH to maintain the oscillation frequency at $f_o = 5$ GHz, which are quite extreme values. Thus, a high-Q resonator should be used. The derivative increases from $9.10 \times 10^{-9}\Omega^{-1}\cdot$ S in the original design to $2.9 \times 10^{-8}\Omega^{-1}$S, which is more than three times the original value. As will be shown, this increase in the frequency selectivity is very convenient for a low phase noise design, as well as the lower sensitivity (for $C_T \cong C_s$) to active device elements, subject to noise fluctuations.

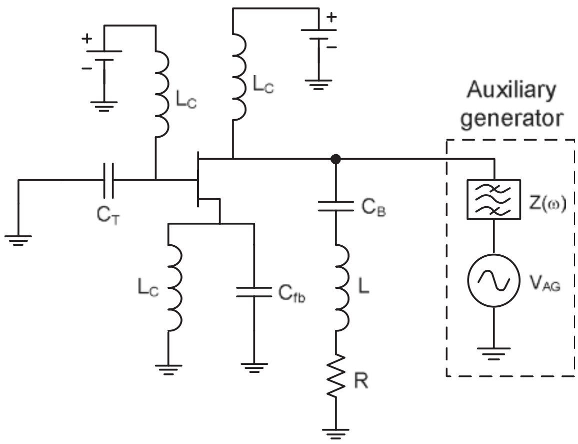

FIGURE 1.6 FET-based oscillator. The transistor is a NEC3210 biased at $V_{GS} = -0.25V$ and $V_{DS} = 2.25$ V. The capacitive termination C_T, together with the feedback capacitance C_{fb}, provide negative resistance at the drain port. The circuit topology matches the schematic representation of Fig. 1.5. The voltage auxiliary generator, connected in parallel at the transistor output node, is used for various analysis techniques presented in this chapter.

In the following, the load inductance $L = 0.2$ nH calculated originally will be considered instead of the high-Q load. This will allow a more general analysis of the oscillator dynamics, without the simplifications allowed by high-frequency selectivity. The circuit fulfills the oscillation startup conditions $Z_T^r(I \cong 0, \omega_o')) < 0$, $Z_T^i(I \cong 0, \omega_o') = 0$, and $\partial(Z_T^i(I \cong 0, \omega_o')/\partial\omega > 0$ at the frequency $f_o = 5$ GHz. Evaluation of the admittance function $Y_T(V \cong 0, \omega) = 1/[Z_N^r(\omega) + jZ_N^i(\omega)] + 1/(R_L + jL\omega)$ shows a shift in the resonance frequency to the value $f_o = 5.2$ GHz (see Fig. 1.7). The total small-signal conductance has the negative value $Y_T^r(V \cong 0, \omega_o) < 0$, and there is a positive slope versus frequency of the susceptance $\partial Y_T^i(V \cong 0, \omega_o)/\partial\omega > 0$, with an excess of negative conductance in small-signal mode. Thus, the startup conditions are fulfilled. The pole analysis of this circuit, with a numerical technique, provides the unstable pair of complex-conjugate poles $2\pi(0.48 \pm j5.012) \times 10^9\text{s}^{-1}$.

When using a commercial harmonic balance simulator, the nonlinear admittance function $Y_T(V, \omega)$ can be obtained with an auxiliary generator. The auxiliary generator is an artificial generator used for simulation purposes only. The voltage auxiliary generator at the frequency ω_{AG} is introduced in parallel at a circuit node (Fig. 1.6). Note that any voltage generator is a short circuit at any frequency different from the one that it delivers (ω_{AG}). To prevent the short circuiting of frequency components $\omega \neq \omega_{AG}$, the voltage generator is connected in series with an ideal bandpass filter, fulfilling $Z_f(\omega = \omega_{AG}) = 0$ and $Z_f(\omega \neq \omega_{AG}) = \infty$. The ratio between the current auxiliary generator current I_{AG} flowing into the circuit, and the voltage delivered, V_{AG}, provides the function $Y_{AG}(V_{AG}, \omega_{AG})$. This admittance function agrees with the total admittance $Y_T(V, \omega)$, depending on both the node

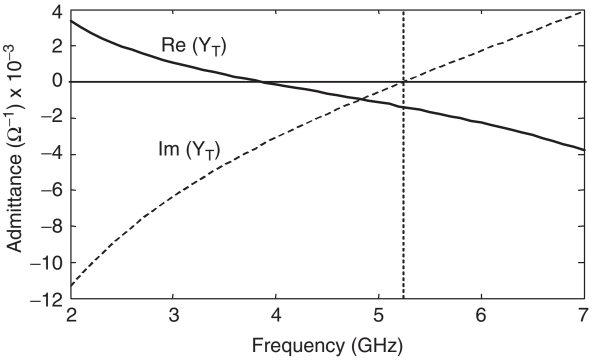

FIGURE 1.7 Small-signal admittance analysis of the FET-based oscillator of Fig. 1.6. There is excess negative conductance at the resonance frequency $f_o = 5.2$ GHz, so the startup of an oscillation at about this frequency can be expected for this particular design.

voltage amplitude $V = V_{AG}$ and the frequency $\omega = \omega_{AG}$ considered in all the preceding analyses. Thus, $Y_{AG} = Y_T$. An analogous procedure can be carried out to determine variations of the total impedance versus the branch current $Z_T(I, \omega)$. For this analysis, a current generator $I_{AG} = I$, at the frequency $\omega = \omega_{AG}$, is introduced in series at the circuit branch selected. To prevent open circuiting of frequency components $\omega \neq \omega_{AG}$, the current generator is connected in parallel with an ideal bandpass filter, fulfilling $Z_f(\omega = \omega_{AG}) = \infty$ and $Z_f(\omega \neq \omega_{AG}) = 0$. The input impedance function $Z_{AG} = Z_T(I, \omega)$ is given by the ratio between the voltage drop at the auxiliary generator V_{AG} and the current delivered, I_{AG}.

In the FET-based circuit considered here, the voltage auxiliary generator at the resonance frequency $f_o = 5.2$ GHz is connected in parallel at port 2 (see Figs. 1.5 and 1.6). By sweeping the auxiliary-generator amplitude V_{AG} from the small-signal conditions, it is possible to analyze the variation of the total admittance function Y_T versus the voltage amplitude at $f_{AG} = \mathrm{f_o}$. The function $Y_{AG}(V_{AG}, f_o)$ is represented in Fig. 1.8. After a small-signal interval of nearly constant value, the conductance $\mathrm{Re}[Y_{AG}]$ increases with the voltage amplitude, as expected in physical devices. On the other hand, the susceptance $\mathrm{Im}[Y_{AG}]$ also varies with the voltage amplitude, due to the nonlinear behavior of the block containing the transistor. The susceptance $\mathrm{Im}[Y_{AG}]$ increases with the amplitude. Thus, a smaller oscillation frequency than the one corresponding to the small-signal resonance of Fig. 1.7 should be expected. Optimization of the auxiliary generator voltage V_{AG} and frequency ω_{AG} to fulfill the goal $Y_{AG}(V_{AG}, \omega_{AG}) = 0$ allows us to obtain the steady-state oscillation amplitude $V_o = 4.4$ V and frequency $f_o = 4.4$ GHz. A multiharmonic analysis has actually been carried out for this calculation. More details are given in Chapter 5. The significant variation of the oscillation frequency is due to the low-frequency selectivity of the resonant consisting of the nonlinear block capacitance and the load inductance $L = 0.2$ nH. A high-quality factor load such as the one discussed at the beginning of the subsection would reduce the amplitude dependence of the imaginary part

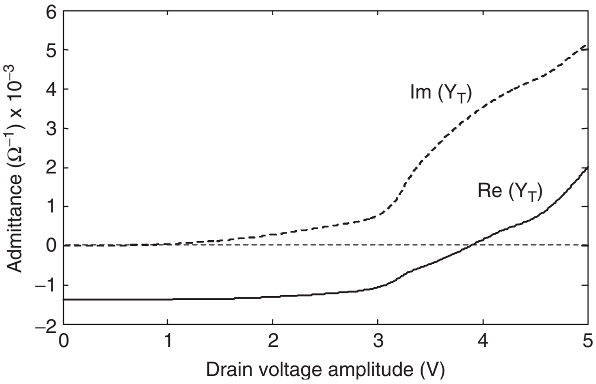

FIGURE 1.8 Variation of the admittance at port 2 versus the amplitude of a voltage auxiliary generator at the frequency $f_o = 5.2$ GHz introduced in parallel at the same port.

of the total admittance function $Y_T^i(V, \omega)$. Then the resonance frequency under small-signal conditions would be much closer to the actual oscillation frequency.

For validation, a time-domain simulation of the free-running oscillator has been carried out, with the results presented in Fig. 1.9. This shows that as predicted by the analysis of Fig. 1.7, the oscillation actually starts up. Steady state is reached after a transient. The envelope of the transient is initially exponential $e^{\sigma t}$ and then evolves gradually to the constant steady-state value. According to previous discussions, the exponent σ depends on the net negative conductance G_T and the quality factor of the resonant circuit. It is given by $\sigma = -\omega_o G_T/2G_L Q$. The steady-state oscillation obtained has the frequency $f_o = 4.4$ GHz and first-harmonic voltage amplitude $V = 4.4$ V at port 2. In agreement with the admittance function variation versus the voltage amplitude $Y_T(V, \omega_o)$, shown in Fig. 1.8, the steady-state oscillation frequency is smaller than the one predicted by small-signal analysis.

Note that the integration from a different initial condition provides a time-shifted steady-state solution with an identical waveform. In (1.12) it was shown that for a one-harmonic analysis of the oscillator, in terms of the node voltage $v(t) = \mathrm{Re}[Ve^{j\omega_o t}]$, any phase shift $v(t) = \mathrm{Re}[Ve^{j(\omega_o t+\phi)}]$ provides an equally valid solution. When considering several harmonic components, the solution will be invariant with respect to the phase of only one of these harmonic components. Otherwise, aside from the time shift, there would be a change in the waveform itself, which is not the case in periodic oscillation. In general frequency-domain analysis, considering two or more state variables, the solution will be invariant with respect to the phase of only one harmonic component of one of these state variables.

To illustrate we apply the stability condition (1.23), derived for a one-port and one-harmonic analysis, to our FET-based oscillator. The termination and feedback elements of the transistor were calculated to obtain negative resistance at the drain node, so this will be the reference node selected for stability analysis. Condition (1.23) is evaluated with the aid of the same auxiliary generator as that used to determine $Y_T(V_o, \omega_o)$ (Fig. 1.8). The derivatives about the free-running oscillation

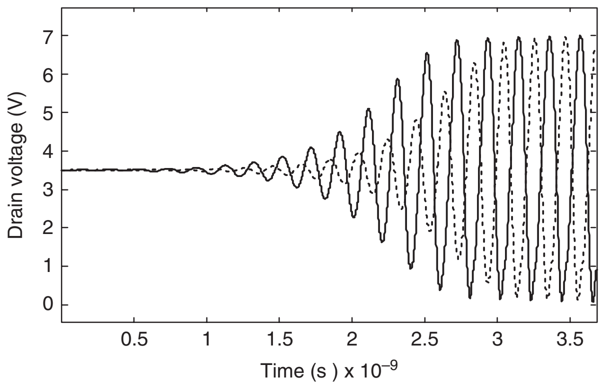

FIGURE 1.9 Time-domain analysis of the oscillator of Fig. 1.6. The envelope of the transient is initially exponential, evolving gradually to a constant steady-state value. The oscillation frequency is $f_o = 4.4$ GHz. Integration from different initial conditions gives rise to time-shifted steady-state waveforms which are equally valid oscillator solutions.

(V_o, ω_o) are obtained through finite differences. Initially, the generator amplitude is kept constant at the oscillation value $V_o = 4.4$ V, performing a frequency sweep about $f_o = 4.4$ GHz. The result is presented in Fig. 1.10. Note that the steady-state oscillation fulfills $\mathrm{Re}[Y_T] = 0$ and $\mathrm{Im}[Y_T] = 0$. Compared with the small-signal analysis of Fig. 1.7, the resonance frequency has decreased from 5.2 GHz to 4.4 GHz. On the other hand, the slope of $\mathrm{Im}[Y_T]$ (the dashed line) remains positive at the resonance frequency, as in the small-signal analysis of Fig. 1.7. Next, the generator frequency is kept constant at f_o and the generator amplitude is swept about $V_o = 4.4$ V. When representing $Y_T(V, f_o)$ and $Y_T(V_o, f)$ in the plane defined by $\mathrm{Re}[Y_T]$ and $\mathrm{Im}[Y_T]$, Fig. 1.11 is obtained. The solid-line curve corresponds to the function $Y_T(V, f_o)$. The dashed-line curve corresponds to the function $Y_T(V_o, f)$.

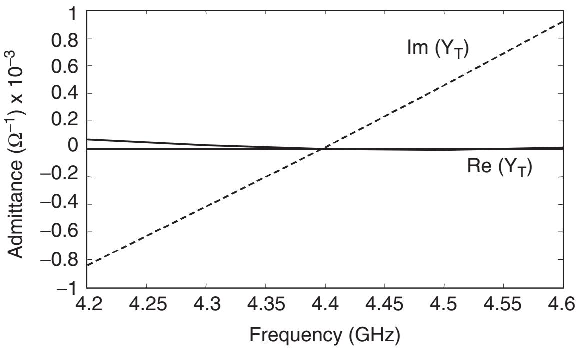

FIGURE 1.10 FET-based oscillator. Determination of the derivatives $\mathrm{Re}[\partial Y_T/\partial f_o]$ and $\mathrm{Im}[\partial Y_T/\partial f_o]$ about the free-running oscillation point V_o, f_o using a voltage auxiliary generator.

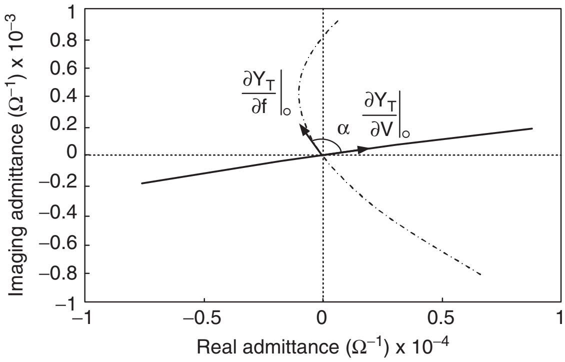

FIGURE 1.11 Representation of the curves $Y_T(V, f_o)$ and $Y_T(V_o, f)$ on the plane defined by $\mathrm{Re}[Y_T]$ and $\mathrm{Im}[Y_T]$. The origin, with $\mathrm{Re}[Y_T] = 0$ and $\mathrm{Im}[Y_T] = 0$, corresponds to the free-running oscillation $f_o = 4.4$ GHz and $V_o = 4.4$ V. The derivatives $\partial Y_{To}/\partial V$ and $\partial Y_{To}/\partial f$, agree, respectively, with the tangents to the origin of the curves $Y_T(V, f_o)$ and $Y_T(V_o, f)$.

The origin, with $\mathrm{Re}[Y_T] = 0$ and $\mathrm{Im}[Y_T] = 0$, corresponds to the free-running oscillation $f_o = 4.4$ GHz and $V_o = 4.4$ V. The derivatives $\partial Y_{To}/\partial V$ and $\partial Y_{To}/\partial f$ agree, respectively, with the tangents to the origin of the curves $Y_T(V, f_o)$ and $Y_T(V_o, f)$.

The derivative with respect to the voltage amplitude takes the value $\partial Y_T/\partial V_o = 5.529 \times 10^{-4} + j0.0012\Omega^{-1}/\mathrm{V}$. In turn, the derivative with respect to the frequency is $\partial Y_T/\partial \omega_o = -3.177 \times 10^{-14} + j6.929 \times 10^{-13}$. Thus, the term in (1.23) has the value $S = 4.2268 \times 10^{-16}$. Its positive sign indicates a stable solution. Note that the product in (1.23) will be positive for an angle $\alpha_{v\omega}$, defined as $\alpha_{v\omega} = \mathrm{ang}(\partial Y_{To}/\partial\omega) - \mathrm{ang}(\partial Y_{To}/\partial V)$, between 0 and π. Thus, the sign of σ_o can be determined graphically by tracing $\partial Y_{To}/\partial V$ and $\partial Y_{To}/\partial f$ in a polar plot (Fig. 1.11).

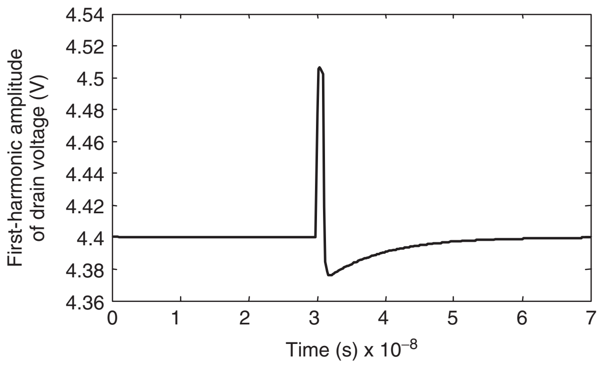

FIGURE 1.12 Oscillatory solution: reaction of the voltage amplitude at the drain node to an instantaneous perturbation applied at $t_p = 30$ ns. The oscillatory solution is stable, so the amplitude recovers its initial value after an exponential transient.

Figure 1.12 shows the effect of a perturbation on voltage amplitude at observation port 2. Instantaneous perturbation is applied at the time $t_p = 30$ ns. In agreement with the formulation (1.22), the amplitude perturbation follows an exponential transient $\Delta V(t) = \Delta V_o e^{\sigma_o t}$. Because the oscillatory solution is stable ($S > 0$), the exponent σ_o has a negative sign: $\sigma_o = -3.87 \times 10^9 S^{-1}$. Therefore, the transient leads back to the original value of the oscillation amplitude, $V_o = 4.4$ V.

1.4 FREQUENCY-DOMAIN FORMULATION OF AN OSCILLATOR CIRCUIT

The oscillator admittance–impedance analysis presented so far assumes a sinusoidal oscillation $v(t) = V_o \cos \omega_o t$. However, the inherent nonlinearity of the oscillator circuit will generate some harmonic content. As already stated, the relevance of the harmonic components will be higher for a smaller quality factor of the load circuit. The objective here is to derive the circuit equations when considering harmonic components up to a certain order N. This will show how the previous analysis at the fundamental frequency generalizes to N harmonic terms. The objective of introducing this formulation here is to provide the necessary background for the phase noise analysis in Chapter 2 and the analysis of frequency dividers in Chapter 4.

1.4.1 Steady-State Formulation

For the frequency-domain analysis of a given nonlinear circuit, the circuit variables are represented in a Fourier series. For simplicity, a single state variable $v(t)$ and a single nonlinearity of current type $i(v)$ are considered. The voltage variable is expressed as $v(t) = \sum_{k=-N}^{N} V_k e^{jk\omega_o t}$, with V_k complex coefficients. Note that because $v(t)$ is a real variable, the Fourier series contains both negative and positive harmonic frequencies $k\omega_o$, fulfilling $V_{-k} = V_k^*$. Due to the orthogonality of the Fourier frequency basis, a circuit of the form of Fig. 1.4 can be formulated by applying Kirchhoff's laws independently at the various harmonic frequencies $k\omega_o$. This provides a system of the form

$$\begin{aligned}
H_{-N} &= V_{-N} + Z_L(-N\omega_o) I_{-N}(V_{-N}, \ldots, V_o, \ldots, V_N) = 0 \\
&\vdots \\
H_o &= V_o + Z_L(0) I_o(V_{-N}, \ldots, V_o, \ldots, V_N) + E_{dc} = 0 \\
&\vdots \\
H_k &= V_k + Z_L(k\omega_o) I_k(V_{-N}, \ldots, V_o, \ldots, V_N) = 0 \\
&\vdots \\
H_N &= V_N + Z_L(N\omega_o) I_N(V_{-N}, \ldots, V_o, \ldots, V_N) = 0
\end{aligned} \tag{1.33}$$

where H_k are complex error functions. Note that the bias sources should be included in the dc term. As an example, a series voltage source E_{dc} has been considered in (1.33). The total number of equations is $2N + 1$, as each harmonic function H_k has real and imaginary parts, except the one corresponding to dc, given by H_o, which is real valued. The equation system (1.33) constitutes the harmonic balance formulation of the oscillator circuit, containing a single nonlinearity of current type only. As written in (1.33), it is valid only for current-type nonlinearities. It cannot be applied in the case of capacitive nonlinearities. As shown in Chapters 3 and 5, the capacitive nonlinearities are described in terms of the harmonic components of the corresponding nonlinear charge $q(v)$. Once the harmonic components $Q_{-N}, \ldots, Q_k, \ldots, Q_N$ are determined, the harmonics of the current through the capacitance are easily obtained from $-jN\omega_o Q_{-N}, \ldots, jk\omega_o Q_k, \ldots, jN\omega_o Q_N$.

As shown in (1.33), Kirchhoff's laws are fulfilled independently at each harmonic component. The key point is that each harmonic component of the nonlinear current depends on all the harmonic components of the node voltage, as they are linked through the constitutive relationship $i(t) = i(v(t))$. Analytically, the various harmonic terms of $i(t)$ would be obtained by calculating $i(t) = i\left(\sum_{k=-N}^{N} V_k e^{jk\omega_o t}\right)$. Note that use of the Fourier expansion from $k = -N$ to $k = N$ allows as to introduce $v(t)$ directly in the constitutive relationship $i(t) = i(v(t))$. This is why the harmonic balance system is generally expressed by considering positive and negative frequencies, even if we know that the harmonic terms at $k\omega_o$ and $-k\omega_o$ fulfill the Hermitian symmetry relationship $V_{-k} = V_k^*$. To understand the dependence $I_k(V_{-N}, \ldots, V_o, \ldots, V_N)$ of each harmonic component of $i(t)$ on all the harmonic components of $v(t)$, consider the particular case of a polynomial characteristic $i(t) = i(v(t))$. The expansion $i(t) = i\left(\sum_{k=-N}^{N} V_k e^{jk\omega_o t}\right)$ clearly gives rise to a mixed dependence of each I_k on different harmonic coefficients $V_{-N}, \ldots, V_o, \ldots, V_N$. In practice, the components $I_k(V_{-N}, \ldots, V_o, \ldots, V_N)$ are obtained numerically using inverse and forward Fourier transfers. Under any variation of $(V_{-N}, \ldots, V_o, \ldots, V_N)$, the waveform $v(t)$ is calculated with an inverse Fourier transform, then the waveform $i(t)$ is obtained from the relationship $i(v(t))$, and finally, the harmonic components I_k are calculated with a forward Fourier transform. Details of this calculation are given in Chapter 5.

System (1.33) is a nonlinear algebraic system which is usually resolved by employing the well-known Newton–Raphson algorithm. Note that in an oscillator circuit, the frequency ω_o is an unknown to be determined, so the system, in the form (1.33), is unbalanced, as it contains $2N + 1$ equations in $2N + 2$ unknowns, given by the real and imaginary parts of all the harmonic components of $v(t)$, plus the oscillation frequency ω_o. To solve this problem, either the real or imaginary part of one of the harmonic components of $v(t)$ will be set arbitrarily to zero, which is allowed by the autonomy of the steady-state oscillation.

As an example of the formulation (1.33), consider a case in which both the dc and first-harmonic component are taken into account in the oscillator solution, so the unknown voltage is expressed as $v(t) = V_o + V_1 e^{j\omega_o t} + V_{-1} e^{-j\omega_o t}$, with

$V_1 = V_{-1}^*$. The steady-state system is given by

$$\begin{aligned} H_o &\equiv V_o + R_L(0) I_o(V_o, V_1, V_{-1}) = 0 \\ H_1 &\equiv V_1 + Z_L(\omega_o) I_1(V_o, V_1, V_{-1}) = 0 \\ H_{-1} &\equiv V_{-1} + Z_L(-\omega_o) I_{-1}(V_o, V_1, V_{-1}) = 0 \end{aligned} \tag{1.34}$$

where, for simplicity, no bias sources are considered. This one-harmonic example is considered again later in the section.

The general system (1.33) can be written in matrix form as

$$\overline{H}_s = \overline{V}_s + [Z_L(k\omega_o)] \overline{I}_s(\overline{V}_s) = 0 \tag{1.35}$$

where the vector $\overline{V}_s$ is made up of the steady-state terms $\overline{V}_s = [V_o \quad V_1 \quad V_{-1} \quad \cdots \quad V_N \quad V_{-N}]$, the vector $\overline{I}_s$ is given by $\overline{I}_s = [I_o \quad I_1 \quad I_{-1} \quad \cdots \quad I_N \quad I_{-N}]$, and the linear matrix $[Z_L(k\omega_o)]$ is the diagonal matrix:

$$[Z_L(k\omega_o)] = \begin{bmatrix} R_L(0) & 0 & 0 & & 0 \\ 0 & \ddots & & & \\ & & Z_L(k\omega_o) & & \\ & & & \ddots & 0 \\ 0 & 0 & & 0 & Z_L(-N\omega_o) \end{bmatrix} \tag{1.36}$$

where k indicates the varying integer order of the harmonic coefficient, that is, $0, \ldots, k, -k, \ldots, N, -N$.

For conceptual purposes it is interesting to obtain the Jacobian matrix associated with system (1.33), which has the form

$$[JH] = [I_d] + [Z_L(k\omega_o)] \left[\frac{\partial \overline{I}}{\partial \overline{V}} \right]_s \tag{1.37}$$

with $[I_d]$ being the identity matrix and $\left[\partial \overline{I}/\partial \overline{V}\right]_o$ the Jacobian matrix of the nonlinear function, consisting of the derivatives of the various harmonic components of the current with respect to the harmonic components of the independent voltage. As an example, in the case of the system (1.34), comprising the dc and first-harmonic component, the Jacobian matrix $\left[\partial \overline{I}/\partial \overline{V}\right]_s$ is given by

$$\left[\frac{\partial \overline{I}}{\partial \overline{V}} \right]_s = \begin{bmatrix} \dfrac{\partial I_o}{\partial V_o} & \dfrac{\partial I_o}{\partial V_1} & \dfrac{\partial I_o}{\partial V_{-1}} \\ \dfrac{\partial I_1}{\partial V_o} & \dfrac{\partial I_1}{\partial V_1} & \dfrac{\partial I_1}{\partial V_{-1}} \\ \dfrac{\partial I_{-1}}{\partial V_o} & \dfrac{\partial I_{-1}}{\partial V_1} & \dfrac{\partial I_{-1}}{\partial V_{-1}} \end{bmatrix}_s \tag{1.38}$$

Determination of this matrix is much simpler than it seems. It is sufficient to take into account the fact that the derivative of the kth harmonic of the nonlinear current with respect to the mth harmonic of the voltage can be obtained as

$$\begin{aligned}\frac{\partial I_k}{\partial V_m} &= \frac{1}{T}\frac{\partial\left(\int_0^T i(t)e^{-jk\omega_o t}dt\right)}{\partial V_m} = \frac{1}{T}\int_0^T \frac{\partial i(t)}{\partial v(t)}\frac{\partial v(t)}{\partial V_m}e^{-jk\omega_o t}\,dt \\ &= \frac{1}{T}\int_0^T g(t)e^{jm\omega_o t}e^{-jk\omega_o t}\,dt \\ &= G_{k-m} \end{aligned} \tag{1.39}$$

with $g(t)$ being the time-domain derivative $g(t) = \partial i(t)/\partial v(t)$ and G_{k-m} being the $(k-m)$th harmonic component of $g(t)$. Taking the property above into account, the Jacobian matrix $\left[\partial\overline{I}/\partial\overline{V}\right]_s$ can be rewritten

$$\left[\frac{\partial I}{\partial V}\right]_s = \begin{bmatrix} G_0 & G_{-1} & G_1 \\ G_1 & G_0 & G_2 \\ G_{-1} & G_{-2} & G_0 \end{bmatrix}_s \tag{1.40}$$

The matrix (1.40), with equal diagonal elements G_0, is the conversion matrix associated with $g(t)$. Therefore, the matrix $[\partial\overline{I}/\partial\overline{V}]_s$ can be obtained from the Fourier series expansion of $g(t)$. Note that it is necessary to double the number of harmonic components considered in the Fourier series expansion of $g(t)$, which now goes from $-2\omega_o$ to $2\omega_o$. These results are easily extended to any number N of harmonic terms.

It has been shown in previous sections that an arbitrary variation of the phase origin of the oscillator solution provides another solution. Because of this, the Jacobian matrix associated with system (1.35), used in the Newton–Raphson algorithm, is singular at steady-state oscillation. To understand this singularity of $[JH]$, consider a time shift τ of the steady-state waveform. This will give rise to the phase shift $-k\omega_o\tau = k\alpha$ of the various harmonic terms, where $\alpha = -\omega_o\tau$ has been introduced. The phase-shifted solution must also be a solution of (1.35). Therefore, it is possible to write

$$\frac{\partial\overline{H}_s}{\partial\alpha} = \left[\frac{\partial\overline{H}_s}{\partial\overline{V}_s}\right]\frac{\partial\overline{V}_s}{\partial\alpha} = \overline{0} \tag{1.41}$$

Because the second factor of equation (1.41) is different from zero, the Jacobian matrix must be singular. In the numerical resolution of (1.35) with the Newton–Raphson algorithm, the singularity problem of the Jacobian matrix can be circumvented by arbitrarily setting to zero the imaginary part of one of the harmonic components (e.g., $V_1^i = 0$). As stated earlier, this also leads to a well-balanced system, with $2N+1$ equations in $2N+1$, given by the real and imaginary parts of all the harmonic components of $v(t)$ except $V_1^i = 0$ and the oscillation frequency ω_o.

1.4.2 Stability Analysis

The stability analysis presented in Section 1.3.2 assumed a small frequency perturbation $\Delta\omega \ll \omega_o$. However, the perturbation frequency is not necessarily small, as in the case of instabilities leading to a division by 2 of the oscillation frequency. For a more general stability analysis, the limitation $\Delta\omega \ll \omega_o$ must be eliminated. In the following, a small-amplitude perturbation of complex frequency $s = \sigma + j\omega$ is considered, with $\omega \in (0, \omega_o)$. Stability analysis is used once the steady-state oscillation has been determined by applying the Newton–Raphson algorithm to the system (1.33). The small perturbation at the initial time t_o will give rise to small amplitude increments in the voltage and current vectors, given by ΔV and ΔI, respectively. Thus, it will be possible to consider a first-order Taylor series expansion of the nonlinearity $\overline{I}(\overline{V})$ about the steady-state solution $\overline{V}_s$, so $\overline{I}(\overline{V})$ is replaced by $[\partial\overline{I}/\partial\overline{V}]_s\Delta\overline{V}$. The perturbed oscillator equations are written

$$[JH(jk\omega_o + s)]\Delta\overline{V}(s) = \left\{[I_d] + \left[Z_L(jk\omega_o + s)\right]\left[\frac{\partial\overline{I}}{\partial\overline{V}}\right]_s\right\}\Delta\overline{V}(s) = 0 \quad (1.42)$$

Note that the system (1.42) contains two different frequency variables, the steady-state frequency ω_o and the complex frequency s, generated as a result of perturbation at t_o. The formulation is similar to that used in the conversion matrix approach [23], although the small-signal frequency is complex in this case. The perturbation gives rise to a transient variation of the harmonic components that is taken into account by means of dependence on the complex frequency s. Note that unlike the analysis of Section 1.3, the imaginary part of the sideband frequency s is not limited to small values. It can take any value in the interval $(0, \omega_o)$. Note that particularizing s to the case of small frequency variations, the impedance matrix $[Z_L(jk\omega_o + s)]$ can be expanded in a Taylor series, so it is possible to write $[Z_L(jk\omega_o + s)] \cong Z_L(jk\omega_o) + (\partial Z_L/\partial(jk\omega_o))s$. It is easily seen that placing this in (1.42) and limiting analysis to the fundamental frequency ω_o, an equation equivalent to (1.26) is obtained. Therefore, the analysis technique (1.18 and 1.26) is a particularization of the more general stability analysis (1.42) to the case of a small perturbation frequency$\Delta\omega$.

System (1.42) is a homogeneous linear system, so for the perturbed solution $\Delta\overline{V}$ to differ from zero, the associated characteristic determinant must be zero $\det\{[I_d] + [Z_L(jk\omega_o + s)][\partial\overline{I}/\partial\overline{V}]_s\} = 0$, with $[I_d]$ the identity matrix. Note that the increment $\Delta\overline{V}(s)$ necessarily differs from zero since an instantaneous perturbation was actually applied at t_o. Because s is the complex frequency of the perturbation, evolution of this perturbation will depend on the roots s of the characteristic determinant $\det[JH(k\omega_o + s)]$. For $s = 0$, the characteristic determinant agrees with the determinant of the Jacobian matrix $\det[JH] = 0$ of the harmonic balance system [see (1.37)]. In (1.41) it was shown that this Jacobian matrix is singular, $\det[JH] = 0$. Therefore, one of the roots of the characteristic determinant will be $s = 0$. This zero root is due to the system autonomy. For this perturbation to vanish exponentially in time, all the rest of the roots must have a negative real part.

To transform the analysis of the characteristic system (1.42) into a pole analysis, a small-signal current source $I_{in}(s)$ is introduced in parallel with the nonlinear element. The current source at the frequency s will generate the sidebands $k\omega_o + s$. The original system (1.42), with the input $I_{in}(s)$, will be ruled by

$$\{[I_d] + [Z_L(jk\omega_o + s)] \left[\frac{\partial \overline{I}}{\partial \overline{V}} \right]_s \} \Delta \overline{V}(s) = \left[Z_L(jk\omega_o + s) \right] \begin{bmatrix} I_{in}(s) \\ \vdots \\ 0 \end{bmatrix} \tag{1.43}$$

Any output $Y(s)$ selected will be linearly related to the increment $\Delta\overline{V}(s)$, in the form $Y(s) = B\Delta\overline{V}(s)$, with B a row matrix. Unless pole–zero cancellations occur, all possible transfer functions will have the same denominator, due to the division by the characteristic determinant $\det\{[I_d] + [Z_L(jk\omega_o + s)][\partial\overline{I}/\partial\overline{V}]_s\}$. The system poles will agree with the roots of this determinant. In particular, it is possible to define the transfer function $Z_{in}(s) = \Delta V_1(s)/I_{in}(s)$, where $\Delta V_1(s)$ is the lowest sideband ($k = 0$) of node voltage perturbation. Clearly, this frequency-domain analysis is totally equivalent to the one presented for a dc solution in Section 1.2. However, unlike in dc analysis, two frequencies are involved in the linearization (1.43), one coming from the perturbation s and the other from ω_o, associated with the steady-state regime.

In the circuit shown in Fig. 1.1, with the cubic nonlinearity $i(v) = av + bv^3$, the terms in the Jacobian matrix (1.40) are given by $G_o = a + 3/2bV_o^2$, $G_1 = 0.0$, and $G_2 = 3/4bV_o^2$. The matrix $[Z_L(jk\omega_o + s)]$ is obtained directly from the inverse of the linear admittance $Z_L(\omega) = [G + j(C\omega - 1/(L\omega))]^{-1}$, with ω a generic frequency. The characteristic determinant is second order in s, so it has two different roots. Due to fulfilment of the oscillation condition (1.35), one root is $s = 0$, associated with the solution autonomy. The second real root is $-0.32 \times 10^9 s^{-1}$, so the oscillation is stable.

1.5 OSCILLATOR DYNAMICS

In this section the oscillator circuit is studied as a dynamic system [10,24] which will provide a geometric viewpoint of oscillator behavior and valuable background for an understanding of stability and phase noise. This study will be a general one, with no limiting assumptions in terms of state variables, harmonic content, or frequency of perturbations.

1.5.1 Equations and Steady-State Solutions

The nonlinear differential equations ruling circuit behavior are generally expressed in terms of a vector of state variables $\overline{x}$. This vector consists of the minimum number of variables such that its knowledge at time t_o together with that of the system input for $t > t_o$ determine the circuit response for $t > t_o$. Different choices are possible. As an example, the second-order nonlinear equation (1.9) can be split into two first-order equations by using the two state variables $x_1(t) = v(t)$ and $x_2(t) = dv/dt$. In lumped circuits, a common choice for the state variables in $\overline{x}$ is the set consisting of all inductor currents $i_{L1}, i_{L2}, \ldots$ and all capacitor voltages $v_{C1}, v_{C2}, \ldots$. The system order agrees with the number of reactive elements in the circuit. For circuits containing ideal transmission lines, the system order is ideally infinite, as the transmission lines are described with exponential terms of the form $\exp(A + sB)$, with s the Laplace frequency and A, B constant 2×2 matrixes (see Section 5.2, Chapter 5). A Taylor series expansion of this exponential would give rise to time derivatives of increasingly high order. If the time delay associated with each transmission line is not too high, it is possible to transform the differential equation system into a system of differential difference equations, due to the presence of the delayed variables $x_{T_1}(t + \tau_1) \cdots x_{T_M}(t + \tau_M)$, with M the number of transmission lines and $\tau_1, \ldots, \tau_M$ their corresponding time delays [25]. Other ways to tackle the simulation of distributed elements are presented in Chapter 5.

Because the main purpose of this section is to provide a general explanation of the oscillator dynamics, only the case of lumped-element circuits is considered. The vector containing the circuit state variables will be $\overline{x} \in R^N$. The time-domain equations will be written using Kirchhoff's laws together with the constitutive relationships of the nonlinear elements. This will provide a system of differential algebraic equations. In some cases, these time-domain equations can be expressed in *state form* [24]:

$$\begin{aligned} \dot{\overline{x}} &= \overline{f}(\overline{x}) \\ \overline{x}(t_o) &= \overline{x}_o \end{aligned} \tag{1.44}$$

Here $\overline{f}$ is a vector of nonlinear smooth functions (i.e., having continuous derivatives with respect to $\overline{x}$ up to infinite order). It must be noted that in free-running oscillators the function $\overline{f}$ does not depend explicitly on time. This is because it does not contain any time-varying external generators. As an example, in the parallel resonance oscillator of Fig. 1.1 the state variables are the voltage across the capacitor $v_c(t)$ and the current through the inductance $i_L(t)$. Thus, the state variable vector is defined as $\overline{x} = (v_c, i_L)^T$. Applying Kirchhoff's laws, it is possible to write

$$\begin{aligned} \frac{dv_c}{dt} &= -\frac{i_L}{C} - \frac{v_c}{RC} - i_{nl}(v_c) = -\frac{i_L}{C} - \frac{v_c}{RC} - \frac{(av_c + bv_c^3)}{C} && \text{(a)} \\ \frac{di_L}{dt} &= \frac{v_c}{L} && \text{(b)} \end{aligned} \tag{1.45}$$

Clearly, equation system (1.45) is formally similar to the general equation (1.44), with a two-dimensional nonlinear function $\overline{f}$ that does not depend explicitly on time. A dc solution can generally be found for any circuit described by (1.44) by setting $\dot{\overline{x}} = 0$ and solving $\overline{f}(\overline{x}_{DC})$. This is the dc solution that always coexists with the oscillatory solution, as shown in previous sections. However, in a well-designed oscillator, this dc solution must be unstable. Thus, integration of the circuit differential equations from any initial condition $\overline{x}_0 \neq \overline{x}_{dc}$ must provide a transient leading to a periodic steady-state oscillation $\overline{x}_s(t)$.

Another property of autonomous systems already discussed is that any arbitrary time translation of the steady-state solution $\overline{x}_s(t)$ provides another valid solution $\overline{x}_s(t-\tau)$. Actually, the initial conditions $\overline{x}_o$ considered for the integration of (1.44) may be associated with any time value t_o, because the function $\overline{f}$ does not depend explicitly on time. When integrating the circuit equations (1.44) from different initial values $\overline{x}_o$, the same steady-state waveform, with different time shifts, is obtained (see Fig. 1.9).

The situation is different for circuits that have a time-varying independent source such as a sinusoidal generator. When employing Kirchhoff's laws, this source will give rise to an explicit time dependence of the nonlinear differential equation system, which in state form will be written $\dot{\overline{x}} = \overline{f}(\overline{x}, t)$. Note that in the common case of a periodic source with period T, the nonlinear function $\overline{f}$ will also be periodic, with the same period T.

For compactness of the formulation, the same formal equation (1.44) is often used for both autonomous and nonautonomous periodic systems. Actually, a nonautonomous system can be expressed as an autonomous system if the time t is included in the state variable vector, which becomes $\overline{x}'$. The new variable t is unbounded, as time tends to infinity. A different variable related to time can be chosen instead. For a periodic nonlinear function $\overline{f}$, the angle variable $\theta = (2\pi/T)t$ is used, with T being the independent source period [24]. The variation of this new variable can be limited to the range $[0,2\pi)$. Defining the new state vector as $\overline{x}' = (\overline{x}, \theta)$, the equations of the nonautonomous periodic system are expressed as

$$\begin{aligned} \dot{\overline{x}} &= \overline{f}(\overline{x}, \theta) \\ \dot{\theta} &= \frac{2\pi}{T} \end{aligned} \tag{1.46}$$

As gathered from (1.46), the dimension of the nonautonomous periodic system increases in one respect to that of an autonomous system containing the same number of reactive elements. Note that this is merely a change in the formal expression of the system, since the dependence on the time reference is, of course, maintained under this change.

By *forced circuits* we mean circuits with an independent time-varying source that do not oscillate or circuits that exhibit an oscillation synchronized to the independent periodic source. When integrating the nonlinear differential equations that describe these circuits from the same initial time t_o and different initial values of the state vector $t_o, \overline{x}_o$ or $t_o, \overline{x}'_o$, the same steady-state waveform at the same time values (not shifted in time) will be obtained. Thus, the time-varying generator of the forced circuit prevents solution invariance versus time translations. This invariance is a property of autonomous circuits only. Here by the general term *autonomous circuit* we mean free-running oscillators or circuits containing oscillations that are not synchronized to the independent sources.

When analyzing a system such as (1.46), the designer usually performs a representation versus time of the solutions obtained. An alternative way to observe these solutions is by using the phase space [26]. In the phase space, each axis corresponds to a different state variable x_i. Then, an instantaneous representation of the time values of these variables $x_i(t)$ is carried out, as is done, for example, when tracing the load cycle of a transistor-based circuit. Plotting the numerical values of all the variables at a given time t provides a description of the state of the system at that time. When time evolves, the solution follows a "trajectory" or set of sequential points versus the implicit time variable. The evolution of the system is indicated by a path, or trajectory, in the phase space. The phase space enables a geometric and therefore comprehensible representation of complex behavior. In the case of a nonautonomous circuit, a time-related variable must be included, such as θ or the generator value $e_{\text{in}}(t)$. In practice, the phase space representation is limited to three state variables, so a projection of the phase space is actually obtained, which is usually enough to identify the most relevant properties.

As an example, Fig. 1.13 shows a phase space representation of the solutions of a FET-based oscillator. The variables chosen are the drain voltage v_D and the current through the load inductance i_L. The unstable dc solution, given by the constant voltage $v_D = 3.5$ V and current $i_L = 0$ (after the dc block), provides a point in this representation. The periodic steady-state solution gives rise to a closed trajectory termed a *cycle*, because the circuit variables repeat their values after one period. Actually, in a phase-space representation, the steady-state solutions give rise to bounded sets called *limit sets*. Dc solutions give rise to points called *equilibrium points*, and periodic solutions give rise to *cycles*. Other types of steady-state solutions give rise to other geometric figures.

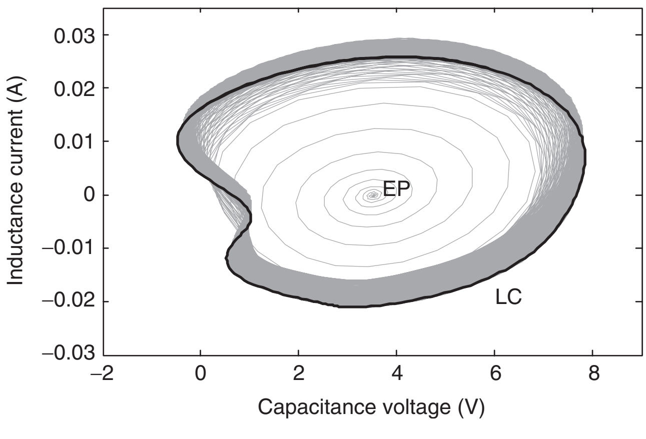

FIGURE 1.13 Phase space representation of the solutions of the FET-based oscillator of Fig. 1.6. The dc solution gives rise to the equilibrium point, indicated as EP. The steady-state oscillation gives rise to the limit cycle, LC. The spiral-like trajectory corresponds to the startup transient.

In a phase space representation [10], transients are open trajectories leading from one limit set to another. In the case of Fig. 1.13, the spiral trajectory from the equilibrium point (EP) to the cycle (LC) corresponds to the startup transient, leading from an unstable dc solution to steady-state oscillation. In a noiseless system, after reaching the cycle, the solution keeps turning in the cycle for a time tending to infinity. In practice, the stable cycle is continuously recovering from the small perturbations that are always present in real life. A single instantaneous perturbation kicks the system out of the cycle, but because the cycle is stable, an exponential transient leads the solution back to it. Due to the continuous noise influence, the solution trajectory will actually surround the cycle. The same is true for any other type of steady-state regime observed in real life.

As already indicated, when represented in phase space, steady-state solutions give rise to bounded sets. The type of limit set and its dimension depend on the particular type of steady-state solution. In general, the steady-state solutions of nonlinear systems can be classified into four principal types: dc solutions, periodic solutions, quasiperiodic solutions, and chaotic solutions. The main characteristics of each type of solution are summarized briefly next.

1.5.1.1 Constant Solution Constant solutions are only possible in circuits with no time-varying input generators. As already seen, they are obtained by imposing $\dot{\overline{x}} = 0$. Because there is no time variation of the state variables, the representation of a constant solution in phase space gives rise to a point called the *equilibrium point* (Fig. 1.13). The geometric dimension of the point is zero.

1.5.1.2 Periodic Solution The periodic solution, well known to designers, fulfills $\overline{x}(t + nT) = \overline{x}(t)$, with n an integer and T the solution period. The circuit variables can be expanded in a Fourier series with one fundamental frequency $\omega_o = 2\pi/T$. For a free-running oscillator, the period T will depend on the values of the circuit elements and bias generators. In a forced circuit the period T is determined by the input generator. The periodic solution of a free-running oscillator gives rise to an isolated closed trajectory in the phase space (see the cycle in Fig. 1.13), known as the limit cycle. For a sinusoidal oscillator with no harmonic content, this cycle will be a circumference. Whatever the dimension of the system in R^N, the cycle will have one dimension because it is a line. The trajectories surrounding the limit cycle are open, corresponding to transients. This is why the limit cycle is an isolated closed trajectory in the phase space. In stable steady-state oscillation, all these neighboring trajectories lead to the cycle. The stable cycle must be attracting for all its surrounding neighborhood, which must have the same dimension as the entire phase space R^N. Note that the cycles of an ideal LC oscillator (with no resistance) are not isolated because any initial condition provides a different cycle (see Section 1.2). In a conservative oscillator, for arbitrarily close initial values, arbitrarily close cycles would be obtained. Thus, they are not limit cycles.

It must be remembered that the phase space of an autonomous system does not contain time or a time-related variable. Due to the invariance versus time translations of autonomous systems, all possible steady-state oscillations $\overline{x}_o(t - \tau)$

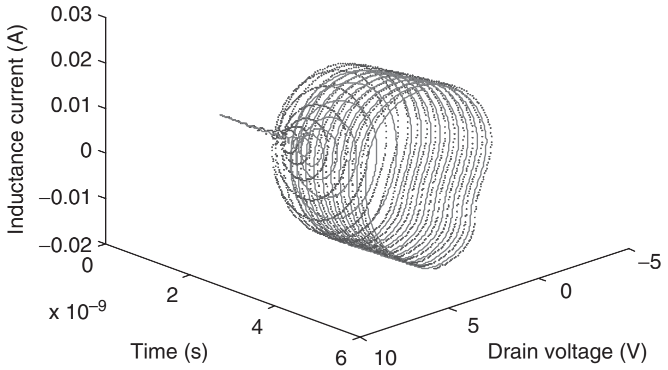

FIGURE 1.14 Solutions of the FET-based oscillator obtained when integrating the circuit equations for two different initial values. Although the solutions are time shifted, they provide the same limit cycle, which is obtained from the projection of these solutions over the plane defined by the drain voltage and inductance current.

lie on the same limit cycle. This is shown clearly in Fig. 1.14, where the solutions obtained when integrating the equations of the FET-based oscillator of Fig. 1.6 are shown for two different initial conditions. It is, in fact, the same analysis as that performed in Fig. 1.9. The difference is that two different state variables, the drain voltage v_D and the inductance current i_L, have been considered here for a three-dimensional representation versus time. The two time-shifted steady-state solutions give rise to the same limit cycle, obtained by projecting the figure over the plane defined by v_D and i_L.

The situation is different for the periodic solution of a forced system. For a given phase value of a forcing periodic source, the periodic solution is unique. The cycle is actually due to this source (not generated by the circuit). As shown in (1.46), time can be considered as a state variable of the nonautonomous system. Because time is unbounded, either the periodic source value $g_{\text{in}}(t)$ or the angle $\theta = \omega t$ should be assigned to one of the axis of the phase space representation. Therefore, a different cycle, with an identical shape, is obtained for each phase value of the input source.

1.5.1.3 Quasiperiodic Solution In an "almost-periodic" solution, no period can be defined [24]. However, for each $\varepsilon > 0$ there exists a time-interval length $l(\varepsilon)$ such that each real interval of length $l(\varepsilon)$ contains at least one number τ (the *translation number*) fulfilling $|\overline{x}(t+\tau) - \overline{x}(t)| < \varepsilon$. The quasiperiodic solutions can be expanded in a Fourier series with a finite number M of nonrationally related (*incommensurable*) fundamentals $\omega_{f1}, \omega_{f2}, \ldots, \omega_{fM}$ and are thus expressible as a sum of periodic waveforms [26]. Two frequencies, ω_{f1} and ω_{f2}, are incommensurable if $\omega_{f1}/\omega_{f2} \neq m/n$, with m and n integers. A key aspect of quasiperiodic solutions is that the number M of required fundamental frequencies is uniquely defined, but not the set of these fundamental frequencies. Actually, $\omega_{f1}, \omega_{f2} + \omega_{f1}$ span the same set of frequencies as ω_{f1} and ω_{f2}. For a simple explanation of why the solution cannot be periodic, note that it is not possible to obtain a time value T fulfilling $A\cos\omega_{f1}t + B\cos\omega_{f2}t = A\cos(\omega_{f1}t + \omega_{f1}T) + B\cos(\omega_{f2}t + \omega_{f2}T)$. Satisfying this would require that $\omega_{f1}T = n\cdot 2\pi$, $\omega_{f2}T = m\cdot 2\pi$, with m and n integers. Then the ratio ω_{f1}/ω_{f2} would be rational, which is against our initial assumption of incommensurable fundamentals.

A quasiperiodic solution with two fundamental frequencies is easily obtained when connecting a periodic generator at the frequency ω_{in} to an existing oscillator at the frequency ω_{o}. Although other regimes are possible (see Chapter 3), for a wide range of input generator frequency and power, mixer-like behavior, with two incommensurable fundamentals, ω_{in} and ω_{o}, will be observed, with the ω_{o} value influenced by the input generator. Note that it would be equally possible to consider the fundamental frequency basis ω_{in}, $|\omega_{\text{in}} - \omega_{\text{o}}|$. The circuit is said to operate in an autonomous quasiperiodic regime. An interesting aspect of this type of regime is that despite the existence of an independent periodic source connected to the circuit, different initial values $\overline{x}_{\text{o}}$ at the initial time t_{o} give rise to time-shifted solutions with the same pattern. This is due to the fact that the oscillation is not synchronized to the input source and can have any phase shift with respect to this source.

Figure 1.15 shows the quasiperiodic solution obtained when introducing a generator at $f_{\text{in}} = 6.33$ GHz in the oscillator of Fig. 1.6, with original free-running oscillation frequency $f_{\text{o}} = 4.4$ GHz. It is clear that when representing a quasiperiodic solution in the phase space, no closed cycle can be obtained because the solution is not periodic. In the particular case of two incommensurable fundamental frequencies, the steady-state trajectory lies on the surface of a 2-torus. This is in close relationship with the fact that two fundamental frequencies give two independent rotations in phase space. As an example, Fig. 1.16 shows the three-dimensional representation of the quasiperiodic solution of the FET-based circuit. As time tends to infinity, the torus surface gets covered entirely by the solution trajectory. Because

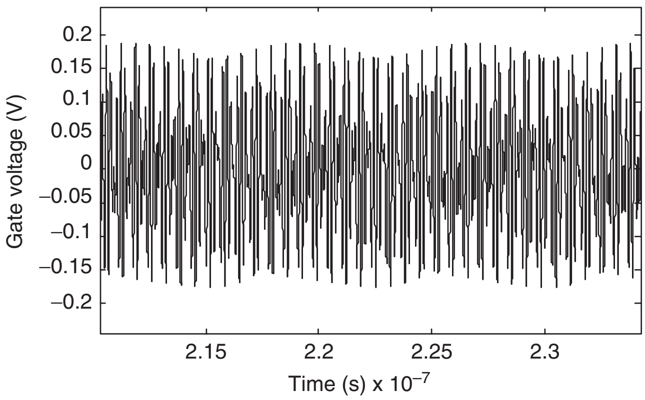

FIGURE 1.15 Time representation of the quasiperiodic solution of a FET-based oscillator at the original free-running frequency $f_{\text{o}} = 4.4$ GHz when a generator is introduced at $f_{\text{in}} = 6.33$ GHz.

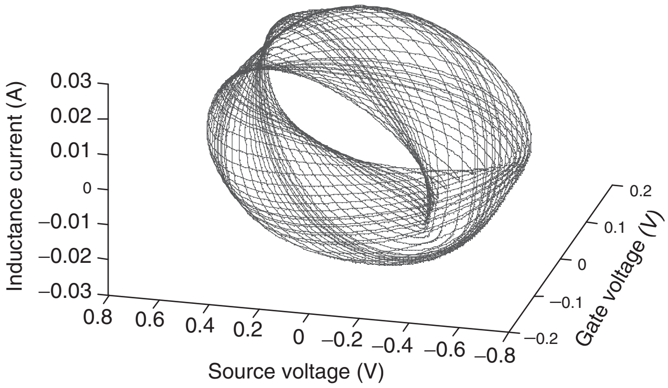

FIGURE 1.16 Phase space representation of the quasiperiodic solution of a FET-based oscillator. The steady-state solution lies on the surface of a 2-torus. This surface is covered entirely by the solution trajectory, as time tends to infinity.

the solution lies on the torus surface, it has two dimensions in the phase space. Note that a three-fundamental quasiperiodic solution would have three dimensions.

1.5.1.4 Chaotic Solution Chaotic solutions are neither periodic nor quasiperiodic [27]. Thus, they exhibit a continuous spectrum, at least for some frequency intervals. When performing frequency-domain measurements, chaotic solutions are often mistaken for noise or interference. However, the power measured is usually too high to be due to noise only. Chaotic solutions are quite common in practice. Actually, the minimum mathematical requirement for an autonomous circuit to exhibit this type of solution is that it contain at least three reactive elements plus one nonlinear element [28,29]. As an example, the commonly used Colpitts oscillator can exhibit chaotic solutions for some transistor bias voltages and linear element values.

Chaotic solutions are characterized by a sensitive dependence on initial conditions, meaning that solutions with arbitrarily close initial values diverge exponentially in time. Figure 1.17 presents simulations of a chaotic Colpitts oscillator, designed originally for the oscillation frequency $f_o = 1$ GHz. This figure shows the time evolution of the collector voltage when integrating the circuit equations from two close initial values. Initially the waveforms seem to overlap, but as time evolves they diverge and become quite different from each other. Compare the situation with that of a periodic or quasiperiodic periodic solution, giving the same steady-state waveform whatever the initial value is $\overline{x}_o$ at t_o. As we know, this waveform will be time-shifted for different $\overline{x}_o$ values in the case of autonomous behavior. Comparing Fig. 1.17, corresponding to a chaotic solution, with Fig. 1.15, corresponding to a quasiperiodic solution, it can be noted that the chaotic solution is nonperiodic and highly irregular. The quasiperiodic waveform usually looks like a periodic signal modulated with another periodic signal of incommensurate frequency. In the example in Fig. 1.18, the amplitude is clearly modulated and the frequency is modulated too, as the zero crossings are not uniformly spaced [26].

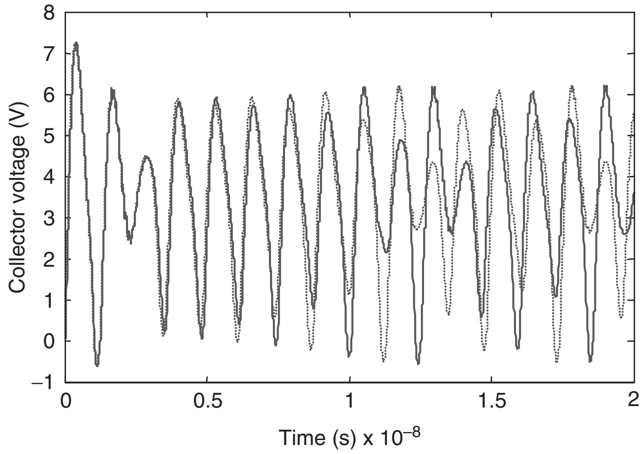

FIGURE 1.17 Time evolution of the collector voltage in a chaotic Colpitts oscillator when integrating the circuit equations from two close initial values. Initially, the waveforms overlap, then diverge, and after a little time become quite different from each other.

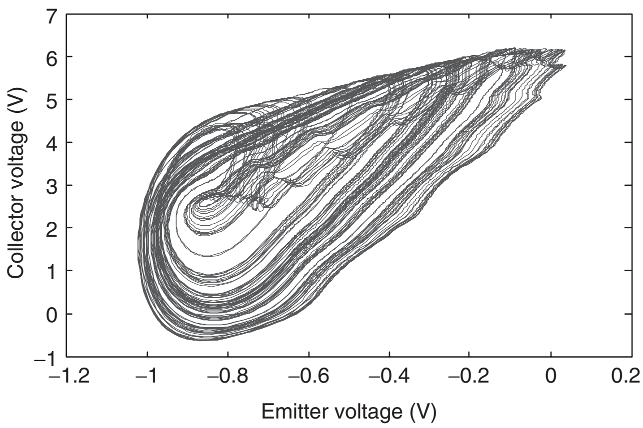

FIGURE 1.18 Phase space representation of a chaotic solution corresponding to a Colpitts oscillator. The bounded set obtained is not covered entirely by the trajectory; it has a fractal dimension. In close relation with this fractal dimension, the bounded set exhibits a self-similar structure.

When represented in phase space, the steady-state chaotic solution gives rise to a bounded figure, which unlike a limit cycle or a torus, is not entirely covered by the trajectory. As an example, Fig. 1.18 shows the phase space representation of a chaotic solution of a Colpitts oscillator. Some sections of the figure are not filled by the trajectory even when the simulation time tends to infinite. Owing to this fact, the dimension of the figure is fractal. The meaning of fractal dimension is explained in the following. A figure will have an entire dimension Dim if we can break it into an integer number N^{Dim} of self-similar figures. As an example, a line can be broken into N self-similar pieces. A square can be broken into N^2 self-similar pieces, and a cube can be broken into N^3 pieces. In each case the total number of pieces is N^{Dim} and the magnification factor of each piece, to recover the original figure, is N. As the reader can verify, the dimension of the figure can be obtained by setting Dim = log(number of pieces) − log(magnification of each piece). The chaotic bounded sets are characterized by a self-similar structure, meaning that they look the same for any scale of magnification. However, because some pieces are missing, as in Fig. 1.18, the definition of dimension introduced provides a fractional number.

1.5.2 Stability Analysis

As shown in previous sections, not all the steady-state solutions of a given circuit will be observable physically. To be observable, a given solution must be robust versus the small perturbations that are always present in real life (e.g., those coming from noise or any fluctuation of the bias sources). *Stable* means robust versus small perturbations. If a small perturbation is applied to a stable solution, the system will return to it exponentially in time. In contrast, if a small perturbation is applied to an unstable solution, the system will evolve to a different steady-state solution after an initially exponential transient. The solution obtained after the transient will be a stable solution and thus will be physically observable.

Note that for stability analysis, no assumption is made as to the value of the instantaneous perturbation applied. The only condition is that it has to be small. This is because two or more stable steady-state solutions may coexist and a large perturbation may lead the system to the a different stable solution. Thus, the stability definition is local in nature: it refers only to the system behavior near the steady-state solution [24]. The stability or instability of a given steady-state solution depends on the system and the particular solution, but not on the value of the applied small perturbation. This necessary restriction to small perturbations is advantageous, as it allows linearization of the circuit equations about the particular steady-state solution. Because an arbitrary perturbation will have components in any direction of an N-dimensional phase space, the stable steady-state solution must be attracting for all the neighboring trajectories. This is why stable solutions are also called *attractors*. An example of an attractor is the limit cycle of Fig. 1.13, which attracts, as can be seen, all its neighboring trajectories in the phase space.

We can express the solution of (1.44) in terms of its initial value as $\overline{x}(t, \overline{x}_o)$. The basin of attraction for a given steady-state solution $\overline{x}_s$ is the set of initial conditions $\overline{x}_o$ such that the system evolves to this solution as time tends to infinity: $\lim_{t\to\infty} \overline{x}(t, \overline{x}_o) = \overline{x}_s$ [24]. For an N-dimensional system with only one stable solution, the basin of attraction for this solution will be the entire space R^N. This single stable solution is said to be *globally asymptotically stable*. For a system with two or more coexisting stable solutions, each solution will have a different basin of attraction. The basins of attraction are disjoint because the solution of a system $\dot{\overline{x}} = \overline{f}(\overline{x})$, with $\overline{f}$ smooth, is unique, so the trajectories cannot intersect. If they did, using the intersection point $t_o, \overline{x}_o$ as the initial value for the system integration, the system might tend to either of the coexisting steady-state solutions, which is, of course, impossible. A key fact is that the dimension of each of the disjoint basins of attraction of the coexisting stable steady-state solutions agrees with the dimension N of the entire space. This is because each solution is stable. The union of the basins of attraction will be equal to R^N.

The circuit of Fig. 1.19a constitutes an example of bistable behavior. The nonlinearity is $i(v) = av + bv^3$. The circuit equations are obtained by adding the branch currents, which can be solved for three different dc solutions:

$$G_1 v + G_2 v + av + bv^3 = 0 \tag{1.47}$$

The three solutions are given by $V_{dc1} = 0$, which, as will be shown later, is unstable, and $V_{dc2} = 1$ V and $V_{dc3} = -1$ V, which are stable. Each of the stable solutions V_{dc2} and V_{dc3} has its own basin of attraction. Taking v and the current through

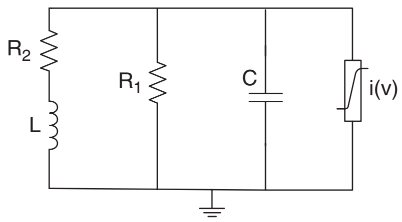

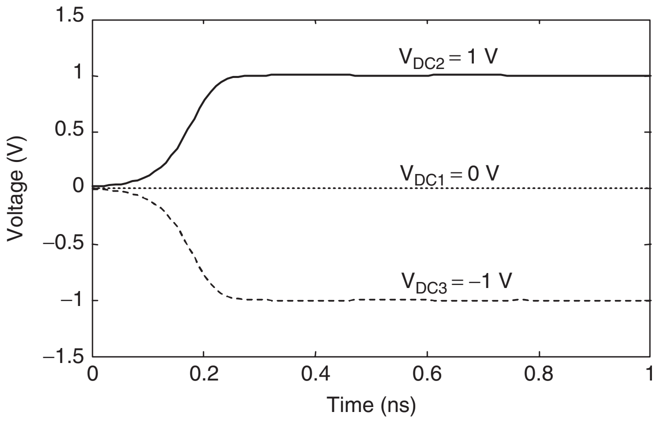

FIGURE 1.19 Cubic nonlinearity circuit with three dc solutions: $V_{dc1} = 0$, $V_{dc2} = 1$ V, and $V_{dc3} = -1$ V. The circuit element values are $L = 1$ nH, $C = 0.5$ pF, $R_2 = 100\ \Omega$, and $G_1 = 0.01\ \Omega^{-1}$. (a) Circuit schematic. (b) Solutions obtained for the two initial values: $i_{Lo} = 0$ and $v_o = 0.01$ V (solid line) and $i_{Lo} = 0$ and $v_o = -0.01$ V (dashed line).

the inductance i_L as state variables, the initial points $i_{Lo} = 0$ and $v_o > 0$ belong to the basin of attraction of $V_{dc2} = 1$ V, whereas the initial points $i_{Lo} = 0$ and $v_o < 0$ belong to the basin of attraction of $V_{dc3} = -1$ V. As an example, Fig. 1.19b shows the solution obtained when integrating the system equations from $i_{Lo} = 0$ and $v_o = 0.01$ V, which evolves to $V_{dc2} = 1$ V, and the solution obtained when integrating the system equations from $i_{Lo} = 0$ and $v_o = -0.01$ V, which evolves to $V_{dc2} = -1$ V.

For the stability analysis of a given steady-state solution $\overline{x}_s(t)$, either constant or time varying, a small perturbation is applied at a given time instant t_o, and from this value the system is allowed to evolve according to its own dynamics. Thus, beginning at this time value, the system analyzed is a perturbed system in which the stimulus that was applied is no longer present. Due to the effect of the instantaneous perturbation, the solution becomes $\overline{x}_s(t) + \Delta\overline{x}(t)$. Because the perturbation is small, it will be possible to expand the nonlinear equation system (1.47) in a Taylor series around $\overline{x}_s(t)$. The expansion is carried out only up to first order (higher order is rarely necessarily), which provides the following linear time-varying system:

$$\begin{aligned} \dot{\overline{x}}_s(t) + \Delta\dot{\overline{x}}(t) &= f(\overline{x}_s(t)) + Jf(\overline{x}_s(t))\Delta\overline{x}(t) && \text{(a)} \\ \Delta\dot{\overline{x}}(t) &= Jf(\overline{x}_s(t))\Delta\overline{x}(t) && \text{(b)} \end{aligned} \tag{1.48}$$

where $Jf(\overline{x}_s(t))$ is the Jacobian matrix of the nonlinear function f in (1.48), evaluated at the steady-state solution $\overline{x}_s(t)$. Because $\overline{x}_s(t)$ fulfills (1.44), equation ((1.48)a) can be simplified to ((1.48)b). For the steady-state solution $\overline{x}_o(t)$ to be stable, the perturbation $\Delta\overline{x}(t)$ must vanish exponentially in time. This will depend on the properties of the Jacobian matrix $Jf(\overline{x}_s(t))$ evaluated at this particular solution. Because the Jacobian matrix is evaluated at the steady-state solution, it will have the same periodicity or nonperiodicity of this solution. Therefore, the difficulties of the stability analysis are totally dependent on the solution type. The simplest case will be that of a dc solution, providing a constant Jacobian $Jf(\overline{x}_{dc})$. For a periodic solution of period T, the Jacobian matrix will also be periodic, with the same period T.

1.5.2.1 Stability Analysis of a dc Solution In a dc solution $\overline{x}_{dc}$, the Jacobian matrix is constant. Then equation (1.44) becomes a time-invariant linear system given by $\Delta\dot{\overline{x}} = Jf(\overline{x}_{dc})\Delta\overline{x}(t)$, since $Jf(\overline{x}_{dc})$ is a constant matrix. The general solution of this linear system is [27]

$$\Delta\overline{x}(t) = \sum_{n=1}^{N} c_k e^{\lambda_k t}\overline{u}_k = c_{c1}e^{(\sigma_{c1}+j\omega_{c1})t}\overline{u}_{c1} + c_{c1}^* e^{(\sigma_{c1}-j\omega_{c1})t}\overline{u}_{c1}^* + c_{r1}e^{\gamma_{r1}t}\overline{u}_{r1} + \cdots \tag{1.49}$$

where the exponents λ_k, $k = 1$ to N, which may be real or complex conjugate, are the eigenvalues of the Jacobian matrix $Jf(\overline{x}_{dc})$, the vectors $\overline{u}_k$ are the eigenvectors of this matrix, and c_k are constants that depend on the initial conditions, thus on the instantaneous perturbation applied. Note that for the expression (1.49) to be valid, all the eigenvalues $\lambda_k, k = 1$ to N of the Jacobian matrix $Jf(\overline{x}_{\mathrm{dc}})$ are assumed different, which is the general case. For a double eigenvalue λ_j, the coefficient of the associated exponential term $e^{\lambda_j t}$ will depend linearly on time, as $(c_{oj} + c_{1j}t)e^{\lambda_j t}$. For three repeated real eigenvalues λ_j, the exponential term $e^{\lambda_j t}$ will have the quadratic dependence $(c_{oj} + c_{1j}t + c_{2j}t^2)e^{\lambda_j t}$. This is easily generalized to any number of repeated eigenvalues, whose presence will require calculation of generalized eigenvectors. Note, however, that the presence of repeated eigenvalues is rare in practical circuits unless they contain perfect symmetries. Thus, this possibility will be discarded in most derivations. Exceptions are the Rucker and N-push oscillators with symmetric topology that we study in Chapter 10.

The application of the Laplace transform to $\Delta\dot{\overline{x}} = Jf(\overline{x}_{\mathrm{dc}})\Delta\overline{x}(t)$ provides the following system in the Laplace variable $s : (sI_N - Jf(\overline{x}_{\mathrm{dc}}))\Delta\overline{X}(s) = 0$, with I_N the identity matrix in the space R^N. Clearly, the eigenvalues $\lambda_k, k = 1$ to N, of $Jf(\overline{x}_{\mathrm{dc}})$ agree with the roots of the characteristic determinant $\det(sI_N - Jf(\overline{x}_{\mathrm{dc}})) = 0$. It is possible to define a closed-loop transfer function associated with this linearized system as was done in Section 1.2. For that, an arbitrary input $U(s)$ is introduced into the system and an arbitrary output $Y(s)$ is selected:

$$
\begin{aligned}
(sI_N - Jf(\overline{x}_{\mathrm{dc}}))\Delta\overline{X}(s) &= G(s)U(s) \\
Y(s) &= F\Delta\overline{X}(s)
\end{aligned}
\tag{1.50}
$$

where $G(s)$ is a $N \times 1$ matrix and $F(s)$ is a $1 \times N$ matrix. The closed-loop transfer function will be

$$
H(s) = \frac{F[sI_N - Jf(\overline{x}_{\mathrm{dc}})]^{+}G(s)}{\det\,[sI_N - Jf(\overline{x}_{\mathrm{dc}})]}
\tag{1.51}
$$

Unless pole–zero cancellations occur, giving rise to changes in the numerator and denominator of (1.51), all possible closed-loop transfer functions that one may define in the linearized system will have the same denominator. This denominator agrees with the characteristic determinant, and its roots, which correspond to the system poles, agree with the exponents λ_k of (1.49). When dealing with a dc solution here, the exponents λ_k will be called, indistinctly, eigenvalues or poles.

It will be assumed that there are no repeated (multiple) eigenvalues and that no eigenvalue is zero. The time evolution of the perturbation $\Delta\overline{x}(t)$ will be determined by the eigenvalues λ_k, because c_k and $\overline{u}_k$ are constant. For stability, all the eigenvalues must have a negative real part. This means that the perturbation will vanish exponentially in time and the system will return exponentially to the original steady-state solution $\overline{x}_{\mathrm{dc}}$. The linearized solution of a practical circuit will generally contain many eigenvalues (or poles), as many as the dimensions of the state variable vector $\overline{x}$, which in lumped circuits agrees with the total number of inductors plus capacitors. Typically, an unstable solution contains only a few unstable poles. Common situations are one real pole $\gamma > 0$ or a pair of complex-conjugate poles $\sigma \pm j\omega$, with $\sigma > 0$, with all the rest of the poles on the left-hand side of the complex plane.

From an inspection of (1.49), not all the eigenvalues λ_k will have the same weight on the transient response to the perturbation. This transient will be dominated by the eigenvalues with maximum real part σ_c or γ_r. In an unstable state, this real part will be positive. In a stable solution, the transient will be dominated by poles of smaller absolute value, abs(σ_c) or abs(γ_r). The associated frequencies will be observed during the transient response. In the common case of a single dominant pair of complex-conjugate poles $\sigma_c \pm j\omega_c$, an oscillation at the pole frequency ω_c, with amplitude decaying to zero will be observed during the transient response. Obviously, the response will be longer for a smaller absolute value of σ_c. As already shown, this can be due to a high quality factor for the resonance at ω_c. However, it can also be due to circuit operation close to instability, with the pair of complex-conjugate poles $\sigma_c \pm j\omega_c$ very near the imaginary axis. Actually, the observation (in simulation) of slower transients versus the variation in a circuit parameter such as bias voltage usually indicates that the circuit is approaching instability at the frequency of the transient.

According to (1.49), for any eigenvalue on the right-hand side of the complex plane, the perturbation $\Delta\overline{x}(t)$ tends to infinity over time. This unbounded growth of the perturbation is, of course, totally unrealistic. Expression (1.49) is a solution of the linearized system $\Delta\dot{\overline{x}} = Jf(\overline{x}_{dc})\Delta\overline{x}(t)$, which assumes a small perturbation $\Delta\overline{x}$. For any eigenvalue on the right-hand side of the complex plane, this assumption soon becomes invalid. After a very short time, the linearization is no longer applicable. The solution does not tend to infinity but to a different steady-state solution that cannot be predicted with the linearization.

Each eigenvalue of the Jacobian matrix $Jf(\overline{X}_{dc})$ is associated with a particular eigenvector, and the set of N vectors spans the space R^N. For illustration it will be assumed that m eigenvalues of a solution $\overline{x}_{dc}$ have a negative real part and $q = N - m$ eigenvalues have a positive real part. This type of solution, having stable and unstable eigenvalues or poles, is called a *saddle*. The solution is unstable because not all the eigenvalues have a negative real part. The m vectors associated with eigenvalues that have a negative real part $\overline{u}_1, \ldots, \overline{u}_m$ span, close to $\overline{x}_{dc}$, the stable eigenspace of this solution. The q vectors associated with eigenvalues that have a positive real part $\overline{u}_{m+1}, \ldots, \overline{u}_N$ span, close to $\overline{x}_{dc}$, the unstable eigenspace of this solution. Thus, unstable solutions may have stable eigenspaces, which is the most common situation in practical circuits, due to the usually high dimension of the system of differential equations determined by the number of reactive elements. For an unstable real pole, the unstable eigenspace will have one dimension and be defined by a single eigenvector, providing a straight line in the space R^N. In the case of two complex-conjugate poles, the unstable eigenspace will have two dimensions, defined by the two associated eigenvectors, corresponding to a plane in the space R^N.

Because the eigenvectors correspond to linearization of the original nonlinear system about the dc solution $\overline{x}_{dc}$, they are meaningful only in the neighborhood of this solution. At a larger distance from $\overline{x}_{dc}$, the stable and unstable eigenspaces become the stable and unstable manifolds associated with this solution. A manifold is a connected set in R^N instead of the disjoint junction of two or more nonempty subspaces [27]. All the points in the manifold have a continuous time derivative. The manifold can be closed, like a limit cycle, or it can be open, starting or ending in a steady-state solution or limit set. The stable manifold of $\overline{x}_{dc}$ is the set of initial values $\overline{x}_o$ such that $\lim_{t\to\infty} \overline{x}(t, \overline{x}_o) = \overline{x}_{dc}$. Close to $\overline{x}_{dc}$ the stable manifold is tangent to the stable eigenspace spanned by $\overline{u}_1, \ldots, \overline{u}_m$ [24]. The unstable manifold of $\overline{x}_{dc}$ is the set of initial values $\overline{x}_o$ such that $\lim_{t\to-\infty} \overline{x}(t, \overline{x}_o) = \overline{x}_{dc}$. Note the negative sign in the time limit, indicating that the system actually gets away from $\overline{x}_{dc}$ as time increases. Close to $\overline{x}_{dc}$ the unstable manifold is tangent to the unstable eigenspace spanned by $\overline{u}_{m+1}, \ldots, \overline{u}_N$. As already stated, because an arbitrary perturbation will have components in the N dimensions of the phase space, any dc solution with an unstable eigenspace or manifold will be unstable and physically unobservable. For the dc solution to be stable, the dimension m of its stable eigenspace must agree with the total system dimension N, so $m \equiv N$. Thus, the dc solution must be an attractor, that is, attracting for all the directions of the phase space.

Figure 1.20 shows an illustration of the eigenspaces of a dc solution in an R^3 system located in the plane in the center of the spiral [27]. Because it is an R^3 system, there are three eigenvalues associated with the dc solution. In this particular example, two eigenvalues are complex conjugate $\lambda_{1,2} = \sigma \pm j\omega$, with $\sigma < 0$. The associated eigenvectors define the stable eigenspace E_S associated with this dc solution. The third eigenvalue is real and positive, $\lambda_3 = \gamma > 0$. Its associated eigenvector defines a straight line that constitutes the unstable eigenspace of the dc solution. Note that due to the negative σ, the trajectories assume positions close to the straight line. The spirals shrink very quickly, so the system mostly evolves along a line corresponding to the unstable eigenspace E_U when getting away from the dc solution. Thus, the eigenvalue $\lambda_3 > 0$ totally dominates the transient behavior. However, as the distance to the dc point increases, the eigenspace evolves into a nonlinear manifold. It is no longer a straight line but generally a curve tending to a different steady-state solution that cannot be predicted using linear analysis.

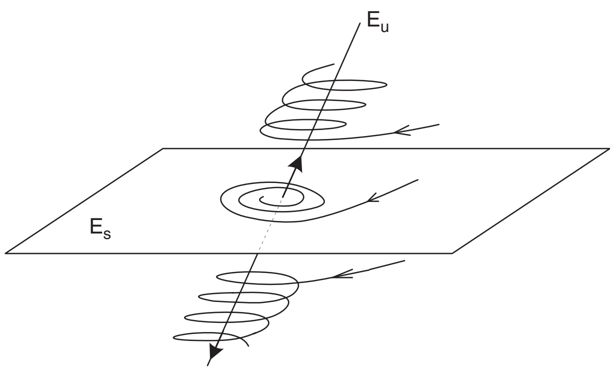

FIGURE 1.20 Eigenspaces of a dc solution in an R^3 system located in the plane in the center of a spiral. Because it is an R^3 system, there are three eigenvalues associated with the dc solution. The corresponding eigenvectors define stable and unstable eigenspaces.

Note that even though the new steady-state solution to which the solution evolves cannot be determined using the linearized analysis of (1.49), in most cases it will be possible to predict its constant or oscillatory nature and, in the latter case, the fundamental frequency of the oscillation. Exceptions can be encountered, however, because the linearization (1.49) has local validity only. As an example, for a dominant pair of complex-conjugate poles $\sigma \pm j\omega$, with $\sigma > 0$, the transient predicted by (1.49) will be oscillatory at the frequency ω, with exponentially growing amplitude. The system is expected to evolve to steady-state oscillation at about the frequency ω. In the case of a real pole γ on the right-hand side of the complex plane, no oscillation will be generally observed. The system is expected to evolve under a monotonic transient to a different dc solution (see Fig. 1.19b). Note that relaxation oscillations [24] are also possible in the presence of positive real poles.

To illustrate, the stability analysis described previously will be applied to the dc solution $v_{c,\mathrm{dc}} = 0$, $i_{L,\mathrm{dc}} = 0$ of the second-order nonlinear system (1.45). The linearized system is given by

$$\begin{bmatrix} \Delta\dot{v}_c(t) \\ \\ \Delta\dot{i}_L(t) \end{bmatrix} = \begin{bmatrix} \dfrac{-G_T + 3bv_{c,\mathrm{dc}}^2}{C} & \dfrac{-1}{C} \\ 1/L & 0 \end{bmatrix} \begin{bmatrix} \Delta v_c(t) \\ \Delta i_L(t) \end{bmatrix} = \begin{bmatrix} \dfrac{-G_T}{C} & \dfrac{-1}{C} \\ 1/L & 0 \end{bmatrix} \begin{bmatrix} \Delta v_c(t) \\ \Delta i_L(t) \end{bmatrix} \tag{1.52}$$

where $G_T = 1/R + a$. As expected, the eigenvalues of the Jacobian matrix agree totally with the complex-conjugate poles $\sigma \pm j\omega$ calculated in (1.11), and are given by

$$\lambda_{1,2} = -\frac{G_T}{2C} \pm \frac{1}{2}\sqrt{\frac{G_T^2}{C^2} - \frac{4}{LC}} = 10^9 \pm j9.5 \times 10^9 \tag{1.53}$$

Because there are eigenvalues with a positive real part, the dc solution is unstable. The two complex-conjugate eigenvalues have two associated complex-conjugate eigenvectors spanning a two-dimensional space. The unstable manifold agrees, in this simple case, with the entire space R^2. If G_L is increased continuously, $G_T = a + G_L$ decreases, and at $G_T = 0$ the pair of poles crosses the imaginary axis to the left-hand side of the complex plane. The dc solution $v_{c\_\mathrm{dc}} = 0, i_{L\_\mathrm{dc}} = 0$ is stable for $G_T > 0$, unstable for $G_T < 0$, and undergoes a qualitative stability change at the critical value $G_L = |a|$. Note that the decaying transient, with oscillatory behavior, will be very slow for $G_L = |a| + \varepsilon$ with positive ε, that is, when approaching the critical value $G_L = |a|$. A qualitative change in the solution stability when a parameter is modified continuously is known as *bifurcation*. As has been shown, the values of the solution poles will generally change when varying a circuit parameter, such as G_L or L. Because of this, one real pole or a pair of complex-conjugate poles may cross the imaginary axis, giving rise to a qualitative change in the solution stability. Two complex poles may also turn into two real poles, or vice versa. This change in the nature of the poles may happen in either the left- or right-hand side of the complex plane, and does not give rise to a bifucation. However, the total pole number remains unchanged and is equal to the system order N. Note that for the large inductance value $L > 4C/G_T^2 = 0.1nH$, the linearized system will have two real eigenvalues of the same or different sign γ_1, γ_2, whose associated eigenvectors also span the entire space R^2.

As a second example, the stability of the three coexisting dc solutions of the circuit of Fig. 1.19b will be analyzed. These three dc solutions, calculated with (1.47), are $V_{\mathrm{dc}1} = 0$, $V_{\mathrm{dc}2} = 1$ V, and $V_{\mathrm{dc}3} = -1$ V. For each stability analysis, the nonlinear element is replaced by its linearization about the corresponding dc solution $\partial i(V_{\mathrm{dc}i})/\partial v$, obtaining the linearized differential equation system

$$\begin{bmatrix} \Delta \dot{v}_c(t) \\ \Delta \dot{i}_L(t) \end{bmatrix} = \begin{bmatrix} \dfrac{-G'_T(V_{\mathrm{dc}i})}{C} & \dfrac{-1}{C} \\ \dfrac{1}{L} & \dfrac{-R_2}{L} \end{bmatrix} \begin{bmatrix} \Delta v_c(t) \\ \Delta i_L(t) \end{bmatrix} \tag{1.54}$$

with $G'_T(V_{\mathrm{dc}i}) = G_1 + a + 3bV_{\mathrm{dc}i}^2$ and $R_2 = 1/G_2$. $V_{\mathrm{dc}2} = 1$ V and $V_{\mathrm{dc}3} = -1$ V have the same two poles, which are complex conjugate: $p_{1,2} = -6 \times 10^{10} \pm j2 \times 10^{10}$. They fulfill $\mathrm{Re}[p_{1,2}] < 0$, so $V_{\mathrm{dc}2}$ and $V_{\mathrm{dc}3}$ are stable. The two poles of $V_{\mathrm{dc}2} = 0$ V are real, with the values $p_1 = -8.385 \times 10^{10}$ and $p_2 = 2.385 \times 10^{10}$. Thus, the solution $V_{\mathrm{dc}2} = 0$ V is unstable and unobservable. The eigenvector associated with p_1, which is $\overline{u}_1 = (16.148, 1)$, spans the stable eigenspace of $V_{\mathrm{dc}2} = 0$. The eigenvector associated with p_2, which is $\overline{u}_1 = (123.852, 1)$, spans the unstable eigenspace of $V_{\mathrm{dc}2} = 0$. In terms of the state variables, this unstable eigenspace can be expressed as $\Delta v = 123.852 \Delta i_L$. It separates the disjoint basins of attraction of the two stable solutions $V_{\mathrm{dc}2}$ and $V_{\mathrm{dc}3}$.

1.5.2.2 Stability Analysis of a Periodic Solution Periodic solutions can be obtained in both autonomous and nonautonomous systems. For compactness, the two types of systems will be described as $\dot{\overline{x}} = f(\overline{x})$. However, in a nonautonomous system, the vector $\overline{x}$ will include $\theta = (2\pi/T)t$ as one of the state variables. In the following, the same dimension N of the vector $\overline{x}$ will be considered in the two cases, so the autonomous system should contain N reactive elements, whereas the nonautonomous system should contain $N-1$ reactive elements.

For the stability analysis of a periodic solution $\overline{x}_{sp}(t)$, with period T, a small perturbation will be applied at a particular time instant t_o, giving rise to the increment $\Delta\overline{x}(t)$ in the circuit state variables. Due to the small value of the increment $\Delta\overline{x}(t)$, the nonlinear system (1.55) can be linearized about $\overline{x}_{sp}(t)$. This leads to the time-varying linear system

$$\Delta\dot{\overline{x}}(t) = Jf(\overline{x}_{sp}(t))\Delta\overline{x}(t) \tag{1.55}$$

where the Jacobian matrix $Jf(\overline{x}_{sp}(t))$ is periodic with the same period T as the steady-state solution $\overline{x}_{sp}(t)$. The stability of the periodic solution will be determined by the time evolution of $\Delta\overline{x}(t)$. The general form of this perturbation is [24]

$$\begin{aligned} \Delta\overline{x}(t) &= \sum_{i=k}^{N} c_k e^{\lambda_k t}\overline{u}_k(t) \\ &= c_{c1}e^{(\sigma_{c1}+j\omega_{c1})t}\overline{u}_{c1}(t) + c_{c1}^* e^{(\sigma_{c1}-j\omega_{c1})t}\overline{u}_{c1}^*(t) + c_{r1}e^{\gamma_{r1}t}\overline{u}_{r1}(t) + \cdots \end{aligned} \tag{1.56}$$

where the complex vectors $\overline{u}_k(t), k = 1$ to N, are periodic with the same period T as the periodic solution, and the complex exponents λ_k are constant. The complex constants $c_k, k = 1$ to N, depend on the initial conditions (i.e., on the applied instantaneous perturbation). Note the similarity with the general expression of the perturbation of a dc regime (1.49). The only difference is the periodicity of the vectors $\overline{u}_k(t)$. Because these vectors are periodic, the extinction (or not) of the perturbation will depend only on the real part of the exponents λ_k in (1.56). This transient will be dominated by the terms associated with exponents with maximum real part σ_c or γ_r. Calculation of the exponents λ_k requires a Floquet analysis of the time-periodic linear system (1.57). Note that the λ_k are constant and cannot be the eigenvalues of the periodic matrix $Jf(\overline{x}_{sp}(t))$. Their calculation is carried out in several steps, outlined below.

Because system (1.55) has N dimensions, it will also have N linearly independent solutions $\Delta\overline{x}_1(t), \Delta\overline{x}_2(t), \ldots, \Delta\overline{x}_N(t)$. This means that the solution obtained for any initial value $\Delta\overline{x}_o$ can be expressed as a linear combination of N independent solutions. However, different sets of N independent solutions can be chosen. A useful set is the one obtained by integrating the linear system (1.55) successively from initial condition vectors $\Delta\overline{x}_{ok}$ given by columns of the N-order identity matrix I_N. Each independent solution $\Delta\overline{x}_{ck}(t)$, with $k = 1$ to N, is determined by integrating (1.55) from $\Delta\overline{x}_k = [0, \ldots, 1, \ldots, 0]^T$, where the "1" is located at the kth position. A matrix $[W_c(t)]$ can then be defined by the N independent solutions $\Delta\overline{x}_{ck}(t)$ obtained in this manner. It is called a *canonical fundamental solution matrix*, $[W_c(t)] = [\Delta\overline{x}_{c1}(t), \Delta\overline{x}_{c2}(t), \ldots, \Delta\overline{x}_{cN}(t)]$. Note that $[W_c(t)]$ is not periodic since, as gathered from (1.56), it will contain products of periodic terms and exponential terms.

Any particular initial value vector $\Delta\overline{x}_o$ of an N-dimensional system can be written $\Delta\overline{x}_o = [I_N]\Delta\overline{x}_o$. Knowing the canonical matrix $[W_c(t)]$ and the initial value $\Delta\overline{x}_o$ at $t_o = 0$, the solution $\Delta\overline{x}(t)$ can be calculated through a simple matrix–vector product:

$$\Delta\overline{x}(t) = [W_c(t)]\Delta\overline{x}_o \tag{1.57}$$

To illustrate some other properties of $[W_c(t)]$, the auxiliary matrix $[V(t)] = [W_c(t+T)]$ will be defined, which is the same matrix $[W_c(t)]$ as that evaluated at the time incremented in one period of the steady-state solution: $t + T$. We emphasize that due to the exponential factors, $[W_c(t)]$ is not periodic. However, the Jacobian matrix $Jf(\overline{x}_{sp}(t))$ is indeed periodic. Because of this, $[V(t)]$ is also a fundamental solution matrix of (1.55), as can easily be verified:

$$[\dot{V}(t)] = [\dot{W}_c(t+T)] = [Jf(\overline{x}_{sp}(t+T))][W_c(t+T)] = [Jf(\overline{x}_{sp}(t))][V(t)] \tag{1.58}$$

Thus, all the components of $[V(t)]$ fulfill (1.55). Because $[V(t)]$ is a fundamental (but not canonical) solution matrix, its columns will be expressible as in (1.57). Therefore, the solution matrix $[V(t)] = [W_c(t+T)]$ can be expressed in terms of the canonical fundamental solution matrix as $[V(t)] = [W_c(t)][V(0)]$, where $[V(0)]$ is the initial condition matrix. Replacing $[V(t)]$ with its original expression $[V(t)] = [W_c(t+T)]$, the following relationship is obtained: $[W_c(t+T)] =$

$[W_c(t)][W_c(T)]$. Note that unlike $[W_c(t)]$, the matrix $[W_c(T)]$ evaluated at $t = T$ is constant and will have constant eigenvalues and eigenvectors. The eigenvalues, assumed different, will be $m_k, k = 1$ to N, and the associated eigenvectors will be $\overline{w}_k$.

The eigenvectors $\overline{w}_k$ of $[W_c(T)]$ are linearly independent, so when taking these vectors as initial values for linear system integration, a set of N independent solutions is obtained. For each $\overline{w}_k$, the following relationship is fulfilled:

$$\begin{aligned}\Delta\overline{x}_{fk}(t+T) &= [W_c(t+T)]\overline{w}_k = [W_c(t)][W_c(T)]\overline{w}_k = [W_c(t)]m_k\overline{w}_k \\ &= m_k[W_c(t)]\overline{w}_k = m_k\Delta\overline{x}_{fk}(t) \end{aligned} \tag{1.59}$$

where m_k is the eigenvalue of $[W_c(T)]$ associated with the eigenvector $\overline{w}_k$. The N solutions $\Delta\overline{x}_{fk}(t)$ form a set of independent solutions in terms of which any general solution $\Delta\overline{x}(t)$ of (1.55) can be expressed. It is easily shown that each solution $\Delta\overline{x}_{fk}(t)$ fulfills $\Delta\overline{x}_{fk}(t+nT) = [W_c(T)]^n\Delta\overline{x}_{fk}(t) = m_k^n\Delta\overline{x}_{fk}(t)$. Due to this property, the solutions $\Delta\overline{x}_{fk}(t)$ are called *multiplicative*. The N eigenvalues m_k of $[W_c(T)]$ are known as the *Floquet multipliers* of the linearized system (1.55).

It is easily derived that a multiplicative solution fulfilling $\Delta\overline{x}_{fk}(t+nT) = m_k^n\Delta\overline{x}_{fk}(t)$ can be written as $\Delta\overline{x}_{fk}(t) = e^{\lambda_k t}\overline{u}_k(t)$, with $\overline{u}_k(t)$ a periodic vector. Taking into account the form of these independent solutions, the general solution $\Delta\overline{x}(t)$ is written

$$\Delta\overline{x}(t) = \sum_{k=1}^{N} c_k e^{\lambda_k t}\overline{u}_k(t) \tag{1.60}$$

which demonstrates (1.56). The N Floquet multipliers are related to the N exponents in (1.60) through the expressions [24]

$$m_k = e^{\lambda_k T} \qquad k = 1 \text{ to } N \tag{1.61}$$

The exponents λ_k are known as *Floquet's exponents*. At each time instant t, the periodic vectors $\overline{u}_k(t)$ provide N independent directions in which the perturbation is decomposed in a manner similar to the N eigenvectors associated with the linearization about a dc solution [see equation (1.49)]. Each vector $\overline{u}_k(t)$ is obtained by integrating the linearized system (1.55) from the eigenvector $\overline{w}_k$ of the constant matrix $[W_c(T)]$ and dividing by $e^{\lambda_k t}$. Note that the exponents λ_k are calculated directly from the eigenvalues $m_k, k = 1$ to N, of $[W_c(T)]$.

The Floquet multipliers m_k can be real or complex. The relation (1.61) between Floquet multipliers and Floquet exponents is not univocal. Actually, there is an infinite set of exponents $\lambda_k + jm(2\pi/T)$, with m an integer and T the solution period, associated with each multiplier m_k, as can easily be verified by introducing the exponent $\lambda_k + jm(2\pi/T)$ into (1.61).

Writing the time variable as $t = t' + nT$, with n a positive integer, it is possible to introduce the multipliers into the general expression (1.60)

$$\Delta\overline{x}(t' + nT) = \sum_{k=1}^{N} c_k m_k^n e^{\lambda_k t'} \overline{u}_k(t') \tag{1.62}$$

Remember that the objective is to determine the limit value of the perturbation when time tends to infinity. Whether the increment $\Delta\overline{x}(t)$ will decay to zero or grow unboundedly will depend solely on the limit value of m_k^n with n tending to infinity, as the vectors $\overline{u}_k(t)$ are periodic with the same period T as in the steady-state solution. Clearly, if any of the multipliers has a modulus larger than 1, the perturbation will tend to infinity and the solution will be unstable. For the periodic solution to be stable, all the multipliers must have modulus smaller than 1, except the one corresponding to variations tangent to the periodic cycle, with value $m = 1$. It is easily shown that in a nonautonomous circuit, this multiplier is associated with the extra variable θ. The case of a free-running oscillation is considered below. However, an exception is the periodic free-running oscillation, considered below.

As already shown, any arbitrary time shift τ of the periodic solution of an autonomous system $\overline{x}_{sp}(t)$ gives rise to a new solution $\overline{x}_{sp}(t - \tau)$. All the time-shifted solutions lie in the same limit cycle (see Fig. 1.14). Thus, we can assume that the periodic solution of an autonomous system is invariant under displacements along this cycle. The cycle has dimension 1, and at each time value, the tangent to the cycle can be considered as one of the N dimensions into which any small perturbation is decomposed. Perturbations tangent to the limit cycle will not vanish, as the solution is invariant under displacements along this cycle. Due to this invariance, one of the multipliers of the periodic solution will be $m_1 = 1$, which means that the perturbation neither grows nor decays. The associated vector $\overline{u}_1(t)$ is tangent to the cycle at each time value, and thus is equal to the time derivative of the periodic solution $\overline{u}_1(t) = \dot{\overline{x}}_{sp}(t)$. Therefore, $x_1(t) = e^{\lambda_1 t}\overline{u}_1(t) = \dot{\overline{x}}_{sp}(t)$, where the value $\lambda_1 = 0$ has been taken into account. Thus, $\overline{u}_1(t) = \dot{\overline{x}}_{sp}(t)$ must be an independent solution of the linearized system (1.55). This is easily demonstrated by deriving both sides of (1.55) with respect to time, which provides the equality $\ddot{\overline{x}}_{sp} = Jf(\overline{x}_{sp})\dot{\overline{x}}_{sp}$, so the vector $\dot{\overline{x}}_{sp}$, tangent to the limit cycle, fulfills (1.55).

The Floquet multiplier calculation has been used in the stability analysis of the steady-state oscillation at $f_o = 1.59$ GHz of the parallel resonance circuit shown in Fig. 1.1. Because it is a two-dimensional system, two different multipliers are obtained: $m_1 = 1$ and $m_2 = 0.2828$. As already explained, the first is associated with perturbations along the direction of the cycle. The second multiplier is real and has magnitude smaller than 1, which means that the steady-state oscillation is stable. The vector $\overline{u}_1(t)$ agrees with the time derivative of the periodic solution $\overline{u}_1(t) = \dot{\overline{x}}_{sp}(t)$. The vector $\overline{u}_2(t)$ can be calculated as $\overline{u}_2(t) = e^{-\lambda_2 t}\Delta\overline{x}_{f2}(t)$, where $\Delta\overline{x}_{f2}(t)$ is the fundamental solution obtained by integrating the linearized system from the initial condition $\overline{w}_2$, with $\overline{w}_2$ being the eigenvector of $[W_c(T)]$ associated with $m_2 = 0.2828$.

Because the steady solution $\overline{x}_{sp}(t)$ is periodic, it can be expressed in a Fourier series at the oscillation frequency $f_o : \overline{x}_{sp}(t) = \sum_{m=-M}^{M} \overline{X}_m e^{jm\omega_o t}$, where M is the number of harmonic terms considered. Note that the vectors $\overline{u}_k(t)$ in the general expression (1.56) for $\Delta\overline{x}(t)$ are also periodic, with the same fundamental frequency ω_o. Thus, considering two different time scales in $\Delta\overline{x}(t)$, one for the periodic $\overline{u}_k(t)$ and the other for the exponents $e^{\lambda_k t}$, it will be possible to decompose this perturbation in an M-order Fourier series, with time-varying harmonic terms $\Delta\overline{x}(t) = \sum_{m=-M}^{M} \Delta\overline{X}_m(t)e^{jm\omega_o t}$. Note that because N independent variables comprise $\Delta\overline{x}(t)$, each harmonic component $\Delta\overline{X}_m(t)$ will be an N-dimensional vector. Before continuing, note that the harmonic components of a time-domain product $c(t) = a(t)b(t)$ can be obtained as $\overline{C} = Toep(a)\overline{B}$, where $\overline{C}$ and $\overline{B}$ are vectors containing the $2M+1$ harmonic components of $c(t)$ and $b(t)$, respectively, and Toep(a) is a matrix composed of the Fourier coefficients of $a(t)$. The rows of this matrix are permutations of the harmonic components of $a(t)$, such that the product of row m by the harmonic vector $\overline{B}$ provides the mth harmonic component of $c(t)$. Note that the calculation is affected by the truncation error in the Fourier series. One example of this type of matrix was shown in (1.40). The same principle will be applied to the time-domain product $Jf(\overline{x}_{sp}(t))\Delta\overline{x}(t)$ in the system (1.55). On the other hand, the harmonic components of $\Delta\dot{\overline{x}}(t)$ can be related to the harmonic components of $\Delta\overline{x}(t)$. Note that $\Delta\dot{\overline{X}}(t)$ is given by $\Delta\dot{\overline{X}}(t) = \sum_{m=-M}^{M}(\Delta\dot{\overline{X}}_m(t) + jm\omega_o\Delta\overline{X}_m(t))e^{jm\omega_o t}$. Then it is possible to write in matrix form

$$\Delta\dot{\overline{X}}(t) + [jm\omega_o]\Delta\overline{X}(t) = Toep[Jf(\overline{x}_{sp})]\Delta\overline{X}(t) \tag{1.63}$$

with the components of the matrix $Toep[Jf(\overline{x}_{sp})]$ being constant values, since $Jf(\overline{x}_{sp}(t))$ is periodic at ω_o. Note that the dimension of the system (1.63) is $(2M+1)N$ for N independent variables. Applying the Laplace transform to equation (1.63), the following system in the Laplace frequency s is obtained:

$$\left\{[s + jm\omega_o] - Toep\left[Jf(\overline{x}_{sp})\right]\right\}\Delta\overline{X}(s) = 0 \tag{1.64}$$

Note that (1.64) is the characteristic system associated with the system linearization about the periodic solution $\overline{x}_{sp}(t)$. Recent works [30, 31] have rigorously demonstrated that for $M = \infty$ the Floquet exponents λ_k agree with the poles associated with the harmonic linear system (1.64). Because of this, there will be a set of poles $\lambda_k + jm(2\pi/T)$, with $|m| \leq M$ and T the solution period associated with each multiplier m_k. In a free-running oscillator, one of these poles is $s = 0$, so the matrix $[jm\omega_o]-$ matrix $Toep[Jf(\overline{x}_{sp})]$ must be singular. The periodicity $\lambda_k + jm(2\pi/T)$ of the poles associated with a nonlinear system linearization about a periodic regime can be understood intuitively. Consider the particular case of an instability of the periodic regime at ω_o due to a pair of complex-conjugate poles $\sigma \pm j\omega$, with $\sigma > 0$. The instability will lead to the generation of an incommensurable frequency ω. This will give rise to sidebands of the form $m\omega_o \pm \omega$ in the oscillator spectrum, so the circuit reacts as if it had "sources" of instability at all the sidebands, originated by the periodic poles.

As an example, the analysis presented will be applied to the FET-based oscillator of Fig. 1.6. The system dimension is $N = 13$, due to a relatively large number of inductors and capacitors. The steady-state oscillation frequency is $f_o = 4.39$ GHz.

The two pairs of dominant poles, extracted through numerical calculation, are $p_{1,2} = 0 \pm j4.39$ GHz and $p_{3,4} = -0.071 \pm j0.404$ GHz. Note that the frequency of $p_{1,2}$ agrees with the oscillation frequency $f_o = 4.39$ GHz, so these poles correspond to the Floquet multiplier $m = 1$ and are due to the autonomy of the oscillator solution. On the other hand, the pair of poles $p_{3,4} = -0.071 \pm j0.404$ GHz correspond to the complex-conjugate multipliers $m_{1,2} = 0.9881 \pm j0.0503$, of absolute value $|m_{1,2}| = 0.9894$. Thus, the steady-state oscillation is stable.

There are three main types of instability of a periodic solution associated with the three different possible situations: one unstable real multiplier $m_u > 1$, one unstable real multiplier $m_u < -1$, and a pair of complex-conjugate multipliers m_u and m_u^*, with $|m_u| > 1$. The type of instability will generally determine the type of solution to which the system will evolve after a transient.

Instability Due to a Positive Real Multiplier $m_k > 1$ The case of a periodic oscillation with multipliers $m_1 = 1$, $|m_{j \neq k}| < 1$, $j = 1$ to N, and $m_k > 1$ will be considered. This oscillation will be unstable due to $m_k > 1$. The real multiplier $m_k > 1$ is associated with a real eigenvalue γ_k. Thus, the perturbed steady-state oscillation will have a transient dominated by $e^{\gamma_k t}\overline{u}_k(t)$, as gathered from (1.56). Because the real exponent does not introduce any new frequency components, this type of instability will generally lead to a different periodic solution. This type of instability is typically obtained in multivalued solution curves. An example is shown in Fig. 1.21, corresponding to a MOSFET-based oscillator at 0.4 GHz [32]. Variation of the oscillation amplitude has been represented versus the gate bias voltage. The curve is bi-valued in the interval represented, which is due to the existence of a turning point at $V_{GG} = -1.2$ V at which the solution curve folds over itself. The entire curve is composed of solution points of a free-running oscillator regime, so at all the solution points there is a multiplier $m_1 = 1$. The

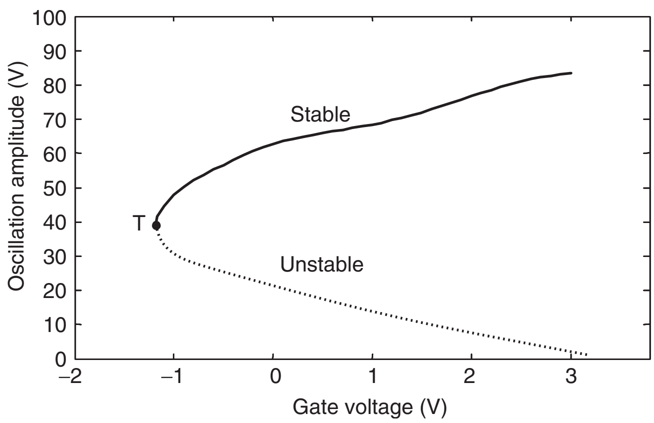

FIGURE 1.21 Variation of the oscillation amplitude versus the gate voltage in a MOSFET-based oscillator. The solution curve is bi-valued, due to the existence of a turning point.

upper section of the curve (the solid line) is stable, with all its Floquet multipliers, except $m_1 = 1$, having magnitude smaller than 1. However, a real multiplier $m_2 < 1$ increases its value when reducing V_{GG} and takes the critical value $m_2 = 1$ at the infinite slope point T. The lower section of the curve (the dashed line) is unstable with a real multiplier $m_2 > 1$. At the turning point T, $m_2 = 1$, which implies a real pole $\gamma_2 = 0$, due to the relationship between the multipliers and the roots of the characteristic determinant associated with (1.64). As demonstrated in Chapter 3, a pole at zero implies a singularity of the system at steady state, thus the infinite value of the curve slope at this point. This example shows again that the stability properties of a given steady-state solution vary when a parameter is modified. At the turning point, a qualitative stability change or bifurcation takes place in the system.

In Fig. 1.22a, the oscillator solutions at the particular bias voltage $V_{GG} = -1$ V have been represented in the phase space. The point designated EP corresponds to the coexisting dc solution. The stability of the dc solution has been analyzed independently and it has been found that this solution is stable. The limit cycle LC1 (the dashed line) has one multiplier, $m_1 = 1$, due to the solution autonomy, plus a second real multiplier, $m_2 = 1.0281$, so this limit cycle is unstable. The fundamental frequency of this solution is $f_o = 0.418$ GHz. The limit cycle LC2 has a multiplier $m_1 = 1$, plus a second, dominant multiplier $m_2 = 0.9863$, so this limit cycle is stable. Its fundamental frequency is $f_o = 0.414$ GHz.

The stable dc solution and the stable limit cycle coexist for the same values of the circuit elements (Fig. 1.22b). The unstable limit cycle is located between these two stable solutions. The unstable manifold of the unstable limit cycles separates their disjoint basins of attraction. To illustrate this idea, Fig. 1.22b shows the system behavior in a plane transversal to the unstable limit cycle LC1. The cycle intersection with this transversal plane gives rise to the point depicted. The stable manifold has dimension $N - 2$, with N the total system dimension. Note that one of the N dimensions corresponds to the cycle and is lost in the intersection with the transversal plane. The stable manifold of dimension $N - 2$ is simply sketched with two arrows pointing toward the cycle intersection point. The unstable manifold has one dimension, and depending on the initial conditions, leads to the stable limit cycle LC1 or the stable equilibrium point EP. According to Figs. 1.21 and 1.22, when reducing the gate bias voltage, the stable and unstable limit cycles LC1 and LC2 approach each other, overlap, and vanish at the turning point. For V_{GG} smaller than a value corresponding to the turning point, the dc solution is the only stable solution.

Instability Due to a Negative Real Multiplier $m_k < -1$ A periodic oscillation with associated Floquet multipliers $m_1 = 1$, $|m_{j\neq k}| < 1$, $j = 1$ to N, and a real multiplier $m_k < -1$ will be considered. This steady-state solution is unstable. Under small perturbations, the transient, ruled by (1.56), will be dominated by the real term $c_k e^{(\sigma + j(\omega_o/2))t}\overline{u}_k(t) + c_k^* e^{(\sigma - j(\omega_o/2))t}\overline{u}_k^*(t)$. To understand this, the relationship between Floquet multipliers and exponents $m_k = e^{\lambda_k T}$ must be taken into account. A real multiplier $m_k < -1$ can be expressed as $m_k = e^{(\sigma + j(1/2)(2\pi/T) + n(2\pi/T))T} =$

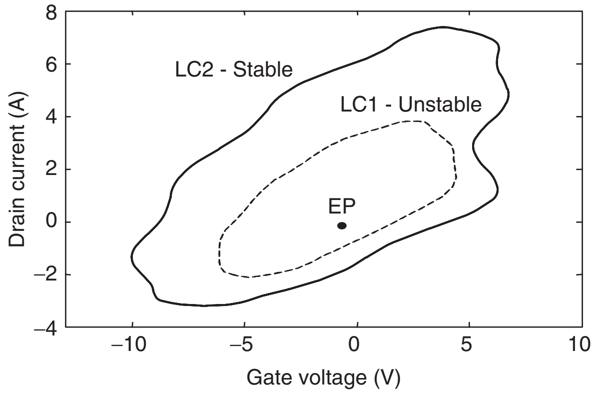

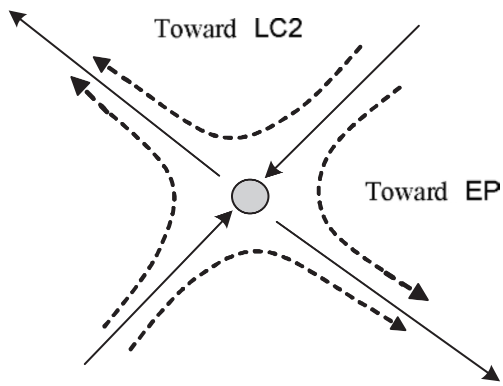

FIGURE 1.22 Phase space representation of coexisting solutions of a MOSFET-based oscillator for $V_{GG} = -1$ V. Both the equilibrium point EP and the outer limit cycle LC2 are stable. The inner limit cycle LC1 is unstable. Its unstable manifold behaves as a separator of the basins of attraction of EP and LC2.

$e^{(\sigma+j(\omega_o/2)+n\omega_o)T} = -e^{\sigma T}$, with n an integer. Because the vectors $\overline{u}_k(t)$ are periodic at the same frequency ω_o of the steady-state oscillation, the initial transient $c_k e^{(\sigma+j(\omega_o/2))t}\overline{u}_k(t) + c_k^* e^{(\sigma-j(\omega_o/2))t}\overline{u}_k^*(t)$ will correspond to an exponentially growing oscillation at the subharmonic frequency $\omega_o/2$. This transient will generally lead to a steady-state regime at the divided frequency $\omega_o/2$.

The frequency division by 2 has been observed in a Colpitts oscillator, discussed below. A stable periodic oscillation at $f_o = 1$ GHz is obtained for the original set of element values, with $L = 10$ nH. This solution has one multiplier, $m_1 = 1$, whereas the remaining multipliers have magnitude smaller than 1. Then the inductance L is swept, recalculating the steady-state solution for each L value. Note that due to the circuit autonomy, the oscillation frequency f_o will vary with L. After obtaining each steady-state solution, the corresponding Floquet multipliers are determined

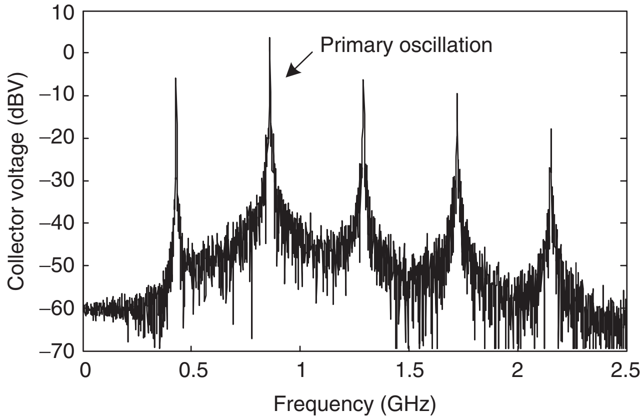

FIGURE 1.23 Subharmonic solution in a Colpitts oscillator. The oscillation at $f_o = 0.808$ GHz exhibites a real multiplier $m = -1.7340$, responsible for generation of the subharmonic frequency $f_o/2 = 0.404$ GHz.

numerically. It is found that when increasing the inductance value, one multiplier, m_2, crosses the circle through the point -1 at the value $L_o = 12.11$ nH. The periodic oscillation at f_o is unstable for $L > L_o$, so it is unobservable. For each $L > L_o$, the system evolves to a stable subharmonic solution at $f_o/2$. Figure 1.23 shows that the stable subharmonic solution emerged from the unstable periodic solution at $L = 16$ nH. This unstable solution has the Floquet multipliers $m_1 = 1$ and $m_2 = -1.734$. The voltage spectrum at the collector node is represented in Fig. 1.23. Both the primary oscillation at 0.870 GHz and the subharmonic components can be distinguished. This subharmonic solution is autonomous and periodic, so it will have a multiplier $m'_1 = 1$. Because it is stable, the remaining multipliers will have magnitude smaller than 1. Note that the unstable nondivided solution coexists with the stable divided solution. It is a mathematical solution that cannot be observed physically.

Instability Due to a Pair of Complex-Conjugate Multipliers $m_k, m_{k+1} = m_k^*, |m_k| > 1$ A periodic solution with a pair of complex-conjugate multipliers $m_k, m_{k+1} = m_k^*, |m_k| > 1$ will be unstable and under small perturbations will generally lead the system to a quasiperiodic solution with two fundamental frequencies ω_o and $\omega'_o = \alpha\omega_o$, with $\alpha \in R$. To understand this, the relationship between Floquet multipliers and exponents $m_k = e^{\lambda_k T}$ must be taken into account. A Floquet multiplier $|m_k| > 1$ can be expressed as $m_k = e^{\sigma + j(\alpha(2\pi/T) + n(2\pi/T))T} = e^{(\sigma + j\alpha\omega_o)T} = e^{(\sigma + j\omega_a)T}$. Because the multipliers m_k and m_{k+1} are the dominant ones, the transient after a small perturbation will initially evolve according to $c_k e^{(\sigma + j\omega_a)t}\overline{u}_k(t) + c_k^* e^{(\sigma - j\omega_a)t}\overline{u}_k^*(t)$. The vector $\overline{u}_k(t)$ is periodic at ω_o, so this transient will contain the two incommensurate frequencies ω_a and ω_o, which will generally lead to a quasiperiodic solution with a mixerlike spectrum at these two fundamental frequencies.

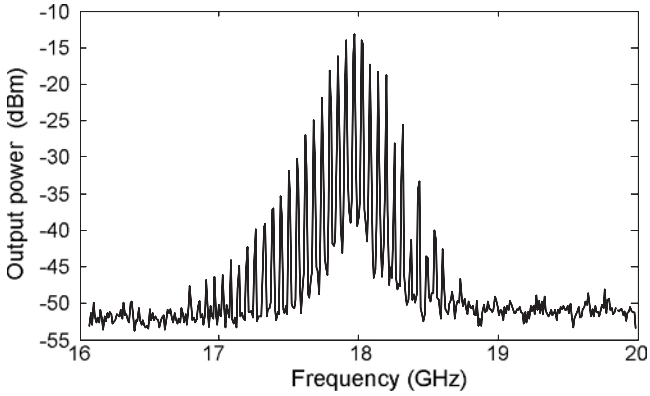

FIGURE 1.24 Output power spectrum of an oscillator at $f_o = 18$ GHz, with a second undesired oscillation at $f'_o = 8.989$ MHz.

As an example, Fig. 1.24 shows the output power spectrum of an oscillator at $f_o = 18$ GHz, with a second undesired oscillation at $f'_o = 8.989$ MHz. The unstable periodic solution had a pair of complex-conjugate multipliers $m_{1,2} = 1.0011 \pm j0.0077$. The nonharmonically related oscillation at $f'_o = \alpha f_o$ emerges from this solution. Mixing the two frequencies gives rise to the spectrum shown in Fig. 1.24. Note that the unstable periodic solution at f_o coexists with a quasiperiodic solution. It is a mathematical solution that cannot be observed physically.

1.6 PHASE NOISE

The phase noise problem in free-running oscillators is linked directly to the invariance of the steady-state periodic solution versus time translations. As shown in Section 1.2, in the frequency domain this gives rise to an irrelevance versus the phase origin. When a small impulse perturbation is applied to a stable periodic solution, the system will return to this solution (due to its stability) with a time shift τ (positive or negative) with respect to the original waveform. This gives rise to a shift $\Delta\phi = -\omega_o\tau$ in the phase origin. Note that the new phase value resulting from the perturbation corresponds to an equally valid oscillator solution. Because the linearized system $\Delta\dot{\overline{x}}(t) = Jf(\overline{x}_{sp}(t))\Delta\overline{x}(t)$ is a time-variant system, the time shift τ of the steady-state solution recovered depends on the particular time t_p of the solution period $(0, T]$ at which the perturbation is applied [8]. This is illustrated in the simulations of Fig. 1.25, which were carried out in the FET-based oscillator of Fig. 1.6. Figure 1.25a shows the steady-state waveform corresponding to the voltage across the gate capacitance $v_G(t)$. A short current pulse will be introduced at the gate node at different time values t_p, analyzing the effect on the drain voltage waveform. Figure 1.25b shows the original steady-state waveform (the solid line) and the time-shifted steady-state waveforms resulting from the use of an instantaneous perturbation of equal magnitude applied at different

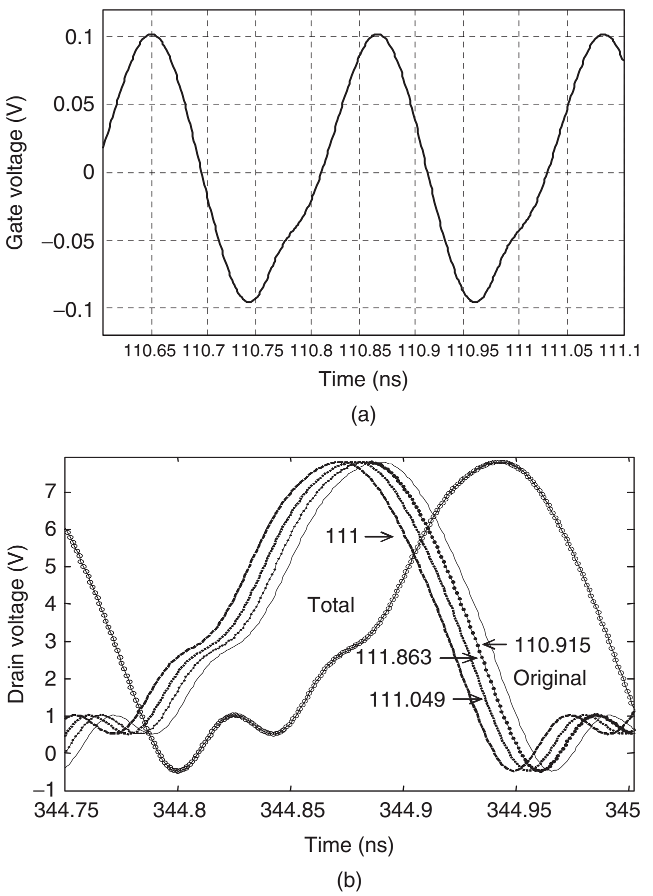

FIGURE 1.25 Time shift of the steady-state solution of the FET-based oscillator of Fig. 1.6 as a result of the introduction of short current pulses at different times. The current perturbations are introduced at the gate node. (a) Gate voltage waveform. (b) Drain voltage waveform. The waveform indicated by "total" is the result of three different perturbations applied at $t_p = 110.915$, 111, and 111.049 ns.

points in time. The curve corresponding to a perturbation applied at $t_p = 110.863$ ns is nearly overlapped with the curve corresponding to a perturbation applied at $t_p = 110.915$ ns, represented by diamonds. The dashed curve corresponds to a perturbation applied at $t_p = 111$ ns. The dotted curve corresponds to a perturbation applied at $t_p = 111.049$ ns. In agreement with Hajimiri and Lee [8], larger time shifts are obtained when a perturbation is applied at points of the waveform with a larger magnitude of the time derivative, due to rapid evolution of the system at these points. When applying several perturbations, the time shift accumulates. This is evidenced by the bold dotted curve, which is obtained as the result of three different perturbations applied at $t_p = 110.915$, 111, and 111.049 ns.

Unlike the test perturbations considered in the analysis shown in Fig. 1.25, the circuit noise sources are not deterministic. Thus, for phase noise analysis it will be necessary to obtain the stochastic characterization of the phase deviation in the presence of noise perturbations. The fundamental background for the understanding and analysis of oscillator phase noise is provided in Chapter 2.

REFERENCES

[1] A. B. Carlson, *Communication Systems*, McGraw-Hill, New York, 1986.

[2] U. L. Rohde, Nonlinear effects in oscillators and synthesizers, *IEEE MTT-S International Microwave Symposium*, Phoenix, AZ, pp. 689–692, 2001.

[3] K. Kurokawa, Injection locking of microwave solid state oscillators, *Proc. IEEE*, vol. 61, pp. 1386–1410, Oct. 1973.

[4] R. A. York, Nonlinear analysis of phase relationships in quasi-optical oscillator arrays, *IEEE Trans. Microwave Theory Tech.*, vol. 41, pp. 1799–1809, Oct. 1993.

[5] R. E. Collin, *Foundations for Microwave Engineering*, 2nd ed., Wiley, New York, 2001.

[6] P. F. Combes, J. Graffeuil, and J. F. Sautereau, *Microwave Components, Devices and Active Circuits*, Wiley, Chichester, UK, 1987.

[7] M. Odyniec, Oscillator stability analysis, *Microwave J.*, vol. 42, p. 6, 1999.

[8] A. Hajimiri and T. H. Lee, A general theory of phase noise in electrical oscillators, *IEEE J. Solid State Circuits*, vol. 33, Feb. 1998.

[9] F. X. Kaertner, Analysis of white and $f^{-\alpha}$ noise in oscillators, *Int. J. Circuit Theory Appl.*, vol. 18, pp. 485–519, 1990.

[10] J. M. T. Thompson and H. B. Stewart, *Nonlinear Dynamics and Chaos*, 2nd ed., Wiley, Hoboken, NJ, 2002.

[11] J. Jugo, J. Portilla, A. Anakabe, A. Suárez, and J. M. Collantes, Closed-loop stability analysis of microwave amplifiers, *IEE Electron. Lett.*, vol. 37, pp. 226–228, Feb. 2001.

[12] A. Anakabe, Detección y eliminación de inéstabilidades paramétricas en amplificadores de potencia para comunicaciones, Ph.D. Thesis, Universidad del Pais Vasco, 2003.

[13] U. L. Rohde, A. K. Poddar, and G. Bock, *The Design of Modern Microwave Oscillators for Wireless Applications*, Wiley, Hoboken, NJ, 2005.

[14] D. J. Vendelin, A. M. Pavio, and U. L. Rohde, *Microwave Circuit Design*, Wiley, New York, 1990.

[15] M. Odyniec (Ed.), *RF and Microwave Oscillator Design*, Artech House, Norwood, MA, 2002.

[16] K. Ogata, *Modern Control Engineering*, Prentice-Hall, Englewood Cliffs, NJ, 1980.

[17] K. Kurokawa, Some basic characteristics of broadband negative resistance oscillators, *Bell Syst. Tech. J.*, vol. 48, pp. 1937–1955, July–Aug. 1969.

[18] P. Gamand and V. Pauker, Starting phenomenon in negative resistance FET oscillators, *Electron. Lett.*, vol. 24, pp. 911–913, 1988.

[19] G. B. Arfken and H. J. Weber, *Mathematical Methods for Physicists*, Academic Press, San Diego, CA, 2001.

[20] J. H. Wilkinson, *The Algebraic Eigenvalue Problem*, Oxford University Press, New York, 1965.

[21] V. Rizzoli and A. Lipparini, General stability analysis of periodic steady-state regimes in nonlinear microwave circuits, *IEEE Trans. Microwave Theory Tech.*, vol. 33, pp. 30–37, Jan. 1985.

[22] S. Mons, J. C. Nallatamby, R. Quéré, P. Savary, and J. Obregón, A unified approach for the linear and nonlinear stability analysis of microwave circuits using commercially available tools, *IEEE Trans. Microwave Theory Tech.*, vol. 47, pp. 2403–2409, Dec. 1999.

[23] S. A. Maas, *Nonlinear Microwave Circuits*, Artech House, Norword, MA, 1988.

[24] J. Guckenheimer and P. Holmes, *Nonlinear Oscillations, Dynamic Systems, and Bifurcations of Vector Fields*, Springer-Verlag, New York, 1983.

[25] M. I. Sohby and A. K. Jastrzebsky, Direct integration methods of nonlinear microwave circuits, *European Microwave Conference*, Paris, pp. 1110–1118, 1985.

[26] T. S. Parker and L. O. Chua, *Practical Algorithms for Chaotic Systems*, Springer-Verlag, Berlin, 1989.

[27] S. Wiggins, *Introduction to Applied Nonlinear Dynamical Systems and Chaos*, Springer-Verlag, New York, 1990.

[28] L. Chua, Editorial in special issue, *IEEE Trans. Circuits Syst.*, vol. 30, pp. 617–619, 1983.

[29] C. P. Silva, Shil'nikov's theorem: a tutorial, *IEEE Trans. Circuits Syst. I Fundam. Theor. Appl.*, vol. 40, pp. 675–682, 1993.

[30] J. M. Collantes, I. Lizarraga, A. Anakabe, and J. Jugo, Stability verification of microwave circuits through Floquet multiplier analysis, *IEEE Asia-Pacific Proceedings on Circuits and Systems*, pp. 997–1000, 2004.

[31] F. Bonani and M. Gilli, Analysis of stability and bifurcations of limit cycles in Chua's circuit through the harmonic-balance approach, *IEEE Trans. Circuits and Syst. I*, vol. 46, no. 8, pp. 881–890, 1999.

[32] S. Jeon, A. Suarez, and D. B. Rutledge, Nonlinear design technique for high-power switching-mode oscillators, *IEEE Trans. Microwave Theory Tech.*, vol. 54, pp. 3630–3639, 2006.